

Development of a mucoadhesive and multiparticulate colon drug delivery system

Inauguraldissertation

zur

Erlangung der Würde eines Doktors der Philosophie
vorgelegt der
Philosophisch-Naturwissenschaftlichen Fakultät
der Universität Basel

von

Daniel Preisig

aus Speicherschwendi, (AR)

Basel, 2017

Original document stored on the publication server of the University of Basel edoc.unibas.ch



This work is licenced under the agreement
„Attribution Non-Commercial No Derivatives – 3.0 Switzerland“ (CC BY-NC-ND 3.0 CH). The
complete text may be reviewed here:

creativecommons.org/licenses/by-nc-nd/3.0/ch/deed.en

Genehmigt von der Philosophisch-Naturwissenschaftlichen Fakultät
auf Antrag von

Prof. Dr. Jörg Huwyler und Prof. Dr. Georg Imanidis

Basel, den 08. Dezember 2015

Prof. Dr. Jörg Schibler

Dekan

To my Friends and my Family

Table of contents

Acknowledgements	iii
Abbreviations	v
Summary	1
1 Introduction	3
1.1 Drug delivery via the oral route	3
1.2 Mucoadhesion	4
1.2.1 <i>The gastrointestinal mucus layer</i>	4
1.2.2 <i>Mucoadhesive polymers</i>	7
1.2.3 <i>Theories of mucoadhesion</i>	8
1.2.4 <i>Mucoadhesive drug delivery systems</i>	9
1.2.5 <i>In vitro methods to study mucoadhesion</i>	10
1.2.6 <i>In vivo methods to study mucoadhesion</i>	12
1.3 Colon drug delivery	14
1.3.1 <i>Anatomy and physiology of the large intestine</i>	14
1.3.2 <i>Diseases of the large intestine</i>	16
1.3.3 <i>Technologies for colon drug delivery</i>	17
1.3.4 <i>Multiparticulate colon drug delivery systems</i>	19
1.3.5 <i>Porous microcarriers for development of mucoadhesive microparticles</i> ...	23
2 Aims	25
3 Peer-reviewed publications	27
3.1 Drug loading into porous microcarriers	27
3.2 Mucoadhesive coating and <i>in vitro</i> evaluation	39
3.3 Preparation of optimized mucoadhesive microparticles	51
4 Clinical study protocol	63

5	Discussions	65
5.1	Drug loading into FCC	65
5.2	Mucoadhesive coating of microparticles	67
5.3	Investigation of <i>in vitro</i> particle-retention.....	69
5.4	<i>In vitro</i> assessment of colonic mucoadhesion and <i>in vivo</i> considerations	71
6	Conclusions and outlook	75
7	Bibliography	77
8	Curriculum vitae	97

Acknowledgements

I want to express my sincerest gratitude to Prof. Dr. Jörg Huwyler who offered me the possibility to perform this PhD project in his group. His motivating attitude and his pleasant personality were a real inspiration, and his scientific inputs were of great value for the realization of this project.

I really want to thank Prof. Dr. Georgios Imanidis for being co-referee of this PhD thesis. The friendly contact to the Institute of Pharma Technology at the University of Applied Sciences and their help in small things is also worth to mention.

The greatest recognition goes to my direct supervisor Dr. Maxim Puchkov. He is an outstanding scientist and a dedicated mentor. His smart guidance was an important driver for the success of this project, and his great sense of humor made it a pleasure to share his office.

I would like to acknowledge our collaboration partner Tillotts Pharma, in particular Dr. Roberto Bravo and Dr. Felipe Varum, for the strong commitment to this project. They gave me exceptional and valuable insights into new areas of formulation development, GMP manufacturing, patenting, and applying for clinical trials. Also, I want to thank Laetitia von Rochow, Sophie Decollogny, and Yalcin Cetinkaya for the good times at the Tillotts laboratories.

I had a great time with my former and current coworkers at the Rosental labs, namely Tanja Stirnimann, Veronika Eberle, Leonie Wagner-Hattler, Roger Roth, Reiji Yokoyama, Marine Camblin, and Darryl Borland. Darryl is acknowledged for proof-reading of the whole manuscript. The support of Dominik Witzigmann and Philip Grossen during the student practicals is also much appreciated.

Highly acknowledged are David Haid, Michael Weingartner, Roger Roth, and Sandy Tognola for their contributions to this PhD project with their Master Theses.

The financial support by the Commission for Technology and Innovation (CTI) is gratefully acknowledged.

Special thanks go to my old and new friends, and I am most thankful for my lovely family, for every heartbeat you have shared with me.

Abbreviations

5-ASA	5-Aminosalicylic acid
AUC	Area under the curve
BCS	Biopharmaceutics Classification System
C _{max}	Maximum plasma concentration
DSC	Differential scanning calorimetry
FCC	Functionalized Calcium Carbonate
HPLC	High-performance liquid chromatography
HPMC	Hydroxypropyl methylcellulose
IBD	Inflammatory bowel disease
IBS	Irritable bowel syndrome
MBZ	Metronidazole benzoate
NCE	New chemical entity
PEG	Polyethylene glycol
PK	Pharmacokinetic
PMC	Pseudomembranous colitis
PVP	Polyvinylpyrrolidone
ROI	Region of interest
ROS	Reactive oxygen species
SEM	Scanning electron microscopy
T _{max}	Time to C _{max}
XRPD	X-ray powder diffractometry

Summary

The physiology of the gastrointestinal tract presents serious barriers and challenges to oral drug delivery. The wide intra- and intersubject variability of gastrointestinal transit time is an important factor that can have a significant influence on drug bioavailability. Mucoadhesive formulations can increase and harmonize the passage time through the gastrointestinal tract, with the potential benefit of more reproducible drug bioavailability. This effect can be enhanced by using multiparticulate drug delivery system instead of single-unit dosage forms as the gastrointestinal transit of the formers is more reproducible and predictable. Delivery of such mucoadhesive multiparticulates to the colon can be of great benefit for local treatment of colonic diseases, such as *Clostridium difficile* infections, inflammatory bowel diseases (IBD) and colon cancer. However, so far no *in vivo* data on the usefulness of oral mucoadhesive formulations in the human proximal colon are available. Therefore, the aim of the work presented in this thesis was to develop a novel formulation platform for delivery of mucoadhesive multiparticulates to the colon for the treatment of *Clostridium difficile* infections. In the scope of the overall project a a proof-of-concept Phase 1 study was aimed therefore a formulation and manufacturing method based on standardized pharmaceutical processes was envisaged.

Functionalized calcium carbonate (FCC, Omyapharm) porous microcarriers were selected as an alternative size range to nanoparticles and pellets. Drug loading of various substances into FCC was carried out on the principle of solvent evaporation and crystallization. The rotary-evaporation and fluidized-bed processes were feasible to achieve high drug loads up to 40% (w/w). Loaded metronidazole benzoate (MBZ) and nifedipine as model drugs for poor aqueous solubility showed increased dissolution rates compared to drug crystals due to enlarged surface area of the loaded drug onto the FCC particles.

Mucoadhesive coating of drug-loaded FCC microparticles was achieved with the cationic polymer chitosan using either a pH-dependent precipitation method, or a spray-coating method in the fluidized-bed process. To test the chitosan-coated microparticles for mucoadhesivity, an *in vitro* method to measure particle retention on porcine colonic mucosa (as model of the human colonic mucosa) was developed. This included the design of a flow-channel device and the validation of marker-ion analysis for quantification of detached microparticles.

Optimized formulations containing MBZ as model drug for local treatment of colonic diseases (*Clostridium difficile* infections) prepared using the fluidized-bed process, resulted in good *in vitro* particle retention. To serve as control, non-mucoadhesive microparticles containing ethylcellulose were developed. These mucoadhesive and non-mucoadhesive microparticles filled into colonic-targeted hard-shell capsules (Tillotts Pharma innovation, outside the scope of the thesis) will be used in a gamma scintigraphy study for a proof-of-concept of mucoadhesion in the human colon as a strategy to increase residence time.

1 Introduction

1.1 Drug delivery via the oral route

Oral intake of a medicine is the most convenient way of drug administration, and the development of an oral dosage form should be the primary goal to ensure a high patient compliance [1]. The small intestine with its enlarged surface area by microvilli still presents the preferred site of drug absorption, but not all drugs are suited for oral administration due to issues of absorption, metabolism, or stability in the gastrointestinal tract potentially resulting in insufficient bioavailability of the drug [2].

The formulation of poorly water-soluble drugs still presents one of the major challenges in pharmaceutical development. Such drugs are prone to dissolve incompletely in the limited volume of intestinal fluids. The solubility-limited drug concentrations in the intestinal lumen can lead to low absorption rates, leading to an overall low bioavailability. Especially, class II and IV drugs of the Biopharmaceutics Classification System (BCS), the latter which are additionally characterized by low permeability through the endothelial membranes, require special formulation strategies. For example solid dispersions [3], lipid formulations [4], or carrier-based formulations in the nano- and microscale can help to reach temporarily increased drug concentrations [5]. The high intra- and interindividual variability of intestinal motility and gastrointestinal residence time presents a serious challenge regarding drug absorption conformity [6]. Mucoadhesive drug delivery systems have gained a lot of attention in the last two decades due to the potential to increase and harmonize gastrointestinal transit time and therefore improve overall drug bioavailability [7].

Local treatment of diseases related to the gastrointestinal tract presents a special application in oral drug delivery. The rationale is to deliver the drug directly to the site of action without being absorbed (or with reduced absorption) and distributed systemically via the blood stream. For example, gastro-retentive drug delivery systems were developed to eradicate *Helicobacter pylori* in the stomach [8,9]. A lot of effort has been undertaken to enable local therapy in the large intestine, and as a result, various coating technologies which dissolve or disintegrate in the distal small intestine or proximal colon have been developed and several medical products are in the market (e.g. Asacol®, Salofalk®, Ipecol®, Entocort®, and Budenofalk®)

The combination of mucoadhesive and colonic-delivery strategies has great potential to improve the efficacy in treatment of colonic diseases such as inflammatory bowel diseases (IBD), *Clostridium difficile* infections, and colon cancer. and serve as well for systemic absorption of drugs which are extensively metabolized in the proximal small intestine (e.g.

peptides) [7,10] or which are substrate to efflux transporters having lower expression levels in the colon than in the jejunum and ileum [11].. However, this combinatory approach requires more research. To cover the scope of this project, a theoretical background on mucoadhesion and colonic drug delivery is given in this introductory Chapter 1.

1.2 Mucoadhesion

Bioadhesion can be defined as the binding of two materials for an extended period of time, provided that at least one of the materials is of biological nature. In terms of drug delivery, mucoadhesion explicitly describes the attachment of a drug carrier system to the mucus layer[12]. The high interest in mucoadhesive formulations is not only due to increased residence timewithin a particular region of the gut, but also due to the potential for systemic drug delivery via other mucosal membranes by allowing an intimate contact with the mucosa, such as buccal and nasal mucosa, circumventing the first-pass effect and allowing a more precise dosing [13,14]. The pioneer work of Nagai *et al.* [15,16] included the development of a nasal insulin delivery system, which showed remarkable bioavailability in beagle dogs, and definitively demonstrated the great potential of mucoadhesive dosage forms. The development of mucoadhesive formulations could also optimize localized therapy of diseases related to the mucosal membranes, since the drug carrier can be brought into close contact with the diseased tissue. Most marketed products are buccal and vaginal drug delivery systems as they have the advantage of direct accessibility at the site of administration [17]. For example, Buccastem® is a buccal bioadhesive tablet containing prochlorperazine maleate against nausea [18], and many bioadhesives vaginal gels containing the contraceptive drug nonoxynol-9 (spermicide) are available in the US and Canada. However, so far no clinical trials have been performed to investigate mucoadhesion in the human large intestine after oral-administration of colonic drug delivery systems. This Chapter 1.2 outlines the challenging aspects of mucoadhesion in the gastrointestinal tract.

1.2.1 The gastrointestinal mucus layer

The function of the mucosal membrane is to protect the underlying epithelial cells and maintain them under moist conditions. The role of the gastrointestinal mucus is rather delicate, as it must be permeable enough for nutrition purposes, and at the same time allowing an efficient protection against mechanical damage during digestion of food due to the viscoelastic properties of the hydrated mucin molecules acting as a lubricant [19]. The mucus layer provides a stable micro-pH environment via bicarbonate secretion and also acts as an effective diffusion barrier between the lumen and the epithelial cells to protect it against chemical degradation from gastric pH, digestive enzymes, and xenobiotics [20–22]. The mucus layer is also an effective diffusion barrier against bacteria and other pathogens, and the impairment of

the mucus layer is an important pathological cause for inflammation [23]. Since the large intestine shows the highest colonization density of bacteria [24], chronic inflammations of the colon (colitis) have higher prevalence compared to inflammations in other sections of the gastrointestinal tract [25]. A total of 10^{14} bacteria are estimated to be in the human gut (10^{11} per gram of feces) [23]. To put this into context, our body consists of 10^{13} human cells [26].

Johansson *et al.* [27] showed evidence that the mucus layer is built up by a firmly attached inner mucus layer and a loose outer layer. It was observed that only the outer mucus layer is colonized, whereas the inner layer is impervious to the normal bacterial flora [28]. Due to the dynamic balance between mucus secretion and erosion, the mucus layer is constantly renewed, and the time required for complete renewal of the mucus layer is defined as the mucus turnover rate. Mucus turnover rate in rats was estimated *in vivo* using an invasive method inapplicable to humans [29]. The authors suggested that mucus turnover rate in humans might be close to the five hours measured in rats, and that the residence time of mucoadhesive dosage forms is then limited to the mucus gel turnover.

Mucus thickness plays a governing role in terms of mucoadhesivity [30], but literature reporting human gastrointestinal mucus thickness is contradictory and diverges among the different *in vitro* and *in vivo* measurement methods. The modified staining of cryostat cross-sections is superior to other *in vitro* methods, since the physiological conditions of the mucus are maintained [31,32]. Mucus thickness was measured in the stomach ($144 \pm 52 \mu\text{m}$), small intestine ($15.5 \mu\text{m}$, no S.D.), cecum ($23.1 \pm 16 \mu\text{m}$), transverse colon ($31.2 \pm 29 \mu\text{m}$), and distal colon ($45.7 \pm 38 \mu\text{m}$). Atuma *et al.* [33] reported an *in vivo* method for the determination of mucus thickness in rats, taking into account the presence of the two different adherent mucus layers. In contradiction to previous studies, mucus thickness was found to be highest in the colon. The loose mucus layer had a thickness of $714 \pm 109 \mu\text{m}$, and the firmly adherent mucus layer was $116 \pm 51 \mu\text{m}$ in thickness. These findings could be extrapolated to humans, suggesting that the thickness of the mucus layer is higher in humans than in rats. In summary, mucus thickness in the human gastrointestinal tract ranges between 15 – 800 μm . However, a strong variation has to be considered between different gastrointestinal sections, individuals, and measurement methods. Especially in a diseased state of the gastrointestinal tract, such as ulcerative colitis and Crohn's disease, the mucus thickness was found to vary significantly [34].

To understand the mechanisms of mucoadhesion, it is important to know the chemical and structural composition of the mucus layers. Besides lipids and inorganic salts, the mucins are the key components of the mucus, which can bind up to 95% of water. [19,35]. Mucins are high-molecular-weight glycoproteins ($0.5\text{-}40 \times 10^6 \text{ Da}$). They are composed of a protein core with attached oligosaccharide branches (2-20 sugar residues). A schematic presentation of a mucin glycoprotein is shown in Fig. 1.1. The sugar residues of the oligosaccharide branches

are composed of galactose, fucose, N-acetylglucosamine, N-acetylgalactosamine, or N-acetylneuraminic acid [35,36]. The sugar residues are attached to distinct amino acids of the protein core controlled by different glycosyltransferase enzymes in the goblet cells [37]. The main bonding types are the N-linked (on asparagine) and O-linked glycosylation (on serine and threonine), from which the latter is more abundant in the human gastrointestinal mucus layer. Depending on the expression level of the core protein (i.e. MUC-1, MUC-2, MUC-3, MUC-13) and glycosyltransferases, different glycosylation products are obtained, resulting in a characteristic glycosylation pattern along the gastrointestinal tract [38]. Important functional groups are the sialic acids and the sulphonate esters, giving an overall negative charge to the intestinal mucus layer [35]. However, the presence of poly-O-acetylated sialic acid in colonic mucins gives these molecules a hydrophobic character and resistance to bacterial enzymatic degradation [39,40]. Intramolecular crosslinking of mucins by disulfide bridges builds up the flat and sheet-like mucin network and the interactions with transmembrane mucins are important for the firmly attached inner mucus layer [41]. At the same time, the creation of large networks makes the mucin insoluble in water and enhances the viscoelastic properties of the outer mucus gel layer [42].

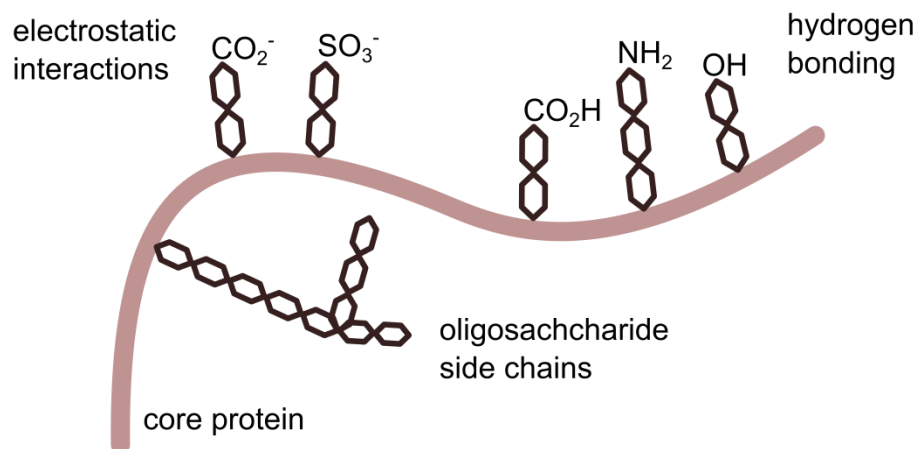


Fig. 1.1: Schematic structure of mucin (adapted from [43])

1.2.2 Mucoadhesive polymers

Most of the excipients used for mucoadhesive functionalization of a dosage form are of a polymeric nature. They usually have hydrophilic functional groups, e.g. carboxylic acids, enabling the formation of H-bonds with the mucin molecules. Examples of COOH -rich polymers with good mucoadhesive properties are poly acrylic acids (Carbopol®) or carboxymethyl cellulose [44]. Other cellulose derivatives such as ethylhydroxyethyl cellulose [45], hydroxypropylmethyl cellulose and hydroxypropyl cellulose [46] were also reported to be mucoadhesive.

One of the most investigated polymers with excellent mucoadhesive properties is chitosan [47–50], a biodegradable and biocompatible cationic amino polysaccharide obtained by partial deacetylation of chitin [51]. The mechanisms involved in the mucoadhesion of chitosan were elucidated by Sogias *et al.* [52] in a systematic study by “switching off” the contributing functional groups and investigating their influence on adhesive interactions. The authors concluded that the attractive interactions between chitosan and mucin are based on multiple adhesive mechanisms, such as electrostatic attraction, hydrogen bonding, and hydrophobic effects, with a major contribution from electrostatic interactions due to the cationic nature of chitosan.

Recent advances in mucoadhesive materials led to a second generation of bioadhesives. For example, thiolated polymers, the so called “thiomers”, can make covalent disulfide bonds with cysteines which are components of the mucin protein core [53]. Therefore, thiomers can target

the mucus layer with high binding strength. The intellectual property of thiomers innovations belong to the start-up company ThioMatrix GmbH.

Lectins are proteins or glycoproteins and also belong to the second generation of bioadhesives. They recognize the receptor-like structures of the cell membranes and bind with high specificity (cytoadhesion). Since lectins do not bind to the mucus layer, they were suggested to present an effective strategy to increase the residence time on mucosal tissues without being affected by the mucus turnover [54].

1.2.3 Theories of mucoadhesion

Mucoadhesion is a complex physicochemical process and more than one mechanism is involved. A number of general theories from surface science describing the phenomenon of adhesion were adapted to explain the mechanisms of mucoadhesion, namely the *adsorption theory*, *electronic theory*, *wetting theory*, *diffusion theory*, *mechanical theory*, and the *fracture theory*, which were well described elsewhere [55].

Adhesive interactions based on the *adsorption theory* are considered to be the major contribution to mucoadhesion. It describes the attraction between the mucins and mucoadhesive polymers on the basis of specific molecular interactions such as ionic bonding, hydrogen bonding, and van der Waals' forces. Hydrophobic effects can occur when the mucoadhesive polymers have an amphiphilic nature. Non-covalent and non-ionic bonds are in general low, but the net result leads to a strong interaction between mucins and polymers. Electrostatic forces are important for cationic polymers, such as chitosan, due to the ionic interactions with the negatively charged mucins. The *chemisorption theory* is a subsection of the *adsorption theory*, and includes the creation of strong covalent bonds as in case of thiomers.

In reality, it is impossible to determine the contributions of different adhesive mechanisms to the overall adhesive strength. Mucoadhesion can be described as a process of consecutive steps which are based on different mechanisms [12,55] as shown in Fig. 1.2. In a first phase (contact stage), the dosage form binds water molecules and swells (wetting theory) facilitating intimate contact with the mucosa. In a second phase (consolidation stage), non-covalent bonds are created (electronic and adsorption theory) and polymer chains interpenetrate into the mucin network (diffusion theory) strengthening the adhesive bond.

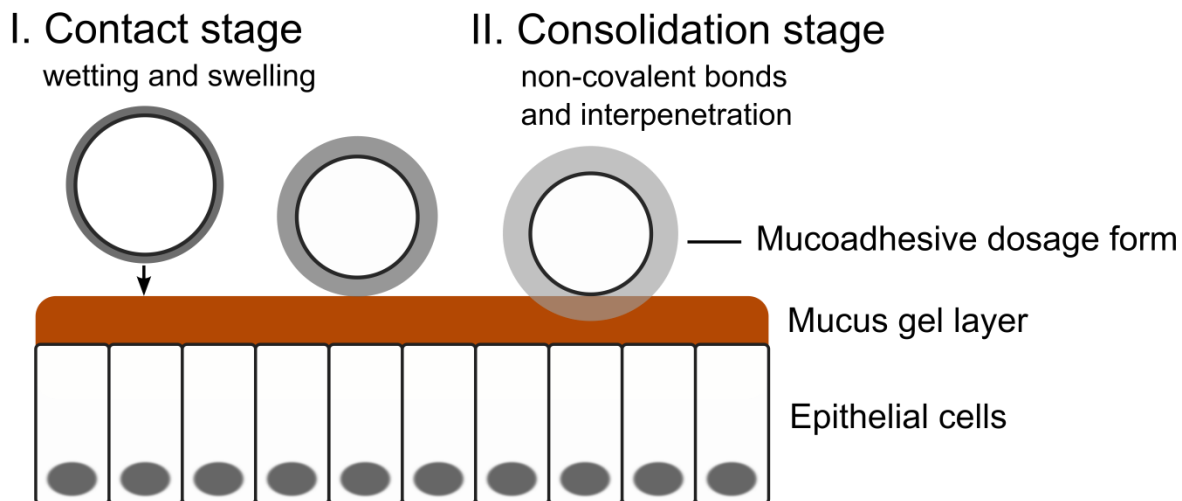


Fig. 1.2: Contact and consolidation stage of the mucoadhesion process [10,49]

1.2.4 Mucoadhesive drug delivery systems

The extensive research in the field of mucoadhesion led to the development of drug delivery systems directed to practically all possible mucosal tissues, such as the nasal [14], buccal [56], ocular [57], vaginal [58], gastric [59], small intestinal [60], and colonic mucosa [61]. Mucoadhesive drug delivery systems are solid or semi-solid dosage forms, i.e. tablets, multiparticulates, patches, films, or gels, depending on the site of administration. For example in buccal delivery, mucoadhesive films were described as highly suitable dosage forms due to the flexibility and comfort [56]. But also gels were produced for buccal delivery, such as ORABASE®, a mucoadhesive paste which protects sore areas in the mouth. Tablets are by far the most developed and investigated mucoadhesive dosage forms, but current market products (e.g. Aftach) are still limited [62].

For gastrointestinal delivery, multiparticulates are favorable compared to single-unit dosage forms due to better distribution along the intestinal wall, and the increased total surface area available for adhesive bonds. Furthermore, the gastrointestinal transit of multiparticulate formulations is less variable than single-units, and transit through the large intestine is slower due to a sieving effect, with monolithic dosage forms moving faster [63,64]. Therefore, considerable amount of work has been carried out on the development of mucoadhesive nanoparticles [65–67], microparticles [68–71], and pellets in the millimeter range [61,72].

1.2.5 *In vitro* methods to study mucoadhesion

In vitro test methods were extensively applied to identify new candidates of mucoadhesive polymers, and to evaluate the mucoadhesive potential of newly developed formulations. The many available techniques can be categorized into direct and indirect methods [73]. Direct methods either measure the force to break a mucoadhesive bond (e. g. tensile detachment [74], atomic force microscopy [75]), or the time a mucoadhesive dosage form can remain on a mucosal surface when exposed to drag forces of a flow (e.g. flow detachment [76], rotating cylinder method [77]). For these experiments, usually animal mucosal tissues are used. Alternatively, artificial substrates can also be applied with the aim of improving the reproducibility of the results [78]. Indirect methods investigate parameters which are related to mucoadhesive properties. For example, the molecular interactions between polymer and mucins can be measured by rheological measurements [79].

In tensile detachment methods, modified balances or tensile testers are typically used to measure the adhesive bond between the polymers and the mucosal tissue. Many research groups adopted and modified the method which was first described by Ch'ng *et al.* in 1985 [74]. The easy sample preparation, the short run time of the experiment, and the high detection sensitivity are advantages which made the tensile test the most applied method in the research of mucoadhesive polymers. The instrument setup should control either the force to be applied or the speed of detachment in order to record a detachment profile. The profile gives information about the change in the force applied as a function of the distance between the polymer sample and the substrate. Earlier studies only reported the maximal force required to detach the mucoadhesive dosage form from the mucosal tissue [74,80–82]. Later, the total work of adhesion was introduced to describe the whole process of detachment, which is simply the area under the curve in the detachment profile [83]. It was suggested that not only the adhesiveness between polymers and mucins, but also their deformation and mechanical properties make a contribution to the complex detachment process [12].

The principle of the flow-detachment method is to measure mucoadhesion based on the resistance to a flow and was first described by Rao and Buri [84][77] as shown in Fig. 1.3. This method was later adapted by other researchers and alternative techniques were reported, namely the falling liquid film method [68], continuous-flow adhesion cell [85], retention model apparatus [76], and particle-retention assay [86]. Since mucoadhesive formulations aim to prolong mucosal residence time, the results of such experiments are mostly given in retained percentage of the initially applied formulation, after a defined period of time. Flow detachment assays were preferably applied to investigate bioadhesion of microparticles [68,84,87–91] and polymer solutions [85,92–94] for drug delivery to the gastrointestinal mucosa. These methods also found application for the evaluation of nasal [95], esophageal

[76] and ocular delivery systems [96]. The disadvantage of a flow-detachment method is the need of a flow device which has to be developed in house. As a consequence, different designs and method parameters were used, which makes it difficult to compare the results between different research groups. Mikos and Peppas [97] were the only ones who used a closed channel. The open channel was used in numerous variations. For example, the flow channel of Rao and Buri [84] was semi-cylindrical and had one nozzle for inlet flow, whereas Bachelor *et al.* [76] have used a flat channel with three nozzles for inlet flow for better distribution of the medium (see Fig. 1.3).

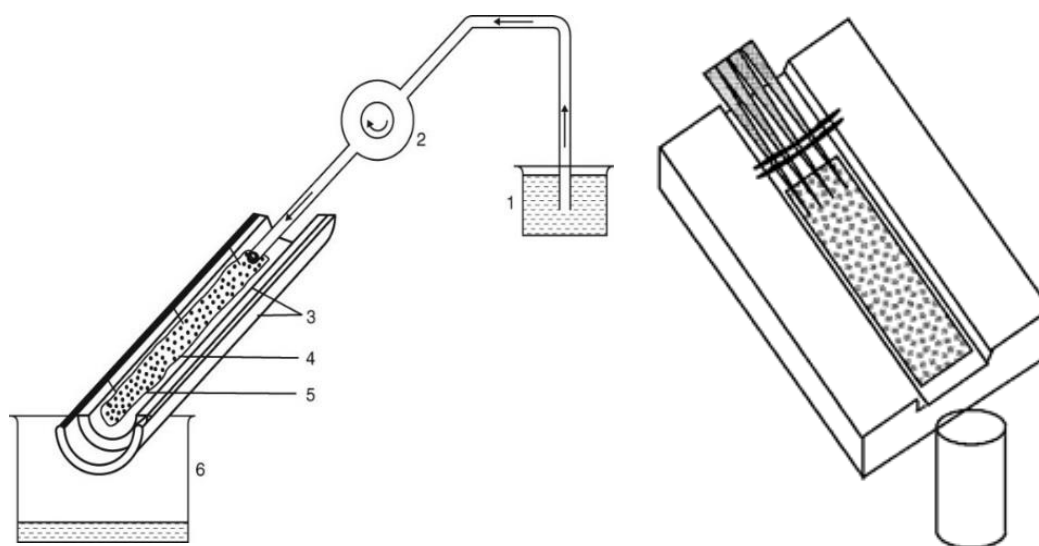


Fig. 1.3: Schematic presentation of two different flow-channel designs reproduced from Rao and Buri (left [84]), and Batchelor *et al.* (right [76]).

In the rotating cylinder method, mucoadhesive microparticles or tablets are also subject to drag forces. However, the difference is that the mucosa covered with adhering particles is moved relative to the medium. The mucosal tissue is mounted around a basket commonly used in USP I dissolution studies, and the mucoadhesive formulation is applied on the substrate. In case of tablets or test discs, the time of adhesion is measured [77], whereas for microparticles the percentage of remaining particles is determined after a specified time [98].

With the rheological approach it is possible to investigate the interactions of polymeric gels with the mucin glycoprotein, since interpenetration of the two polymers can be detected by the change of the rheological properties [99]. In general, the mixture of a hydrated mucoadhesive

polymer and mucin shows increased viscosity when determined experimentally in comparison to the theoretical cumulative viscosity calculated from the individual components. This increased viscosity is due to the molecular interactions, which can be based on chain interlocking, conformational changes, and chemical interaction. Therefore, the relative change in viscosity of the solution, also described as rheological synergism of mucus and polymer, can be used as an indirect quantification of mucoadhesion [79,100].

1.2.6 *In vivo* methods to study mucoadhesion

In vivo methods were applied to evaluate the usefulness of mucoadhesive formulations under physiological conditions. *In vitro* tests are often performed under standardized conditions, and do not resemble the complex environment of the gastrointestinal lumen and mucosa. Especially, in case of mucoadhesive formulations intended for gastrointestinal delivery, factors like volume of fluid available, bowel movement, enzymatic activity, and the presence of food contents are in general difficult to simulate.

In vivo studies with mucoadhesive microparticles can be performed in animals, preferably fasted rats, by oral administration of a known number of microparticles and subsequent dissection of the different intestinal segments [101]. The percentage of the recovered microparticles at different time points and segments can be used to estimate the gastrointestinal transit time of mucoadhesive formulations in comparison to non-mucoadhesive control. To improve the reliability of the quantification method, mucoadhesive microparticles were fluorescently labelled, and the number of particles in the different segments quantified using a fluorescence microscope. Chickering *et al.* [102] have used radiopaque barium to label mucoadhesive microspheres. After oral administration, the feces of the rats were collected by a custom-built sampling robot at pre-defined time intervals. The gastrointestinal lumen and the collected samples were X-rayed and analyzed for particle content.

The gamma-scintigraphy technique is a powerful tool to visually track *in vivo* the fate of orally administered dosage forms throughout the gastrointestinal tract [103,104]. Such clinical trials in humans were also performed for investigation of gastrointestinal transit time of mucoadhesive formulations [105–107]. The principle in gamma-scintigraphy studies is to incorporate a suitable gamma-emitting radioisotope, such as technetium-99m, indium-111, or samarium-153. The radioisotopes can be generated from stable nuclides, such as samarium-152, using neutron activation, which is done in a nuclear reactor by bombardment with neutrons. This means that the preparation of the pharmaceutical dosage form can be conducted with a non-activated marker. However, the high energies during neutron activation can lead to crosslinking or degradation of polymers and drug degradation. For these reasons, only a short activation process is used, and the effect of neutron activation on drug release, drug content

and impurities should be investigated *in vitro* prior to administration *in vivo*. After activation, the dosage form is stored until alpha radiation is harmless, and gamma radiation has decreased to approximately 1 MBq [108]. Gamma rays can be transferred into images using a gamma camera. Samarium-153 is of major clinical relevance, since the relatively short half-life of 46.3 h is well suited for carrying out a visualization study of gastrointestinal transit of dosage forms over few days [109].

Bioavailability studies were also performed for indirect determination of mucoadhesion by comparison to a non-mucoadhesive control formulation [107,110]. Ideally, sustained-release formulations are tested containing a drug which is absorbed only in a short part of the gastrointestinal tract in order that non-mucoadhesive formulations do not reach bioavailability values close to 100%. A significantly increased bioavailability of the mucoadhesive formulation can then be indirectly explained by the prolonged gastrointestinal transit time.

1.3 Colon drug delivery

The large intestine was recognized as a potential site of drug delivery for the local treatment of colonic diseases, as the treatment of chronic inflammatory diseases with potent substances is often accompanied by severe systemic side effects. The main rationale for local drug delivery is to have increased drug concentrations directly at the site of action, with the benefits of decreasing drug doses, plasma concentrations, and adverse drug effects. Colonic drug delivery can also be an efficient strategy to circumvent metabolic degradation by enzymes or active efflux by transporters in the small intestine [111]. Due to the reduced proteolytic activity, the colon has been also often pinpointed as a potential site for delivery and absorption of peptides [10,112]. Time-delayed drug delivery systems were one of the first formulation approaches for colonic delivery. However, due to the wide intra- and intersubject variability of gastrointestinal transit time, these formulations lacked precision of releasing the drug in the colon. Only when the complex environment and physiology of the large intestine was understood in more details, colon-specific characteristics could be identified as a trigger for drug release. As a result, more efficient formulation strategies were developed, for instance coating technologies which are pH-responsive or degradable by the colonic microflora. In this Chapter 1.3, the relevant background knowledge related to colon drug delivery is summarized, and in particular, the current status of the development of multiparticulate colon drug delivery systems was reviewed.

1.3.1 Anatomy and physiology of the large intestine

The large intestine extends from the ileocecal junction to the anus, including distinct segments in following order: cecum, ascending colon, transverse colon, descending colon, sigmoid colon, and rectum (see Fig. 1.4). The main functions of the large intestine are the resorption of water and electrolytes, and retention of the solid stool until a convenient time of defecation. In healthy humans, the chyme coming from the ileum to the colon has a mean flow rate of 1-2 liter per day. The absorptive capacity of the colon can be up to 4 liter per day, and the residual water content in the stool is less than 10% [19]. According to the results of an MRI study conducted by Schiller et al. [113], the fluid volume in the large intestine was highly variable among the subjects, and also depending on food intake. In fasted state, the total colonic fluid volume ranged from 1-44 ml (median = 8 ml), and in the fed state from 2-97 ml (median = 18 ml).

The highly viscous feces are transported towards the rectum by very intense and prolonged contractions, the so-called mass movements or giant migrating contractions. But also segmental contractions to mix the intestinal content, and antiperistaltic contractions towards the ileum to retard the movement of fecal mass are observed [114]. The large intestine has a length of approximately 1.6 m when measured *post mortem*, which is much smaller than the

small intestine (6.0-6.7 m) [115]. There are additional factors why the large intestine is considered to be less effective for drug absorption compared to the small intestine, such as the absence of microvilli and organic nutrient transporters, the increased thickness of the mucus layer, and the higher viscosity of the intestinal content. The latter leads to a lower drug diffusion coefficient, and affects negatively the mixing of the colonic content, reducing the drug concentrations close to the epithelium[19].

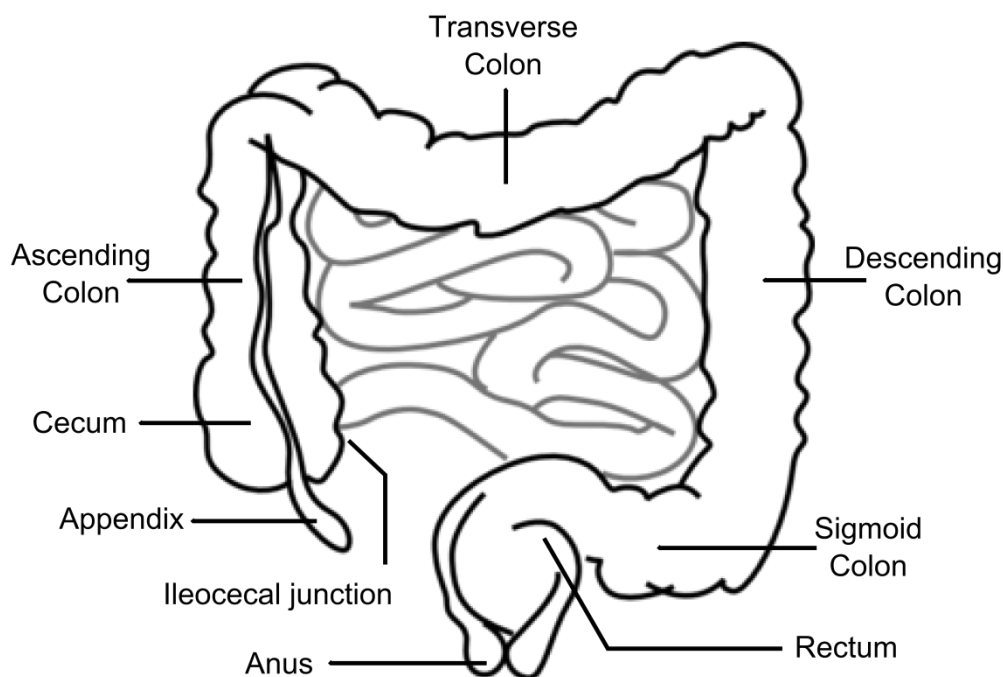


Fig. 1.4: Anatomy of the large intestine (adapted from [19]).

The gastrointestinal transit time is an important factor in the design of targeted drug delivery systems, because it can affect disintegration time of the dosage form, or the location and extent of drug dissolution and absorption. However, the intra- and intersubject variability of transit time, especially through the colon, is very high [2]. The mean transit time of a dosage form through the small intestine is fairly constant, ranging from 3-4 h, in both fed and fasted state, and regardless of the size of the dosage form [116]. Furthermore, it was reported that the physical state of the dosage form, i.e. liquid or solid, does not affect the transit speed through the small intestine [117]. After passage through the small intestine, the dosage form rests in the cecum before it enters the colon for a variable period of time (0-12 h) [7], and multiple-unit formulations were observed to regroup [118]. According to a scintigraphy study of Abrahamsson *et al.* [63], the colonic transit time is different for pellets and tablets, which ranged within 6 to 48 h, and 3.8 to 26 h, respectively. Despite the large variations for both dosage forms and the wide overlapping time range, tablets showed a clear trend of shorter transit time.

The pH in the gastrointestinal tract gradually increases from the stomach to the distal small intestine due to the bicarbonate secretion in the small intestine. The bicarbonate secretion rate is regulated by the hormone secretin and is the highest in the duodenum providing efficient neutralization of the gastric pH [119]. In contrast to the common belief that pH continues rising also along the large intestine up to pH 7-8 [120], various studies have demonstrated the opposite, that pH is highest in the terminal ileum (pH 7.5) and drops significantly in the cecum to pH 6.4-6.0, followed by a gradual increase from the right to the left colon.[121,122]This pH drop in the caecum is mainly due to bacterial fermentation of polysaccharides generating short chain fatty acids (such as acetic, propionic, and butyric acid) which contribute to reduce the pH [123,124].

The human colon is hosting up to 400 different species and subspecies of bacteria [19], and more than 99% of the colonic microflora are obligate anaerobes [24,125]. Most anaerobic species belong to the *Bacteroides*, *Bifidobacteria*, and *Eubacteria*. Other Gram-positive bacteria present in the colon are the *Enterococci*, *Clostridia*, and *Enterobacteria* [126]. The high diversity and colonization of bacteria in the colon compared to the microflora in the stomach and the proximal small intestine stems from the favorable changes of environmental conditions, such as the decreased acidity and motility as well as the presence of a vast amount of nutrients which escape digestion and absorption in the upper small intestine. The chyme, containing polysaccharides indigestible for humans, is fermented by hydrolytic enzymes (β -glucuronidase, β -xylosidase, α -L-arabinosidase, and β -galactosidase), and reductive enzymes (nitroreductase, azoreductase, deaminase, and urea dehydroxylase) [111,127]. In addition to the metabolic activity, we profit a great deal from the high diversity of the gut flora due to secretion of a number of signaling factors supporting our immune system, and due to protection of the intestinal mucosa from overpopulation by pathogenic microbes [128]. It is therefore not surprising that a misbalance of the gut flora can be a crucial factor in the pathogenesis of colonic diseases such as IBD or irritable bowel syndrome (IBS) [125].

1.3.2 Diseases of the large intestine

Ulcerative colitis and Crohn's disease are chronic inflammatory conditions of the gastrointestinal mucosa. They are both referred to IBD due to a number of common features. IBD are more prevalent in developed countries, and the incidence of ulcerative colitis is relatively high with 1.2 to 20.3 cases per 100,000 persons per year [129]. In ulcerative colitis, manifestation of the disease is limited to the rectum and the large intestine, whereas in Crohn's disease the whole gastrointestinal tract from the oral cavity to the rectum can be affected. The main characteristic symptom of IBDs is diarrhea mixed with blood and mucus. The disease can be classified by the severity of the symptoms [130] or by the extent of involved intestinal segments [131]. In contrast to Crohn's disease, ulcerative colitis can have a mild disease

progression, and complete cure is only possible by surgery. In mild to moderate cases of ulcerative colitis, the anti-inflammatory drug mesalazine (e.g. Asacol®) is used as first-line therapy for induction and maintenance of remission [132]. Since autoimmune phenomena are involved in the pathogenesis of IBDs, they are also managed with immunosuppressive drugs such as corticosteroids (prednisone and budesonide), monoclonal antibodies (i.e. infliximab), and others (azathioprine), depending on the severity of the disease and the response of the patient [133]. These medicines can produce strong systemic side effects, including mortality. The most prominent side effects in the treatment with corticosteroids are, besides many others, water retention in the face and acne [134]. The treatment with immunosuppressives is often accompanied by serious infections [135]. Hence, novel formulation strategies targeting the diseased tissue are of high clinical relevance either for existing molecules or new chemical entities (NCEs) [136].

Pseudomembranous colitis (PMC) is an inflammation of the large intestine most often caused by overgrowth of *Clostridium difficile* (*C. difficile*) bacteria. The major cause for PMC is the elimination of the normal microflora during antibiotic therapy allowing pathogenic bacteria to flourish. Therefore, PMC is also referred to *C. difficile* colitis or antibiotic associated colitis. In most cases, the inflammation is caused by the virulence factors toxin A and toxin B. They are internalized by the enterocytes via receptor binding, where they disrupt the cell cytoskeleton and activate an inflammatory immune response [137].

Colon cancer is the third most common type of cancer, and involves around 10% of all cancer cases [138]. In early stage of non-metastatic colon cancer, surgical dissection is the most effective treatment. However, a high risk of recurrence remains, and adjuvant chemotherapy was demonstrated to be inevitable for successful therapy of colon cancer. Besides the standard combination therapy of 5-fluorouracil and leucovorin, additional treatment with other chemotherapeutic compounds such as oxaliplatin, capecitabine, and irinotecan can increase the survival rate depending on the stage of the cancer [139].

1.3.3 Technologies for colon drug delivery

Colon drug delivery systems for oral administration have the advantage to reach the entire large intestine, i.e. from the ileo-colonic region to the rectum, whereas rectally administered formulations, such as suppositories or foams, only reach the lower part of the rectum. Drug delivery to the colon via the oral route can be achieved by advanced formulation technologies triggering the drug release only upon arrival in the ileo-colonic region. Alternatively, the drug itself can be chemically modified to a prodrug which undergoes biotransformation to the active parent drug under colon-specific conditions.

The prodrug approach was successfully applied to the anti-inflammatory drug mesalazine (5-aminosalicylic acid, 5-ASA) used in the treatment of ulcerative colitis and Crohn's disease. Sulfasalazine, olsalazine, and balsalazide are well-known examples for colon-specific prodrugs having a second moiety coupled to 5-ASA via an azo bond ($R^1-N=N-R^2$) [140]. An important characteristic of colon-specific prodrugs is a low and reproducible absorption rate in the small intestine. When administered orally, about 20% of sulfasalazine is systemically absorbed [141]. In the colon, the remaining fraction of sulfasalazine is transformed to 5-ASA and sulfapyridine moieties by bacterial azoreductase which cleaves the azo bond. The absorption of 5-ASA in the colon is relatively low as the bioavailability ranges from 11-33% [140]. Sulfapyridine has been found to be responsible for adverse drug effects. Therefore, 5-ASA prodrugs based on azo-linked polymers have also been developed to decrease systemic absorption and reduce side effects [142]. The azo-coupling to mucoadhesive polymers presents an interesting strategy for more effective local therapy [143,144], but the high amount of polymers needed to reach the required dose of 5-ASA is a drawback of using polymeric prodrugs. Colon-specific prodrugs were also developed for glucosteroids such as dexamethasone, prednisolone, hydrocortisone, and fludrocortisone by coupling the highly polar moieties galactose or glucose via a β -glycosidic bond [145,146].

Time-delayed release systems for drug delivery to the colon follow the principle of having a predetermined lag time for drug release, which matches the transit time through the small intestine. The PulsincapTM technology was one of the first delivery devices based on the lag-time principle [147]. It consists of a capsule with an insoluble body and a soluble cap. The body of the capsule is filled with the drug and closed with a hydrogel plug. After a predetermined time of swelling, the plug is pushed out and the drug starts to release [148]. The problem of variable gastric emptying can be avoided by coating the whole drug delivery system with enteric polymers. In an attempt to improve the PulsincapTM system, an erodible tablet instead of the swelling hydrogel was used [149]. Despite the relatively consistent transit time through the small intestine [116], various studies demonstrated a poor precision of time-delayed delivery systems to release the drug at the intended site [146,147], which might be due to variability in pH and consequent localization of enteric coating dissolution exposing the drug core .

The use of pH-dependent film coatings is the most popular strategy for targeted drug delivery to the colon [120,152,153]. The polymers for pH-triggered drug release are usually methacrylic acid - methyl methacrylate copolymers (Eudragit®, Evonik AG) or hydroxypropyl methylcellulose (HPMC) derivatives such as HP-50 and HP-55, which have a specific and narrow pH range where they start to dissolve. For example, Eudragit® S dissolves at $\text{pH} \geq 7$, which is considered as an optimized enteric coating formulation for colon delivery.

More pH-dependent coating polymers can be found in the review of Madhu et al. [154]. Ashford *et al.* [155] investigated the usefulness of pH-dependent model formulations coated with Eudragit® S by determining the site of disintegration *in vivo* using gamma-scintigraphy. In some cases, disintegration occurred already in the ileum, whereas in another case the tablet travelled until the splenic flexure before the drug was released. This lack of site specificity can be due to the high intra- and intersubject variability of pH and exposure time to the gastrointestinal fluid and also due to the inconsistent acidity gradient along the gastrointestinal tract with the highest pH in the ileum (pH 7.5), followed by the sharp drop of pH in the cecum (6.0).

Biodegradable polymeric film coatings follow the same principle as the prodrugs. They are degraded by the enzymatic activity of colonic bacteria with the advantage of allowing higher drug doses which are released at once. Azopolymers were used for delivery of peptides (insulin and vasopressin) [156,157], and various small molecules [158,159]. Naturally occurring polysaccharides and its derivatives, such as amylose [160], pectin [161], chitosan [162], inulin [163], and dextran [164] are biodegradable polymers which were also exploited in terms of colon-specific targeting. To test the usefulness of such coatings, drug release in appropriate media simulating the enzymatic activity of the colonic microflora can be measured according to Molly *et al.* [165]. However, according to several *in vivo* studies, the reproducibility of such microbially triggered release systems can also be affected by intra- and intersubject variability of the intestinal microflora [150,157,166].

Novel approaches are focusing on the combination of two mechanisms, preferably enzymatic and pH-sensitive systems, since gamma-scintigraphy studies have shown high reproducibility regarding the site of disintegration [167,168]. Such coating systems are less affected by intra- and intersubject variability, because in case that one mechanism fails, there is still a “back-up” mechanism acting as a trigger of complete drug release.

1.3.4 Multiparticulate colon drug delivery systems

There is a clear trend in colon drug delivery to develop multiparticulate formulations rather than single-unit systems. The advantages are similar as for mucoadhesive multiparticulates described in Chapter 1.2.4, i.e. prolonged transit time, closer contact to the diseased tissue, and more reproducible drug release [169,170]. The development of colon-targeted pellet formulations has already led to the launch of several products in the market (Apriso and Salofalk Granu-Stix) [169], whereas colonic-targeted formulations based on microparticles or nanoparticles require further development, especially regarding its toxicity profile and manufacturability at industrial scale.

Most pellet formulations for colon delivery have been prepared by extrusion-spheronization. The drug can be extruded together with a colon-specific polymer such as Eudragit S [171], chitosan [172], or pectin [173]. Another popular method is to prepare drug-loaded pellets which are subsequently film-coated with a pH-dependent or enzymatically-degradable polymer, as described for 5-ASA [160,174–177], budesonide [178], and ibuprofen [171]. Alternatively, drug layering onto nonpareil starter pellets and subsequent film coating with colon-targeting polymers can be carried out using the fluidized-bed process [179,180]. Ionotropic gelation of pectin with zinc or calcium ions was also reported for fabrication of colon-specific pellets, where the drug is incorporated during the crosslinking process [181–183]. Various modifications of such pectin-based pellets have been investigated for colon drug delivery [184–186]. Numerous *in vivo* studies have been carried out showing the potential of colonic-targeted pellets to improve the therapeutic outcome in rats [156,162,176,178,187–193], mice [194], rabbits [195], dogs [196], and humans [197,198].

Nanoparticles for colon drug delivery were first developed and described by Cheng and Lim [199]. Their preparation method of insulin-loaded nanoparticles was based on ionotropic gelation of the bacterial-degradable polymer pectin. The rationale of using nano-sized carriers for colon delivery is a lower transit time and a faster degradation of the coating or matrix upon arrival in the ileo-colonic region [200]. Furthermore, Lamprecht *et al.* have demonstrated a size-dependent accumulation of polystyrene particles in inflamed mucus tissue of colitis-induced rats. Highest binding affinity was observed for nanoparticles (100 nm), whereas relative deposition of microparticles (1 μm and 10 μm) was significantly decreased. As a consequence of these breakthrough results, the development of colon-specific nanoparticles gained a lot of interest, and several *in vivo* studies were carried out as summarized in Table 1.1. Most formulation approaches were based on anti-inflammatory drugs, and incorporation of pH-sensitive polymers (Eudragit® S100) into the particle shell. To test the usefulness of such nanoparticulate drug delivery systems *in vivo*, many researchers used the colitis-induced rat or mouse model to investigate the effect on the extent of inflammation after oral administration. A more recent advancement by Vong *et al.* [201] is the use of redox polymers which specifically accumulate in inflamed tissues (mechanism unclear) and eliminate the reactive oxygen species (ROS), eventually reducing the extent of inflammation.

Table 1.1: *In vivo* evaluation of nanoparticles for colon drug delivery.

Colon-specific polymer	Preparation method	Drug type (drug)	<i>In vivo</i> method	Ref.
Pectin	Iontropic gelation	Peptide (insulin)	(<i>in vitro</i> release studies)	[199]
Chitosan and chitosan derivatives	Polyelectrolyte complexation	Peptide (insulin)	Hypoglycemic effect in rats	[202]
Chitosan and alginate	Double emulsion/solvent evaporation	Anti-inflammatory tripeptide	Reduction of inflammation in colitis-induced mice	[203]
Eudragit® S100	Emulsification-diffusion	Anti-inflammatory (budesonide)	Reduction of inflammation in colitis-induced rats	[204]
Eudragit® S100	Emulsification-diffusion	Anti-inflammatory (curcumin)	Reduction of inflammation and distribution in colitis-induced mice	[205]
Eudragit® S100	oil-in-water emulsion/solvent evaporation	Anti-inflammatory (budesonide)	Reduction of inflammation in colitis-induced mice	[206]
Eudragit® RS PO	Emulsification-diffusion	Fluorescent-marker	Distribution in mice gut	[207]
Eudragit® S100 and azo-polyurethane	oil-in-water emulsion/solvent evaporation	Fluorescent-marker	Distribution in colitis-induced rats	[208]
Redox block copolymer	Self-assembly	Reduction of ROS	Cellular uptake in colitis-induced mice	[201]

Microparticles for colon delivery are an interesting alternative to nanoparticles as they are not internalized by epithelial cells, and hence, there is a much lower risk of systemic drug toxicity. Lorenzo-Lamosa *et al.* [209] have prepared drug-loaded chitosan microspheres by spray-drying which were subsequently encapsulated in Eudragit® L100 and Eudragit® S100 using an oil-in-oil solvent evaporation method. *In vitro* drug release was continuous for several hours when measured at pH 7, whereas no drug dissolution was observed in an acidic buffer. There have been numerous reports on multiparticulate colon drug delivery systems in the micro-size range, most of them based on bacteria-degradable or pH-sensitive release mechanisms. However, only a few have been tested *in vivo*, as summarized in Table 1.2.

Table 1.2: *In vivo* evaluation of microparticles for colon drug delivery.

Colon-specific polymer	Preparation method	Drug type	<i>In vivo</i> method	Ref.
Chitosan and alginate	Spray drying	Anti-inflammatory (budesonide)	Reduction of inflammation in colitis-induced rats	[217]
Chitosan and polyethylene glycol	Emulsion crosslinking solvent evaporation	Anticancer (5-fluorouracil)	Distribution in mice gut (X-ray)	[211]
Chitosan	Spray drying	Antibiotic (levofloxacin)	Pharmacokinetics and distribution in rat gut	[214]
N-Succinyl-chitosan	Spray drying and freeze drying	Anti-inflammatory (5-ASA)	Reduction of inflammation in colitis-induced rats	[216]
Chitosan and Eudragit® S100	Emulsion/ solvent evaporation	Anti-inflammatory (5-ASA)	Reduction of inflammation in colitis-induced rats	[218]
Eudragit® S100	Double emulsion/ solvent evaporation	Peptide (insulin)	Hypoglycemic effect in rabbits	[219]
Eudragit® S100	Oil-in-oil emulsion/ solvent evaporation	Fluorescent marker	Pharmacokinetics in colitis-induced rats	[220]
Eudragit® S100	Spray freeze-drying	Fluorescent marker	Pharmacokinetics and distribution in rat gut	[210]
Eudragit® P-4135F	Double emulsion/ solvent evaporation	Anti-inflammatory (calcitonin)	Pharmacokinetics in rats	[221]
Eudragit® S, L, L55	Oil-in-oil emulsion/ solvent evaporation	Anti-inflammatory (prednisolone)	Pharmacokinetics in rats	[222]
Eudragit® S100 and dextran	Emulsion crosslinking	Anticancer (5-fluorouracil)	Pharmacokinetics and distribution in rat gut	[213]
Assam Bora rice starch	Double emulsion/ solvent evaporation	Antibiotic (metronidazole)	Distribution in rat gut	[215]
Guar gum	Emulsion crosslinking	Anti-inflammatory (budesonide)	Pharmacokinetics and distribution in rat gut	[212]

Pharmacokinetic investigations have often been used for determining the delay of drug release in comparison to control particles. However, for estimation of the colon-delivery potential, pharmacokinetic data have to be compared with gastrointestinal transit time. This was done by measuring the particle distribution in the gut at various time points using different techniques, e.g. fluorescence labeling [205,208,210,211], X-ray analysis [207], or drug quantification by HPLC [212–215]. Most of these multiparticulate colon drug delivery systems based on nanoparticles or microparticles have shown a potential benefit in the animal models. However, so far no clinical trials have been performed in humans to support this view.

Mucoadhesive functionalization of multiparticulate colon drug delivery systems can increase the colonic transit time, and hence, they can improve the therapeutic efficiency. Varum *et al.* [61] have developed mucoadhesive pellets coated with an Eudragit® S double layer system (inner layer pH 8, outer layer unbuffered) to accelerate complete disintegration of the coating

once the pH trigger is reached. Bautzova *et al.* [191] have developed chitosan pellets by extrusion-spheronization, which were subsequently coated with Eudragit® FS 30D. These mucoadhesive pellets showed a significantly better pharmacological effect in the colitis-induced animal model compared to non-mucoadhesive pellets. Mucoadhesive microparticles for colon delivery have also been developed and investigated *in vivo* [215,216]. This literature research about multiparticulate colon drug delivery system has shown that most preparation methods to obtain nano- or microparticles were based on emulsification or ionic-gelation techniques. However, mucoadhesive formulations based on porous nano- or microcarriers were not reported yet.

1.3.5 Porous microcarriers for the development of mucoadhesive microparticles

In general, processing of microcarriers is easier compared to nanocarriers due to the improved flowability of larger particles and the possibility of using standardized processes suitable for scale-up. Pellets in the millimeter range would have even better flowability, but microcarriers are expected to show better mucoadhesive performance due to the increased surface area available for mucoadhesive bonds compared to large tablets or pellets [47,55,69,223]. The increased colonic transit time for smaller particles also favors the use of microcarriers.

The extrusion/spheronization method was often used for preparation of mucoadhesive multiparticulates probably due to the simple preparation method. However, this method is only suited for pellets in the millimeter range. For preparation of mucoadhesive microparticles, drug-loading or drug-layering of microcarriers has the advantage that an established and easy scalable process can be used (such as the fluidized bed process) compared to the emulsification or ionic-gelation methods which are difficult to transfer to industrial scale. Drug loading of porous microparticles might be advantageous in comparison to drug layering of non-porous microparticles since the drug is deposited in the carrier skeleton better stabilizing the mucoadhesive coating during drug dissolution and drug diffusion through the swollen mucoadhesive outer coating.

There are a few candidates of commercially available porous microparticles which could be used as drug carrier for the intended mucoadhesive multiparticulate formulation. However, the particle size is a critical parameter and not all microparticles meet the desired requirements. On the one hand, the microparticles should be as small as possible to have optimal mucoadhesion properties related to the large specific surface area, but on the other hand, the increasing cohesive forces of smaller particles can cause manufacturing issues related to poor powder flowability. The flow properties might be critical for pharmaceutical excipients with median particle diameters <30 µm, as for example observed for microcrystalline cellulose (MCC, Avicel PH 105) and hydroxypropyl cellulose (HPC) with median particle sizes of 20 and 29 µm, respectively [224].

The granulated fumed silica AEROPERL[®] 300 was considered as a potential candidate due to the high porosity, the small particle size (30 μm), and its good flowability properties. However, the small pore size of 30-40 nm [225,226] might be disadvantageous when high drug loads are desired. Neusilin US2 is granulated magnesium aluminometasilicate with small particle size (mean 60-120 μm) and high porosity, but the mean pore size of 5 nm is even smaller than for AEROPERL[®].

FCC (Omyapharm) is a novel pharmaceutical excipient with unique properties, such as small particle size (5-15 μm), high porosity (>70%, v/v), and biodegradability [227–231], and due to its large pore size diameter in the outer stratum (~1 μm), which is promising for high drug loads, it has a relevant advantage compared to alternative microcarriers mentioned before.

Instead of coating individual particles with colon-targeting polymers, the mucoadhesive microparticles were filled into capsules which could be coated with a colonic-targeted coating layer. The feasibility of coating hard-shell HPMC capsules in a pan coater with a colon-specific polymer was already demonstrated [232], and hard gelatin capsules are also feasible for application of enteric coatings [233]. However, hydration and swelling of mucoadhesive polymers inside capsule vehicles has been observed in an *in vivo* study in beagle dogs by McGirr et al. [234] resulting in an incomplete release of the polymer from the capsules. Therefore, dispersibility enhancement was an additional research focus to avoid agglomeration of mucoadhesive microparticles prior to release from the capsule.

2 Aims

Drug delivery of mucoadhesive microparticles to the colon has great potential for local treatment of colonic diseases due to prolonged transit time and improved therapeutic efficacy. However, the large intestine presents a challenging environment, and so far, no *in vivo* data on the usefulness of oral mucoadhesive formulations in the human colon are available, despite extensive preclinical data. The aim of this project was to develop a mucoadhesive and multiparticulate formulation platform for colonic delivery. The formulation concept illustrated in Fig. 2.1 consists of a colonic-targeted capsule filled with the mucoadhesive microparticles. The focus of the work presented here was on the development of the mucoadhesive microparticles, i.e. on the drug loading of porous microcarriers and subsequent coating with a mucoadhesive polymer. The development of the enteric coating of the capsule for colonic targeting is not part of this thesis, as it was carried out by our collaboration partner Tillotts Pharma, based on their patented technology and internal know-how. To achieve a formulation prototype feasible for a Phase 1 study, following three aims were defined and pursued.

I) Evaluation of a suitable porous microcarrier with small mean particle size (10-100 μm) and high loading capacity. The drug loading method should be applicable to metronidazole and ideally to various other drug substances.

II) Development of a coating method to functionalize the drug-loaded microparticles with a mucoadhesive polymer. For optimization of the mucoadhesive microparticles, the development of a particle retention assay was envisaged, including the design of a flow-channel device and the development of a sensitive and reliable particle-quantification method.

III) Method optimization towards a scalable and industrially applicable method for preparation of mucoadhesive microparticles to manufacture of clinical batches for a Phase-1 study.

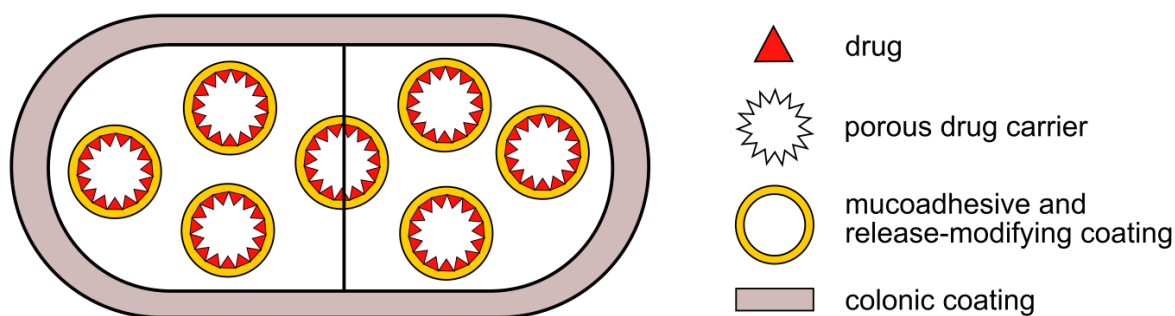


Fig. 2.1: Proposed formulation concept of the mucoadhesive and multiparticulate colon drug delivery system.

3 Peer-reviewed publications

3.1 Drug loading into porous microcarriers

Drug loading into porous calcium carbonate by solvent evaporation

Daniel Preisig¹, David Haid¹, Felipe J. O. Varum², Roberto Bravo², Rainer Alles¹, Jörg Huwyler¹, Maxim Puchkov¹

¹ Department of Pharmaceutical Sciences, University of Basel, Klingelbergstrasse 50, 4056 Basel, Switzerland

² Tillotts Pharma AG, Baslerstrasse 15, 4310 Rheinfelden, Switzerland

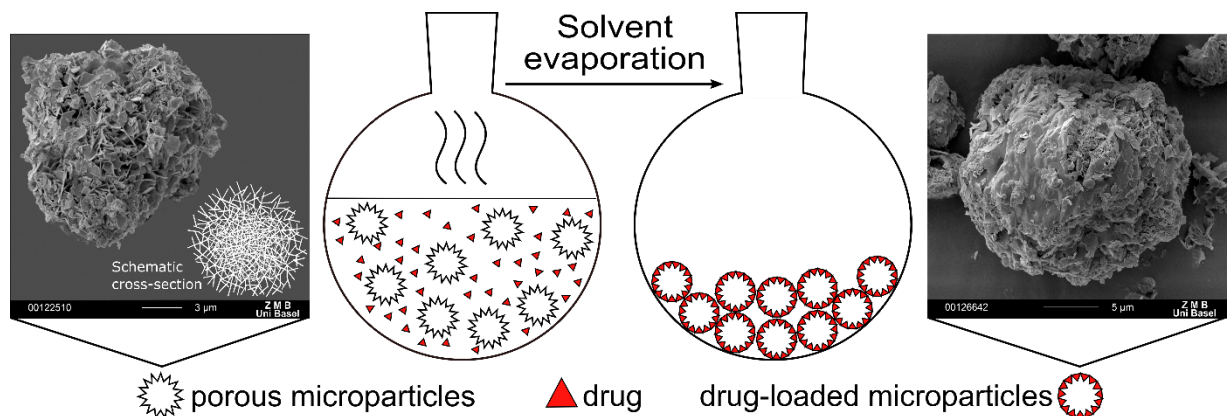


Fig. 3.1: Graphical abstract of the publication.



Research paper

Drug loading into porous calcium carbonate microparticles by solvent evaporation



Daniel Preisig^a, David Haid^a, Felipe J.O. Varum^b, Roberto Bravo^b, Rainer Alles^a, Jörg Huwlyer^{a,*}, Maxim Puchkov^a

^a Department of Pharmaceutical Sciences, University of Basel, Basel, Switzerland

^b Tillotts Pharma AG, Rheinfelden, Switzerland

ARTICLE INFO

Article history:

Received 31 October 2013

Accepted in revised form 3 February 2014

Available online 22 February 2014

Keywords:

Drug loading

Solvent evaporation

Microparticles

Calcium carbonate

Poorly water-soluble drugs

Drug release

ABSTRACT

Drug loading into porous carriers may improve drug release of poorly water-soluble drugs. However, the widely used impregnation method based on adsorption lacks reproducibility and efficiency for certain compounds. The aim of this study was to evaluate a drug-loading method based on solvent evaporation and crystallization, and to investigate the underlying drug-loading mechanisms. Functionalized calcium carbonate (FCC) microparticles and four drugs with different solubility and permeability properties were selected as model substances to investigate drug loading. Ibuprofen, nifedipine, losartan potassium, and metronidazole benzoate were dissolved in acetone or methanol. After dispersion of FCC, the solvent was removed under reduced pressure. For each model drug, a series of drug loads were produced ranging from 25% to 50% (w/w) in steps of 5% (w/w). Loading efficiency was qualitatively analyzed by scanning electron microscopy (SEM) using the presence of agglomerates and drug crystals as indicators of poor loading efficiency. The particles were further characterized by mercury porosimetry, specific surface area measurements, differential scanning calorimetry, and USP 2 dissolution. Drug concentration was determined by HPLC. FCC–drug mixtures containing equivalent drug fractions but without specific loading strategy served as reference samples. SEM analysis revealed high efficiency of pore filling up to a drug load of 40% (w/w). Above this, agglomerates and separate crystals were significantly increased, indicating that the maximum capacity of drug loading was reached. Intraparticle porosity and specific surface area were decreased after drug loading because of pore filling and crystallization on the pore surface. HPLC quantification of drugs taken up by FCC showed only minor drug loss. Dissolution rate of FCC loaded with metronidazole benzoate and nifedipine was faster than the corresponding FCC–drug mixtures, mainly due to surface enlargement, because only small fractions of amorphous drug (12.5%, w/w, and 8.9%, w/w, respectively) were found by thermal analysis. Combination of qualitative SEM analysis and HPLC quantification was sufficient to prove the feasibility of the solvent-evaporation method for the loading of various drugs into FCC. Mechanistic investigation revealed that a high specific surface area of the carrier is required to facilitate heterogeneous nucleation, and large pore sizes (up to 1 μm) are beneficial to reduce crystallization pressures and allow drug deposition within the pores. The solvent-evaporation method allows precise drug loading and appears to be suitable for scale-up.

© 2014 Elsevier B.V. All rights reserved.

1. Introduction

In recent years, porous drug carriers emerged as a promising material, not only to deliver the drug to a specific site of action,

Abbreviations: BCS, biopharmaceutics classification system; DL, drug load; DSC, differential scanning calorimetry; FCC, functionalized calcium carbonate; IBU, ibuprofen; LK, losartan potassium; MBZ, metronidazole benzoate; NP, nifedipine; RSD, relative standard deviation; SEM, scanning electron microscopy; SSA, specific surface area.

* Corresponding author. Department of Pharmaceutical Sciences, University of Basel, Klingelbergstrasse 50, 4056 Basel, Switzerland. Tel.: +41 (0)61 267 15 13.

E-mail address: joerg.huwlyer@unibas.ch (J. Huwlyer).

<http://dx.doi.org/10.1016/j.ejpb.2014.02.009>

0939-6411/© 2014 Elsevier B.V. All rights reserved.

but also to control or improve drug release [1]. A typical example is mesoporous silica nanoparticles with tunable particle and pore size [2]. These particles are suggested to be useful to improve oral bioavailability of poorly water-soluble drugs [3]. After adsorption to the pores, the drug remains entrapped in an amorphous state possessing much higher internal energy relative to the crystalline form and leading to enhanced in vitro dissolution rate [4,5]. Diffusion-controlled, sustained-release kinetics were also described due to the extensive porous network and thus long diffusion pathways [2]. However, the synthesis of silica nanoparticles is a complex process. This makes it a rather expensive material, and toxicity studies

with this engineered nanomaterial have not yet eliminated all health concerns [6,7]. For the development of a carrier-based formulation to control drug release and to target specific sites in the gastrointestinal tract where no systemic absorption of the particles is desired, microparticles are preferred to nanoparticles, since cellular uptake is significantly lower [8] making them toxicologically less problematic [6,9].

The main requirements concerning material properties of the carrier particles are sufficient mechanical strength, biocompatibility, and biodegradability. The number of materials for the design of porous drug delivery systems is therefore limited. Pharmaceutically exploited materials as an alternative to silicon dioxide include magnesium aluminometasilicate [10], aluminosilicate [11], calcium silicate [12], calcium carbonate [13], calcium phosphate [14], titanium dioxide [15], zirconium dioxide [16], and other ceramics [17,18]. However, in contrast to porous silicon dioxide, drug loading of these materials remains a challenge because little is known about drug-loading mechanisms. We decided to use porous calcium carbonate microparticles as a model material to study mechanisms of drug loading since this substance has several properties qualifying it for oral drug delivery.

Calcium carbonate is widely used as food additive, and concerns about biocompatibility in the gastrointestinal tract can therefore be excluded. Furthermore, toxicological tests in HeLa cells proved biocompatibility of porous calcium carbonate particles in the micrometer [19] and nanometer range [20]. Chemical decomposition of calcium carbonate is fast under acidic conditions in the stomach by liberation of carbon dioxide. In the case of enteric-coated capsule or tablet formulations, chemical decomposition of calcium carbonate microparticles might play a minor role due to the relatively high pH in the small and large intestine, thus most

of the material will be eliminated by excretion. However, despite the favorable properties of calcium carbonate, the available literature dealing with drug loading into porous calcium carbonate microparticles is sparse, and low drug-loading capacity limits the use of such particles [13,21]. Therefore, alternative calcium carbonate particles with larger pore volume providing higher loading capacity are desired. Functionalized calcium carbonate (FCC) was recently introduced as a novel pharmaceutical excipient [22]. Because of its high porosity, we chose FCC as the model carrier particle to investigate drug loading.

Due to small pore size and enlarged surface area, FCC is able to absorb 10 times more fluid with faster absorption rate than conventional calcium carbonate [23]. So far, 4 types of FCC (S01, S02, S03, and S04) are available, differing in particle size, pore size, pore structure, and specific surface area. FCC S01 was chosen for our study because it has the largest average particle size (17.9 μm) and highest porosity (70%), theoretically providing high loading capacity. Pores of the outer surface are characterized by interconnected “rose-like” petals that are larger than the pores of the inner core (Fig. 1 A and B). This wide range of pore sizes (0.01–1 μm), combining macroporous and mesoporous characteristics, makes FCC S01 a suitable material to investigate pore-size dependent drug deposition.

Drug loading can theoretically be done during synthesis of the carrier material, but practically it is more convenient to use prefabricated carrier particles. This allows to use organic solvents and to load poorly water-soluble drugs. The most common method is based on adsorption of the drug to the carrier particles by impregnation of the particles in a drug solution [11,15,16,24–28]. To reach the equilibrium between adsorbed and solubilized drug, constant stirring or shaking was applied for an extended period of time (12–72 h). Alternatively, this endpoint can be determined

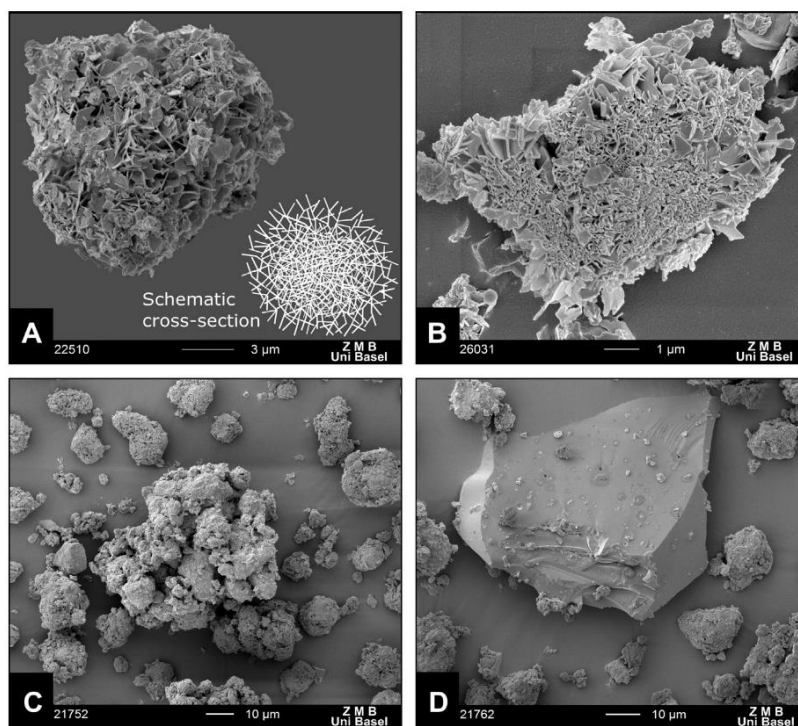


Fig. 1. SEM images of (A) bulk FCC including schematic representation of cross-sectional FCC structure, (B) cross-section of broken FCC, (C) typical agglomerate of drug-loaded FCC (MBZ 40% DL), and (D) an example of a separate drug crystal (MBZ 50% DL).

by adsorption isotherms [29]. However, it is challenging to develop an impregnation method with sufficient payload. A solvent dissolving sufficient amounts of drug is needed to obtain satisfactory drug loads, but strong solute–solvent interactions lead to reduced adsorption to the carrier. Hence, the resulting drug load (DL) can vary considerably, constituting a major challenge when developing a reproducible impregnation method.

An alternative to drug loading by impregnation is the solvent- evaporation method which can be performed under reduced pressure. Continuous removal of the solvent until complete dryness allows to determine DL directly by adding the masses of drug and carrier material. Otsuka et al. [30] made use of this approach by loading phytanadione into porous silica, which resulted in a distinct mode of drug release that was rapid (1 h) initially but continued slowly over 24 h. Sher et al. [31] loaded ibuprofen into macroporous polypropylene microparticles by evaporating methanol or dichloromethane under ambient conditions and investigated the influence of solvent volume on the adsorption mechanism. To our knowledge, these are the only publications investigating the solvent- evaporation method for drug loading into prefabricated porous materials. In fact, the feasibility of the solvent- evaporation method for drug loading has been questioned since it is considered to deposit the drug as a crystalline layer whose properties and composition cannot be reproducibly controlled [32]. However, we believe that a better understanding of the processes is needed before the solvent- evaporation method can be declared as unsuitable for drug loading of porous carriers.

For in- depth investigation of drug loading by solvent evaporation, four model drugs representing three classes (BCS II–IV) of the biopharmaceutics classification system (BCS) were selected, with a special focus placed on poorly water- soluble drugs. Ibuprofen (IBU) [33] and nifedipine (NP) [34] have good permeability and poor water solubility and were selected as BCS II substances. The potassium salt of losartan (LK) is freely soluble in water but shows low bioavailability [35] and is therefore a BCS III compound. Metronidazole benzoate (MBZ; prodrug of metronidazole) is a BCS IV substance since it is poorly water soluble and is not absorbed in the intestine [36].

The aim of the present study was to investigate the mechanism of drug loading by solvent evaporation. This included determination of the site of drug deposition (inside or outside the pores), analysis of crystallinity, and comparison of theoretical and experimental drug- loading capacities. Moreover, we studied the dissolution kinetics to evaluate the suitability of FCC as an oral drug delivery system.

2. Materials and methods

2.1. Materials

Functionalized calcium carbonate (FCC S01) was kindly provided by Omya, Switzerland. Metronidazole benzoate was donated by Farchemia, Italia. IBU was received from Glatt GmbH, Germany. NP was obtained from Siegfried AG, Switzerland. LK was purchased from Hetero Drugs, India. Ammonium formate, formic acid (98%), NP, and methanol (all HPLC- grade) were obtained from Sigma- Aldrich, Switzerland. Acetonitrile (HPLC- grade) was purchased from VWR, Belgium. Acetone, sodium dihydrogenphosphate dihydrate ($\text{NaH}_2\text{PO}_4 \cdot 2\text{H}_2\text{O}$), sodium hydroxide pellets, and sodium lauryl sulfate (SLS) were purchased from Hanseler AG, Switzerland.

2.2. Drug loading by solvent evaporation

FCC was loaded with MBZ, IBU, LK, and NP at different drug to drug- carrier ratios. This ratio is called drug load (DL) and is defined

as the mass fraction of the active pharmaceutical ingredient (API) as described in Eq. (1). DL can also be expressed as percentage (w/w) [37].

$$\text{DL} = m_{\text{API}} / (m_{\text{API}} + m_{\text{SK}}) \quad (1)$$

where m_{API} is the mass of the API, and m_{SK} is the mass of the skeleton of the porous carrier.

The series of different drug loads included 25%, 30%, 35%, 40%, 45%, and 50% (w/w). The weighted drug was placed in a round- bottom flask and dissolved in the organic solvent (50 ml). Acetone was used for IBU, MBZ, and NP, and methanol was used for LK. The amount of FCC particles (5.0 g) was kept constant for all drug- loading experiments. The suspension was sonicated in a water bath (Retsch, Switzerland) for 5 min to disperse agglomerates and degas the solvent. The solvent was evaporated in a rotary evaporator (Büchi RE 121 or R-114) with a water bath set to 40 °C (Büchi 461 or B-480). Pressure was gradually decreased by 100 mbar per 0.5 h to 20 mbar, and held for 1 h at final pressure. Initial pressure setting was 300 mbar for methanol and 480 mbar for acetone, requiring a total runtime of 2.5 h and 3.5 h, respectively. After removal of the residual solid from the round- bottom flask, the product was gently milled with mortar and pestle, and subsequently sieved through 250 µm and 90 µm mesh screens (Retsch, Switzerland). Drug- loaded FCC was vacuum- dried for 24 h at room temperature (KVTS 11, Salvis AG, Switzerland) under constant nitrogen injection.

2.3. Particle characterization

2.3.1. Drug quantification by HPLC- UV

Drug quantification was performed by isocratic HPLC- UV methods which had been validated for precision, accuracy, range, and linearity in accordance with the quality guidelines of the International Conference on Harmonization (ICH; Q2R1 1994). Drug- loaded FCC (50 mg) was placed in a 10 ml volumetric flask, suspended in 8 ml methanol, and sonicated for 5 min in a water bath. After cooling down to room temperature, methanol was added to a final volume of 10 ml. FCC suspensions were centrifuged for 2 min at 14,000 rpm (Centrifuge 5415C, Eppendorf, Germany). The supernatant was diluted 1:10 with methanol; subsequently 1:10 dilutions were prepared with water- methanol mixtures (90:10 v/v for IBU, LK, and MBZ, and 50:50 v/v for NP). The resulting drug concentrations of the 1:100 dilutions were all within the validated range of the HPLC- UV methods. Samples were filtered (0.45 µm PTFE syringe filters, VWR, USA), and drug concentrations were determined with an HPLC- UV system (Agilent 1100, USA). The area under the curve (AUC) of HPLC- UV chromatograms was converted into drug concentrations according to calibration standards. The experimental drug load (DL_e) was calculated by applying Eq. (1). Samples of IBU- and LK- loaded FCC were prepared in triplicates for each DL level, and each sample was measured in triplicates; thus, the total number of measurements was $n = 9$. Samples of MBZ- and NP- loaded FCC were prepared in duplicates for each DL level, and each sample was measured in triplicates, thus, the total number of measurements was $n = 6$.

A Nucleosil C18 column with 120 mm length, 3 mm inner diameter, and 5 µm particle size (Marchery- Nagel, Switzerland) was used for the separation of IBU, MBZ, and NP, whereas a ProntoSIL C8 column with 125 mm length, 2 mm inner diameter, and 5 µm particle size (Bischoff Chromatography, Germany) was used for the analysis of LK. Mobile phases consisted of ammonium formate (10 mM) and acetonitrile at a volumetric ratio of 50:50. The formate buffer for IBU and LK quantification was adjusted with formic acid to pH 3.5, whereas NP and MBZ were analyzed with buffers of pH 4.0 and 4.5, respectively. Flow rate was 500 µl/min in all cases.

UV-detection of IBU, LK, MBZ, and NP was done at 223, 225, 320, and 235 nm, respectively.

2.3.2. Scanning electron microscopy (SEM)

The outer surface of FCC samples was analyzed with a scanning electron microscope (Nova NanoSEM 230, FEI Company, USA). Samples were sputtered with a 20 nm gold layer by a sputter coating machine (MED 020, BalTec, Liechtenstein).

Clogging and smoothening of the outer pore surface of FCC were indicators of pore filling and provided qualitative evidence for successful drug loading. Another important criterion for evaluating a drug-loading method is loading efficiency, i.e. the extent of drug deposited within the particles. However, direct quantification of drug deposited within the pores is not possible by SEM or any other method. Therefore, SEM image analysis was used for qualitative estimation of drug-loading efficiency by applying a classification system, namely “excellent”, “good”, and “poor”. Loading efficiency was rated as “poor” if numerous agglomerates and separate drug crystals were detected (Fig. 1C and D, respectively). Loading efficiency was rated as “good” if only a few agglomerates and separate drug crystals were detected. If none of these two types of undesired particles were found, complete drug loading into porous microparticles was assumed [38], and loading efficiency was rated as “excellent”.

It is assumed that drug loading becomes less efficient when DL is above the loading capacity of FCC. Based on this assumption, drug loading capacity was defined as the maximum possible DL where loading efficiency is still rated as “good”. Experimentally, loading capacity was determined as the DL (w/w) at which further loading resulted in a significantly higher number of agglomerates and separate drug crystals, i.e. “poor” loading efficiency. Successful qualitative estimation requires SEM images of each DL containing large numbers of particles. Therefore, the images were obtained at the lowest magnification, yet ensuring detection of agglomerates and separate drug crystals.

2.3.3. Particle density

True density (ρ_s , density of the solid only) was determined by helium pycnometry (AccuPyc 1330, Micromeritics GmbH, Germany). Bulk density (ρ_b) of non-loaded FCC was determined by manual densification into a container of known volume and subsequent determination of the sample weight. Bulk density was determined in triplicates.

2.3.4. Mercury porosimetry

Samples of FCC loaded with IBU (40%, w/w), LK (40%, w/w), MBZ (40%, w/w), and NP (35%, w/w), and bulk FCC were characterized by mercury porosimetry for pore-size distribution using a Micromeritics Autopore IV mercury porosimeter. The maximum pressure of mercury applied was 414 MPa, equivalent to a Laplace diameter of $4 \times 10^{-3} \mu\text{m}$. The data were corrected using Pore-Comp (software program of the Environmental and Fluid Modelling Group, University of Plymouth, UK) for mercury and penetrometer effects and also for sample compression [39]. Intraparticle porosity (ϕ_{intra}) was calculated based on Eq. (2).

$$\phi_{intra} = v_{intra} / v_p \quad (2)$$

where v_{intra} is the specific volume of intraparticle voids (ml/g), and v_p is the specific volume of the particle considered as closed (ml/g). The specific volume of particles (v_p) can also be expressed as $v_p = v_{intra} + v_s$, where v_{intra} and v_s are the specific volumes of intraparticle voids and the solid, respectively. Since the specific volume of the solid (v_s , ml/g) is equal to the reciprocal value of the true density of the solid (ρ_s , g/ml), intraparticle porosity was calculated based on the specific intraparticle pore volume (v_{intra}) measured by

mercury porosimetry, and the true density of the solid (ρ_s) measured by helium pycnometry.

$$\phi_{intra} = \frac{v_{intra}}{v_{intra} - \frac{1}{\rho_s}} \quad (3)$$

The validity range of Eq. (3) is excluding pore sizes from 4 nm down to 0.26 nm, because v_{intra} of pores smaller than 4 nm cannot be measured by mercury intrusion, but true density measured by helium pycnometry takes into account pore sizes down to 0.26 nm (kinetic diameter of helium) [40]. Specific surface area (SSA)

SSA was determined with a NOVA 2000e (Quantachrome Instruments, USA) using the 5-point BET method with P/P_0 ranging from 0.1 to 0.3. After degassing for 12 h, samples of drug-loaded FCC and FCC–drug mixtures (with equivalent drug fraction) were measured with nitrogen at constant temperature (77.4 K).

2.3.5. Differential scanning calorimetry (DSC)

Thermal analysis was performed with a DSC 400 (PerkinElmer, USA). Melting enthalpy was measured ($n = 3$) for drug-loaded FCC (ΔH_{load}) and FCC–drug mixtures (ΔH_{mix}). The amorphous content (X_a) in drug-loaded FCC was calculated with Eq. (4) according to Vittez [41] and Shah et al. [42].

$$X_a(\%) = 100 - X_c(\%) = 100 - \frac{\Delta H_{load}}{\Delta H_{mix}} * 100 \quad (4)$$

where X_c is the crystallinity of the drug (mass fraction of crystalline drug). Reference samples contained the same fraction of drug as drug-loaded FCC, but as a mixture of FCC and 100% crystalline standard. After a pre-run to remove traces of water (heating to 120 °C), a temperature scan from –20 °C up to 300 °C was performed in steps of 20 °C/min.

2.3.6. Dissolution USP 2

Drug release of IBU, LK, MBZ, and NP was studied with a USP 2 dissolution apparatus (SOTAX, Switzerland) using samples of drug-loaded FCC for which loading capacity was reached. The sample weights for IBU-loaded (40%, w/w), LK-loaded (40%, w/w), MBZ-loaded (40%, w/w), and NP-loaded (35%, w/w) FCC were 75, 50, 125, and 57 mg, respectively. Physical mixtures of drug and FCC with identical sample weights and drug contents served as reference samples. The samples were measured triplicates, and sink conditions were provided in all experiments. Sodium phosphate dissolution buffer (pH 6.8, 0.05 M) was produced according to the standards of the International Pharmacopoeia. Sodium lauryl sulfate (SLS) was used for IBU (1% SLS, w/v), MBZ (0.01% SLS, w/v) to reduce surface tension of the dissolution medium and to avoid floating of the powder samples. For dissolution experiments of NP the addition of 1% SLS (w/v) was necessary to maintain sink conditions and to enable dissolution since the solubility of NP is only 6 mg/l at 37 °C (Table 1). Paddle speed was 100 rpm, and the temperature of the water bath was set to 37 °C. The dissolution medium was continuously transferred to the UV-spectrophotometer (Amersham Bioscience, Ultrospec 3100 pro) and returned to the dissolution vessels with a peristaltic pump (IPC, Ismatec, Switzerland). Glass-microfiber filters (693, VWR, France) with a particle retention of 1.2 μm were inserted in the filter head of the Hollow Shaft™ sampling system (Sotax, Switzerland). Absorbance was measured every minute at the wavelengths described for the HPLC–UV methods. Path length of the cells was adjusted (0.2 or 1.0 cm) to obtain absorbances in the linear and valid range of the calibration standard.

Table 1
Model drugs and solvents used for drug loading with corresponding solubilities in solvent and water (mg/ml).

Model drug	Solvent	Solubility in solvent (mg/ml)	Solubility in water (mg/ml)
Ibuprofen (IBU)	Acetone	607 (25 °C) [54]	0.041 (25 °C) [55]
Losartan potassium (LK)	Methanol	>1000 (25 °C) ^a	>100 (25 °C) ^a
Metronidazole benzoate (MBZ)	Acetone	256 (25 °C) [56]	0.122 (25 °C) [56]
Nifedipine (NP)	Acetone	250 (20 °C) [57]	0.0056 (37 °C, pH 7) [57]

^a Experimental values.

3. Results

3.1. Quantification of drug load by HPLC-UV

Prior to drug quantification, optimized HPLC-UV methods were validated for range, linearity, precision, and accuracy. Linearity of all calibration standards fulfilled our requirement ($R^2 > 0.999$). Precision (intra-assay) was evaluated by relative standard deviation (%RSD, $n = 3$) and was always below 3% RSD. Accuracy (intra-assay) assessed by separately prepared samples was within 97% and 103%.

HPLC values of experimental drug load (DL_e in w/w%) for particles loaded with LK, MBZ, and NP were close to the theoretical drug load (DL_t). IBU-loaded FCC showed a decrease in drug content DL_e (Table 2) which could be due to drug degradation during the loading process. However, drug degradation was low or negligible for the other three model drugs.

3.2. SEM analysis

In general, SEM image analysis revealed individual and intact particles after drug loading. This implies that milling and sieving did not destroy the porous structure of FCC. At a DL of 25% (w/w), loading efficiency was "excellent" for all drugs, since no agglomerates and separate drug crystals were seen. Fig. 2 shows overview images of MBZ-loaded FCC with DLs of 30% (E), 40% (F), 45% (G), and 50% (H). A DL of 30% and 40% (w/w) caused the formation of only a few agglomerates (depicted by white arrows) indicating "good" loading efficiency. However, the significant increase in agglomerates at a DL of 45% compared to 40% indicates decreased loading efficiency. At 50% DL, much more agglomerates and two separate drug crystals were found (Fig. 2H; dashed arrows). Fig. 1D shows the magnification of the upper crystal. According to the definitions in the method section, drug-loading capacity was thus 40% (w/w) for MBZ. The same method was applied for the other drugs, revealing drug loading capacities of 40% (w/w) for IBU and LK, and 35% (w/w) for NP. Fig. 2E–H shows typical particles of the model drugs at full loading capacity. It should be noted that the upper edges of the typical FCC petals stretch out of the surface, indicating that the pores were filled with the drug rather than just coated.

3.3. Particle density

Non-loaded FCC had a true density of 2.71 ± 0.04 g/ml ($n = 3$) and a bulk density of 0.45 ± 0.01 g/ml ($n = 3$). True densities of

drug-loaded FCC with DLs at maximum loading capacity were 1.71 g/ml (IBU 40%, w/w), 1.88 g/ml (LK 40%, w/w), 1.95 g/ml (MBZ 40%, w/w), and 2.01 g/ml (NP 35%, w/w). True densities of pure compounds amounted to 1.10 g/ml (IBU), 1.36 g/ml (LK), 1.39 g/ml (MBZ), and 1.37 g/ml (NP).

3.4. Mercury porosimetry

By taking the first derivative of the cumulative intrusion curve, pore-size distributions based on equivalent Laplace diameter [43] are shown (Fig. 3A). Because differential curves above 10 μm associated with the coarse packing of the powder are not reproducible, they were excluded.

The measured powder samples showed bimodal pore-size distribution with the main peaks at 4.3 μm , representing the interparticle pore diameters, and a broad pore-size distribution between 4×10^{-3} and 1 μm , representing the intraparticle voids. Discrimination between inter- and intraparticle pores can be done by determining the minimum in the differential curve [39], which was at 1 μm for bulk FCC. However, drug-loaded FCC samples showed no clear minimum. Therefore, a pore size of 1 μm was used to distinguish between inter- and intraparticle pores for all samples. Intraparticle porosity was calculated based on true densities of drug-loaded FCC measured by helium pycnometry (Eq. (3)). Fig. 3B shows a decrease in intraparticle porosity of bulk FCC from 69.2% (v/v) to 43.9% (MBZ), 40.1% (IBU), 34.6% (NP), and 24.0% (LK), reflecting drug deposition in particle pores.

3.5. Specific surface area (SSA)

SSA of FCC S01 was determined to be 35.43 m^2/g . Gas adsorption analysis of drug-loaded FCC and FCC-drug mixtures used as a reference showed that SSA generally decreased with higher DL (Fig. 4). This effect was mainly due to the contribution of drugs as they exhibit much lower SSAs than FCC (i.e. 0.42, 0.54, 0.66, and 0.47 m^2/g for MBZ, IBU, LK, and NP, respectively), thus reducing the SSA of drug-containing FCC samples, irrespective of the location of the drug (i.e. inside or outside the pores). The most striking finding from the plots was the consistently lower SSA values for drug-loaded FCC compared to reference samples. This difference was most pronounced for LK, and still significant for MBZ and NP, whereas the SSA values of IBU-loaded FCC were superimposable with the reference samples. Since SEM pictures of LK- and IBU-loaded particles were comparable, it is evident that the SSA

Table 2
Theoretical drug loads (DL_t) resulting from the sum of weights of drug and drug carrier, and experimental drug loads (DL_e) determined by HPLC-UV quantification are shown, where n corresponds to the total number of measurements as described in the methods section.

DL_t (% w/w)	IBU-loaded FCC DL_e (% w/w, $n = 9$)	LK-loaded FCC DL_e (% w/w, $n = 9$)	MBZ-loaded FCC DL_e (% w/w, $n = 6$)	NP-loaded FCC DL_e (% w/w, $n = 6$)
25.00	24.05 \pm 0.26	26.21 \pm 0.22	25.31 \pm 0.12	24.96 \pm 0.74
30.00	28.29 \pm 0.51	30.49 \pm 0.49	28.26 \pm 0.16	29.74 \pm 0.56
35.00	34.13 \pm 0.15	36.69 \pm 0.95	34.99 \pm 0.19	34.90 \pm 0.93
40.00	38.05 \pm 0.50	41.14 \pm 0.27	40.00 \pm 0.63	39.60 \pm 0.41
45.00	43.05 \pm 0.72	44.81 \pm 0.29	44.11 \pm 0.75	44.91 \pm 1.18
50.00	46.15 \pm 0.27	50.58 \pm 0.84	50.05 \pm 0.18	50.87 \pm 0.11

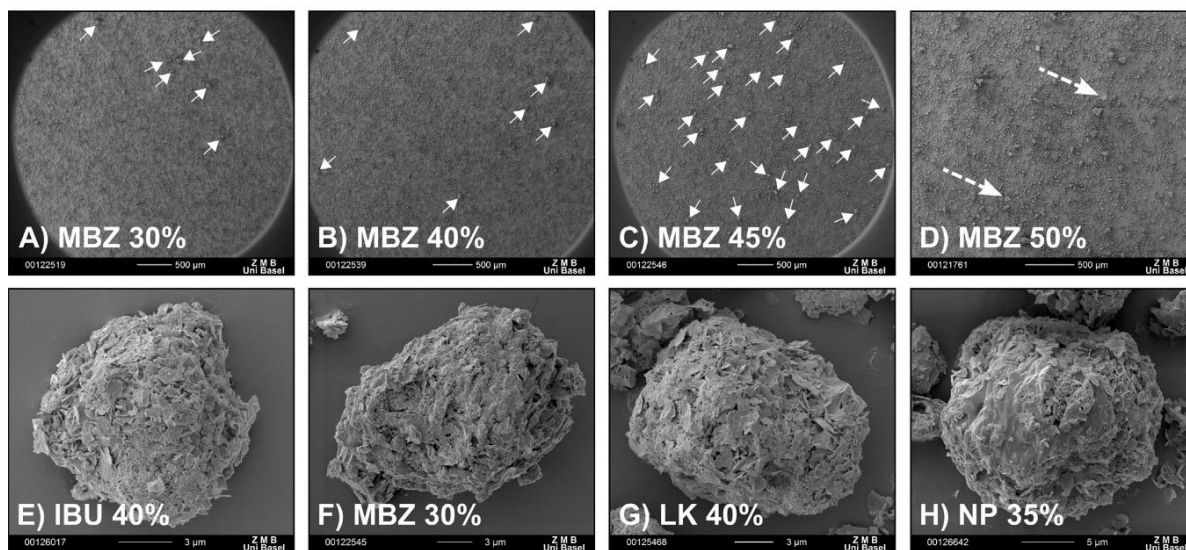


Fig. 2. SEM overview images of MBZ-loaded FCC showing almost no agglomerates (indicated by white arrows) at a DL of 30% (A) and 40% (B). At a DL of 45% (C), a significant increase in agglomerates occurred, and at 50% (D), even separate crystals (dashed arrows) were observed, indicating loading capacity (maximum drug load) at 40% (w/w) for MBZ. SEM images at DLs at maximum loading capacity are shown for MBZ 40% DL (E), IBU 40% DL (F), LK 40% DL (G), and NP 35% DL (H).

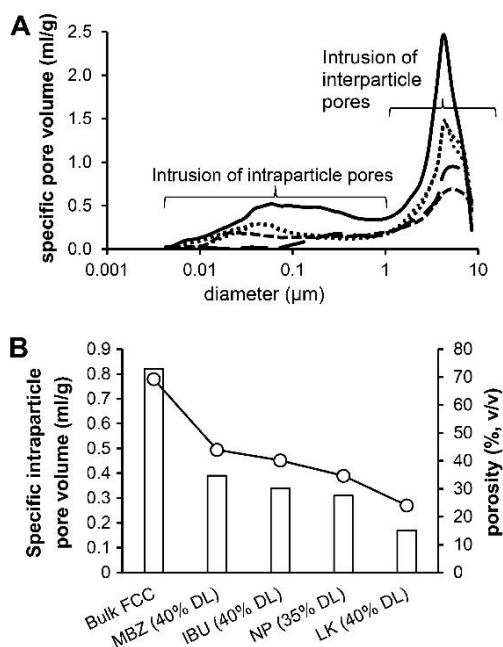


Fig. 3. (A) Representative examples of pore-size distribution of FCC loaded with MBZ (.....) NP (.....), IBU (- - -), and LK (- - -), and of bulk FCC (—) measured by mercury porosimetry. B) Total intruded specific intraparticle pore volume (white bars, ml/g) and intraparticle porosity (-○-%) of drug-loaded FCC and bulk FCC.

reduction after loading of LK was not only a result of pore filling, but rather due to clogging of micropores (<2 nm) presenting the largest fraction of SSA. Completely closed micropores inaccessible for nitrogen gas may only be possible by clogging with amorphous drug.

3.6. DSC analysis

Thermal analysis of drug-loaded FCC showed different heat flow peaks compared to FCC–drug mixtures containing the same amount of drug in 100% crystalline form (Fig. 5). LK-loaded FCC was an exception because no peak occurred, but a glass transition was observed at $130 \pm 5 \text{ }^\circ\text{C}$ (half c_p) suggesting that all loaded LK was converted into an amorphous form. The presence of two heat flow peaks (melting points) of LK-mixed FCC indicated the presence of two LK polymorphs.

Integration of DSC thermograms delivered the melting enthalpies for IBU 40% DL ($\Delta H_{mix} = 39.75 \pm 0.68 \text{ J/g}$, $\Delta H_{load} = 37.10 \pm 0.44 \text{ J/g}$), LK 40% DL ($\Delta H_{mix} = 3.50 \pm 0.02 \text{ J/g}$, $\Delta H_{load} = 0.0 \text{ J/g}$), MBZ 40% DL ($\Delta H_{mix} = 35.32 \pm 2.46 \text{ J/g}$, $\Delta H_{load} = 30.89 \pm 0.12 \text{ J/g}$), and NP 35% DL ($\Delta H_{mix} = 28.30 \pm 0.22 \text{ J/g}$, $\Delta H_{load} = 25.79 \pm 0.11 \text{ J/g}$). The content of amorphous drug was calculated with Eq. (4). Interestingly, small fractions of amorphous drug (χ_a) were found for FCC loaded with IBU (6.7%, w/w), NP (8.9%, w/w), and MBZ (12.5%, w/w).

3.7. Dissolution USP 2

Fig. 6 shows dissolution plots of drug-loaded FCC in comparison with FCC–drug mixtures. Immediate and complete drug release within the first minute was observed for FCC loaded with LK and IBU and corresponding reference formulations. In contrast, FCC loaded with MBZ or NP showed faster drug dissolution in comparison with the drug-mixed FCC. After 3 min, 80% of the drug was released from MBZ-loaded FCC, whereas 80% of the MBZ-mixed formulation was dissolved only after 6 min. FCC loaded with NP released the first 80% of drug 2.5-fold faster than NP-mixed FCC. In summary, drug-loaded FCC provided immediate drug release and showed faster release of NP and MBZ than did the reference samples.

4. Discussion

4.1. Drug loading capacity

To estimate the total available space for loading of a porous material with an API, intraparticle porosity (v/v) should be

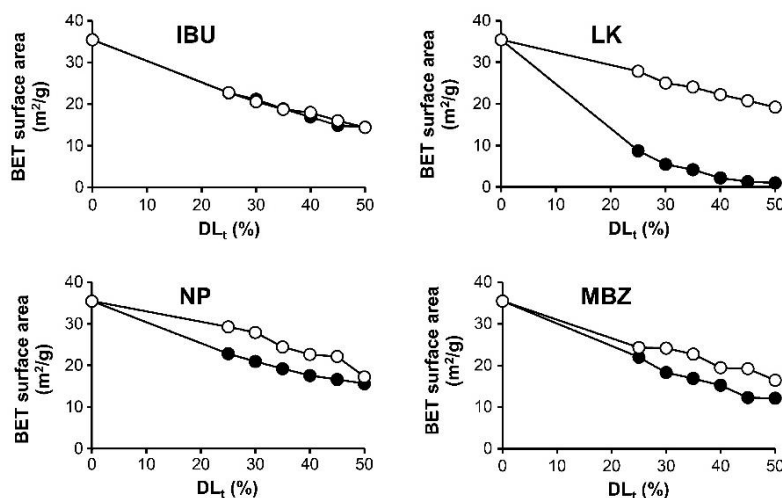


Fig. 4. Specific surface area of drug-loaded FCC (●) and FCC–drug mixtures (○) plotted against theoretical drug loads (DL_t) of IBU, LK, MBZ, and NP.

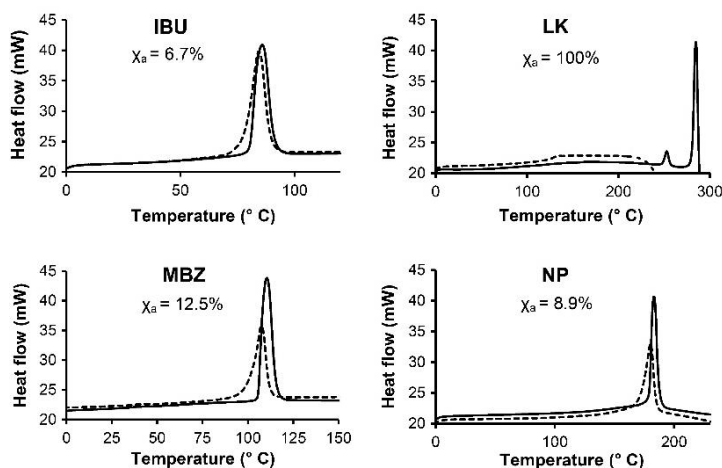


Fig. 5. Representative DSC thermograms of FCC–drug mixtures (—) and drug-loaded FCC (-----) for IBU (40%, w/w), LK (40%, w/w), MBZ (40%, w/w), and NP (35%, w/w). The content of amorphous drug (X_a in%, w/w) is shown for each drug (n = 3).

determined. Mercury porosimetry measurement of bulk FCC revealed a specific intraparticle pore volume of 0.82 ml/g, resulting in an intraparticle porosity of 69.2% (v/v) using true density for calculations of the specific volume of the solid skeleton. Consequently, approximately 70% (v/v) of an FCC particle could theoretically be loaded with drug. This high intraparticle porosity is rather astonishing, but it can be verified by applying a simplified geometrical model as shown below.

It is generally accepted that efficiency of random close packing (RCP) of equisized spherical particles is 64% (v/v); the remaining 36% are interparticle voids [44]. Assuming that FCC particles are spherical and packing efficiency meets the conditions of RCP, the specific particle volume v_p can be approximated as $v_p = v_b * 0.64$, where v_b is the specific bulk volume. Intraparticle porosity can then be expressed as

$$\phi_{intra} = \frac{v_p - v_s}{v_p} = \frac{\rho_b^{-1} * 0.64 - \rho_s^{-1}}{\rho_b^{-1} * 0.64} \quad (5)$$

where ρ_b is the bulk density and ρ_s is the true density of the solid only. Simplification of Eq. (5) yields Eq. (6).

$$\phi_{intra} = 1 - \frac{\rho_b}{\rho_s * 0.64} \quad (6)$$

In order to use Eq. (6), the RCP conditions have to be met. Thus, the fluffy FCC powder was manually densified by means of a punch before bulk density was determined. Experimental values of bulk density (0.45 g/ml) and true density of FCC (2.71 g/ml) yielded an intraparticle porosity of approximately 74% (v/v). The discrepancy of 5% (v/v) between the calculated value and the value obtained by mercury intrusion may be explained by the microporosity and the shape factor of FCC. As described in the methods section, Eq. (3) is only valid for particles with pore sizes above 4 nm. However, SEM and SSA analysis indicated that FCC also consists of micropores (<2 nm), yielding too low values for intraparticle porosity (69.2% v/v) obtained by mercury intrusion and helium pycnometry. Furthermore, FCC particles are not perfectly spherical as shown in Figs. 1 and 2, thus packing efficiency is different to the suggested 64% (v/v) for RCP of spherical objects of equal diameter. Therefore, the calculated porosity (74% v/v) based on Eq. (6) might be overestimated. Since the real value lies in this range

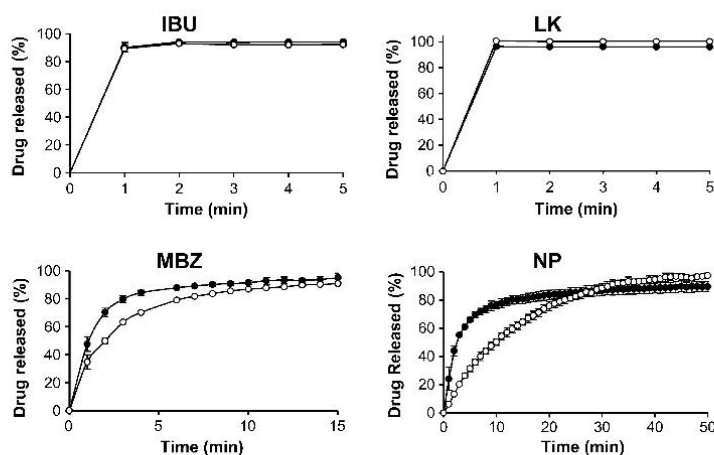


Fig. 6. Drug release from drug-loaded FCC (—●—) in comparison with FCC–drug mixtures (---○---) with same drug content of IBU (40%, w/w), LK (40%, w/w), MBZ (40%, w/w), and NP (35%, w/w). Data points are mean values ($n = 3$), and error bars correspond to standard deviation.

(69.2–74%, v/v), we used 70% (v/v) as the reference value for intraparticle porosity and maximum available space for drug loading. Accordingly, theoretical drug-loading capacity of IBU amounted to 49% (w/w), because $DL = 0.7 \times 1.1 / (0.7 \times 1.1 + 0.3 \times 2.7 \times 100)$, where 0.7 is the volume fraction (intraparticle porosity) which can be loaded with IBU having a true density of 1.1 g/ml, and 0.3 is the volume fraction of the solid having a density of 2.7 g/ml. The calculations for MBZ ($\rho = 1.39$ g/ml) yielded a possible DL up to 54% (w/w).

Comparison with drug-loading capacity by systematic SEM analysis revealed that the particles could not be completely filled. A critical level was observed at 35% (w/w) for NP and at 40% (w/w) for IBU, LK, and MBZ, where numbers of agglomerates and separate crystals started to increase. Above this critical level, the intraparticle pores could not be filled any further, and interparticle voids were also filled with drug causing the formation of agglomerates (Fig. 2B). Recalculation to the volume fractions revealed that only 20% (v/v) of the estimated 70% (v/v) could be loaded with MBZ, amounting to a space-filling efficiency of around 28%. These calculations and comparisons were necessary to understand where the drug was deposited, and also gave interesting insight into the mechanism of drug deposition when using the solvent-evaporation method. Ideally, the resulting product consists exclusively of drug-loaded FCC particles, without agglomerates and separate drug crystals present, because such undesired particles might have a negative effect on drug-release properties. It is therefore mandatory to determine drug loading capacity by a systematic and qualitative method, e.g. SEM image analysis.

4.2. Site of drug deposition

“Excellent” loading efficiency does not necessarily prove that the drug has completely crystallized inside the pores since drug degradation may have occurred. Hence, SEM analysis in combination with HPLC is needed to determine the site and amount of drug deposition. Analysis of porosity and SSA supported the concept of pore filling, but this is not sufficient to unambiguously characterize drug deposition.

Based on SEM images of drug-loaded FCC with low DL (25%, w/w) where no filled pores or separate drug crystals were observed, it can be hypothesized that the drug was deposited as a thin layer on the surface of the outer pores and probably also in deeper regions. With higher DLs (35% and 40% w/w), the FCC surface

became smooth, and most of the outer pores disappeared (Fig. 2). This observation was decisive for the confirmation of pore filling.

The extent of pore filling was quantitatively analyzed by mercury porosimetry. A significant decrease in intraparticle porosity was observed after drug loading, a finding that was most pronounced for LK-loaded FCC samples. The phenomenon was thought to be due to the amorphous drug clogging pores smaller than 0.1 μm , since practically no mercury penetrated below this pore size (Fig. 3A). The lower SSA of drug-loaded FCC compared to mixtures of drug and FCC suggested that the drug was directly associated with the surface of the pores. The mechanism of drug deposition as suggested by the available results is explained below.

4.3. Proposed mechanism of drug deposition in FCC by solvent evaporation

The crystal state of drugs incorporated into FCC particles was investigated by DSC analysis (Fig. 5). For IBU-, MBZ-, and NP-loaded FCC, the amorphous fraction of the drug was around 10% (w/w) which might be due to adsorption into the porous matrix with small pore size, where space limitation prevented the formation of crystalline material, thus retaining the drug in its non-crystalline, amorphous form [45]. However, pore-size distribution estimated by mercury intrusion showed no significant change for pore sizes below 20 nm, suggesting that these small pores were not filled with drug. Entrapment of amorphous drug in pores larger than 20 nm could have occurred, but this is rather unlikely. Alternatively, lower accuracy of the DSC method due to comparison of materials with different porosities could have resulted in the difference of melting enthalpies. Complete amorphization of LK was not due to confinement in small pores, but due to processing in methanol as described elsewhere [46]. Additional DSC measurements of pure amorphous LK after processing in methanol (results not shown) showed a glass transition state at a temperature range similar to that observed for LK-loaded FCC. However, the thermogram of pure amorphous LK also showed recrystallization and occurrence of two polymorphs, which was not observed for LK-loaded FCC, indicating stabilization of the amorphous form in the porous matrix.

The largest fraction of IBU, MBZ, and NP in drug-loaded FCC regained its original crystalline form (see Fig. 5). This crystallization process is assumed to depend on two major events, i.e. nucleation and crystal growth [47]. Nucleation is the initial step when the

solute gathers in clusters. This process is driven by supersaturation of the solute in the solvent. Subsequent precipitation (nucleation) occurs when the cluster reaches a critical size and becomes sufficiently stable. The crystal structure is defined by the distinctive arrangement of the molecules during the nucleation phase. Crystal growth is also driven by supersaturation and can occur in parallel to nucleation. Homogeneous nucleation occurs in the middle of the solution, whereas heterogeneous nucleation is the formation of critical clusters on a pre-existing surface, a so-called nucleation center. Heterogeneous nucleation rate is higher than homogeneous nucleation rate under identical conditions because the formation of a new surface (of the nucleus) requires energy due to surface tensions between the liquid phase and the newly forming solid phase. A pre-existing surface decreases the required energy of surface formation, and the nucleation barrier is lower [48]. These considerations are relevant for initial nucleation in the presence of FCC which provides numerous nucleation centers on its extensive and rough surface. Assuming that drug diffusion into the larger (outer) pores of FCC is fast and no concentration gradient occurs upon evaporation of the solvent, nucleation on the FCC surface, i.e. inside the pores, is preferred. Driven by supersaturation due to continuous evaporation of the solvent, the nuclei start to grow, and the crystals fill the pores. Evidence for heterogeneous nucleation upon solvent evaporation was provided by SSA measurements. The reduced SSA of drug-loaded FCC compared to non-loaded reference samples (Fig. 2) indicated that drug crystals grew directly on the surface of the pores. However, SSA was still relatively high after drug loading of IBU, MBZ, and NP, which is a hint for crystal growth in the larger outer pores (macro- and mesopores), because their contribution to SSA is much lower than the one of micropores. The strongest decrease in SSA was observed for LK-loaded FCC compared to physical mixtures, most probably due to clogging of the micropores by the amorphous drug as shown by DSC and mercury porosimetry. When the pores are filled, drug loading capacity is reached and drug excess leads to the formation of agglomerates. At this stage, drug diffusion into the inner core of the particle is only possible at very slow drying to allow sufficient time.

Crystal growth in porous materials may increase the pressure, thus potentially damaging the material. Typically, this occurs below a pore size of 20 nm [49]. Since crystallization pressure is higher with smaller pore sizes, crystals will preferably grow in the largest pores in materials with multiple pore sizes [49], e.g. FCC. This phenomenon correlated with drug solubility which increased with crystals with positive pressure compared to bulk solubility [50]. These assumptions explain well why the drug preferentially deposited in the larger outer pores of FCC, and why the theoretical drug loading capacity of 70% (v/v) was not reached.

At a late stage of drying, when all remaining solvent is inside the porous matrix, continuing evaporation will lead to an outward flow of the solution (convection) [51]. As a consequence of the mass transfer, drug accumulation and crystallization occur mainly near the surface [51]. These assumptions additionally support the view that drug loading into the inner core is challenging. Inward drug diffusion counteracts the outward mass transfer, potentially leading to more homogeneous drug distribution within the particle, but only when sufficient time for diffusion is given, i.e. when drying is slow enough. Therefore, we hypothesize that drug-loading capacity is dependent on the drying rate and that drug-loading efficiency can be increased if evaporation is slowed.

Our values for loading capacity could still be improved. However, the influence of prolonged drying time was not investigated in this study, because the applied process parameters of the solvent-evaporation method with short drying time (2.5 h or 3.5 h) yielded a sufficiently high DL of 40% (w/w) with good loading efficiencies.

The mechanism of drug loading by solvent evaporation differs fundamentally from the impregnation method, where the adsorption equilibrium controls DL. The adsorption equilibrium essentially depends on physicochemical properties (besides temperature and surface area), especially on drug and solvent polarities [52]. In this study, we showed that crystallization on calcium carbonate templates is not limited to a specific polarity range of the drug. Three highly lipophilic drugs and a salt could be deposited within FCC. In preliminary studies, 16 of 21 model drugs with varying polarities showed excellent loading efficiencies at a DL of 25% (w/w), demonstrating the wide range of applicability of the solvent-evaporation method.

4.4. Release profiles of drug-loaded FCC

A main objective of using porous carriers as a drug delivery system is to improve dissolution rate. Dissolution experiments with the standard USP 2 method have shown that drug loading into porous microparticles can accelerate drug release of poorly water-soluble drugs, e.g. NP and MBZ (Fig. 6). The faster drug dissolution of the loaded drug was attributed to the enlarged surface area compared to micronized drug crystals since only a minor fraction of the loaded drug was considered to be amorphous (approximately 10%). The loaded drug can be considered as a crystalline coating over the pore surface of the microparticles. Increased crystallization pressure in pores leads to locally increased solubility and might be an additional mechanism for faster drug release [50].

Drug release from drug-loaded FCC was investigated without specific formulation strategies (e.g. tablet compaction or additional excipients) to eliminate influences altering the dissolution rate, and to have direct information on the performance of drug-loaded particles. Addition of SLS was necessary to avoid floatation of the particles, but its use is only appropriate for investigation of enteric-coated drug delivery systems targeted to the small or large intestine. It also has to be considered that a certain fraction of suspended FCC and drug particles is sucked through the coarse particle filter and retained in the glass-microfiber filter where temperature and flow conditions are different than in the dissolution vessel.

A significant increase in drug dissolution rate was observed for NP- and MBZ-loaded FCC compared to reference samples, meaning that complete drug dissolution occurred in half the time. This effect might be even higher in vivo than in vitro due to different hydrodynamic conditions and generally decreased dissolution rates compared to the USP 2 apparatus [53]. For the model compounds IBU and LK, little changes in dissolution rate were observed. However, in the case of IBU, loading into FCC proved to be an interesting alternative to the micronization of this poorly soluble drug. For highly soluble compounds such as LK, the use of FCC as a carrier material might be an advantage when low doses have to be administered. In addition, drug-loaded FCC may be coated to modulate drug release, and to obtain, for example, a sustained release formulation.

5. Conclusion

Contrary to common belief, we demonstrated that drug loading by solvent evaporation is simple, fast, and efficient. In particular, the solvent-evaporation method offers three advantages over the widely used impregnation method: (I) the resulting DL can be precisely determined in advance, (II) a high DL can be achieved in a short time, and (III) loading efficiency is good up to the loading capacity of FCC or other porous carriers (i.e. no waste of expensive drugs). The combination of qualitative SEM analysis and HPLC quantification was sufficient to estimate both loading efficiency

and loading capacity, but additional analysis of porosity, SSA, and crystallinity was necessary to elucidate the loading mechanism. It was shown that the extensive surface area of FCC presents a large number of crystallization centers leading to heterogeneous nucleation and drug deposition mainly in the pores, preferably in the larger outer pores. Complete pore filling of the inner core was not possible. Nevertheless, DLs up to 40% (w/w) with good loading efficiencies were achieved. Proof of feasibility of the solvent-evaporation method was mainly attributed to the unique properties of the model carrier used in this study. The large pore sizes (up to 1 μm) decreases crystallization pressures, facilitating drug deposition within the pores, and high DLs were achieved due to the high porosity (70% v/v). Drug-loading capacity could possibly be increased by slowing evaporation, thus allowing enough time for diffusion of drug into the core of the particles.

Dissolution experiments proved that drug release can be accelerated by loading poorly water-soluble drugs into microparticles by the solvent-evaporation method. In contrast to the impregnation method based on adsorption, solvent evaporation led to a low fraction of amorphous drug after drug loading. The faster drug release can be explained by surface enlargement of the drug and locally increased drug solubility. Drug-loaded FCC may be used in capsules or tablets for oral delivery. Possible applications include the formulation of poorly soluble compounds to accelerate their dissolution. Sustained release formulations of highly soluble drugs can be obtained by coating of loaded FCC particles. Technical advantages include the formulation of drugs which are administered at low doses, or the preparation of orally dispersible tablets (ODT's). Indeed, the suitability of FCC for preparation of ODT's was already demonstrated [22]. These findings are promising for the future development of carrier-based drug delivery systems.

Acknowledgements

This project was financially supported by the Swiss Commission for Technology and Innovation (CTI). We thank Dr. M. Dürrenberger and D. Mathys at the Microscopy Center of the University Basel for their technical support in SEM analysis. We also thank Dr. C.J. Ridgway at Omya Inc. for providing analytical data and technical information on mercury porosimetry.

References

- [1] M. Manzano, M. Colilla, M. Vallet-Regí, Drug delivery from ordered mesoporous matrices, *Expert Opin. Drug Deliv.* 6 (2009) 1383–1400.
- [2] S. Wang, Ordered mesoporous materials for drug delivery, *Microporous Mesoporous Mater.* 117 (2009) 1–9.
- [3] Y. Zhang, J. Wang, X. Bai, T. Jiang, Q. Zhang, S. Wang, Mesoporous silica nanoparticles for increasing the oral bioavailability and permeation of poorly water soluble drugs, *Mol. Pharm.* 9 (2012) 505–513.
- [4] M.V. Speybroeck, R. Mellaerts, J.A. Martens, P. Annaert, G.V. den Mooter, P. Augustijns, Ordered mesoporous silica for the delivery of poorly soluble drugs, in: C.G. Wilson, P.J. Crowley (Eds.), *Control. Release Oral Drug Deliv.*, Springer, US, New York, NY, 2011, pp. 203–219.
- [5] B.C. Hancock, M. Parks, What is the true solubility advantage for amorphous pharmaceuticals?, *Pharm Res.* 17 (2000) 397–404.
- [6] H. Kettiger, A. Schipanski, P. Wick, J. Huwyler, Engineered nanomaterial uptake and tissue distribution: from cell to organism, *Int. J. Nanomed.* (2013) 3255.
- [7] L. Yildirimer, N.T.K. Thanh, M. Loizidou, A.M. Seifalian, Toxicology and clinical potential of nanoparticles, *Nano Today* 6 (2011) 585–607.
- [8] M.A. Kobiasi, B.Y. Chua, D. Tonkin, D.C. Jackson, D.E. Mainwaring, Control of size dispersity of chitosan biopolymer microparticles and nanoparticles to influence vaccine trafficking and cell uptake, *J. Biomed. Mater. Res. A* 100A (2012) 1859–1867.
- [9] H.L. Karlsson, J. Gustafsson, P. Cronholm, L. Möller, Size-dependent toxicity of metal oxide particles—a comparison between nano- and micrometer size, *Toxicol. Lett.* 188 (2009) 112–118.
- [10] C. Sander, P. Holm, Porous magnesium aluminometasilicate tablets as carrier of a cyclosporine self-emulsifying formulation, *AAPS PharmSciTech.* 10 (2009) 1388–1395.
- [11] G. Cavallaro, P. Pierro, F.S. Palumbo, F. Testa, L. Pasqua, R. Aiello, Drug delivery devices based on mesoporous silicate, *Drug Deliv.* 11 (2004) 41–46.
- [12] H. Yuasa, D. Asahi, Y. Takashima, Y. Kanaya, K. Shinozawa, Application of calcium silicate for medicinal preparation. I. Solid preparation adsorbing an oily medicine to calcium silicate, *Chem. Pharm. Bull. (Tokyo)* 42 (1994) 2327–2331.
- [13] S. Haruta, T. Hanafusa, H. Fukase, H. Miyajima, T. Oki, An effective absorption behavior of insulin for diabetic treatment following intranasal delivery using porous spherical calcium carbonate in monkeys and healthy human volunteers, *Diabetes Technol. Ther.* 5 (2003) 1–9.
- [14] H. Baradari, C. Damia, M. Dutreih-Colas, E. Laborde, N. Pécout, E. Champion, et al., Calcium phosphate porous pellets as drug delivery systems: effect of drug carrier composition on drug loading and in vitro release, *J. Eur. Ceram. Soc.* 32 (2012) 2679–2690.
- [15] A.A. Ayon, M. Cantu, K. Chava, C.M. Agrawal, M.D. Feldman, D. Johnson, et al., Drug loading of nanoporous TiO₂ films, *Biomed. Mater.* 1 (2006) L11–L15.
- [16] S. Tang, X. Huang, X. Chen, N. Zheng, Hollow mesoporous zirconia nanocapsules for drug delivery, *Adv. Funct. Mater.* 20 (2010) 2442–2447.
- [17] M. Itokazu, T. Sugiyama, T. Ohno, E. Wada, Y. Katagiri, Development of porous apatite ceramic for local delivery of chemotherapeutic agents, *J. Biomed. Mater. Res.* 39 (1998) 536–538.
- [18] A. Krajewski, A. Ravaglioli, E. Roncari, P. Pinasco, L. Montanari, Porous ceramic bodies for drug delivery, *J. Mater. Sci. – Mater. Med.* 11 (2000) 763–771.
- [19] Y. Zhang, Biocompatibility of porous spherical calcium carbonate microparticles on Hela cells, *World J. Nano Sci. Eng.* 02 (2012) 25–31.
- [20] S. Biradar, P. Ravichandran, R. Gopikrishnan, V. Goornavar, J.C. Hall, V. Ramesh, et al., Calcium carbonate nanoparticles: synthesis, characterization and biocompatibility, *J. Nanosci. Nanotechnol.* 11 (2011) 6868–6874.
- [21] N. Qiu, H. Yin, B. Ji, N. Klauke, A. Glidle, Y. Zhang, et al., Calcium carbonate microspheres as carriers for the anticancer drug camptothecin, *Mater. Sci. Eng. C* 32 (2012) 2634–2640.
- [22] T. Stirnimann, N.D. Maiuta, D.E. Gerard, R. Alles, J. Huwyler, M. Puchkov, Functionalized calcium carbonate as a novel pharmaceutical excipient for the preparation of orally dispersible tablets, *Pharm. Res.* 30 (2013) 1915–1925.
- [23] C.J. Ridgway, P.A. Gane, J. Schoelkopf, Modified calcium carbonate coatings with rapid absorption and extensive liquid uptake capacity, *Colloids Surf., Physicochem. Eng. Asp.* 236 (2004) 91–102.
- [24] C. Chamay, S. Bégu, C. Tourné-Péteilh, L. Nicole, D.A. Lerner, J.M. Devoisselle, Inclusion of ibuprofen in mesoporous templated silica: drug loading and release property, *Eur. J. Pharm. Biopharm.* 57 (2004) 533–540.
- [25] L. Gao, J. Sun, L. Zhang, J. Wang, B. Ren, Influence of different structured channels of mesoporous silicate on the controlled ibuprofen delivery, *Mater. Chem. Phys.* 135 (2012) 786–797.
- [26] M. Vallet-Regí, A. Rámila, R.P. del Real, J. Pérez-Pariente, A new property of MCM-41: drug delivery system, *Chem. Mater.* 13 (2001) 308–311.
- [27] S.-W. Song, K. Hidajat, S. Kawi, Functionalized SBA-15 materials as carriers for controlled drug delivery: influence of surface properties on matrix–drug interactions, *Langmuir ACS J. Surf. Colloids* 21 (2005) 9568–9575.
- [28] Y. Zhu, J. Shi, W. Shen, H. Chen, X. Dong, M. Ruan, Preparation of novel hollow mesoporous silica spheres and their sustained-release property, *Nanotechnology* 16 (2005) 2633.
- [29] I. Smirnova, J. Mamic, W. Arlt, Adsorption of drugs on silica aerogels, *Langmuir* 19 (2003) 8521–8525.
- [30] M. Otsuka, K. Tokumitsu, Y. Matsuda, Solid dosage form preparations from oily medicines and their drug release. Effect of degree of surface-modification of silica gel on the drug release from phytonadione-loaded silica gels, *J. Control. Release* 67 (2000) 369–384.
- [31] P. Sher, G. Ingavle, S. Ponrathnam, A.P. Pawar, Low density porous carrier drug adsorption and release study by response surface methodology using different solvents, *Int. J. Pharm.* 331 (2007) 72–83.
- [32] H. Rupprecht, Silicium dioxide and silicates in drug delivery, in: B.W. Müller (Ed.), *Control. Drug Deliv.*, International Publishers Service, Incorporated, 1987, pp. 197–225.
- [33] C. Alvarez, I. Núñez, J.J. Torrado, J. Gordon, H. Potthast, A. García-Arieta, Investigation on the possibility of bioaivers for ibuprofen, *J. Pharm. Sci.* 100 (2011) 2343–2349.
- [34] S.C. Sutton, L.A. Evans, J.H. Fortner, J.M. McCarthy, K. Sweeney, Dog colonoscopy model for predicting human colon absorption, *Pharm. Res.* 23 (2006) 1554–1563.
- [35] M.-W. Lo, M.R. Goldberg, J.B. McCrea, H. Lu, C.I. Furtek, T.D. Bjornsson, Pharmacokinetics of losartan, an angiotensin II receptor antagonist, and its active metabolite EXP3174 in humans, *Clin. Pharmacol. Ther.* 58 (1995) 641–649.
- [36] G.W. Houghton, H.K.L. Hundt, F.O. Muller, R. Templeton, A comparison of the pharmacokinetics of metronidazole in man after oral administration of single doses of benzoylmetronidazole and metronidazole, *Br. J. Clin. Pharmacol.* 14 (1982) 201–206.
- [37] A.D. McNaught, A.R. Wilkinson, *Compendium of Chemical Terminology*, Blackwell Science, Cambridge, UK, 1997.
- [38] V. Ambrogli, L. Perioli, C. Pagano, F. Marmottini, M. Moretti, F. Mizzi, et al., Econazole nitrate-loaded MCM-41 for an antifungal topical powder formulation, *J. Pharm. Sci.* 99 (2010) 4738–4745.
- [39] P.A. Gane, J.P. Kettle, G.P. Matthews, C.J. Ridgway, Void space structure of compressible polymer spheres and consolidated calcium carbonate paper-coating formulations, *Ind. Eng. Chem. Res.* 35 (1996) 1753–1764.
- [40] R.W. Baker, *Membrane Technology and Applications*, John Wiley & Sons, 2012.
- [41] I.M. Vitez, Utilization of DSC for pharmaceutical crystal form quantitation, *J. Therm. Anal. Calorim.* 78 (2004) 33–45.

3.2 Mucoadhesive coating and *in vitro* evaluation

Marker-ion analysis for quantification of mucoadhesivity of microparticles in particle-retention assays

Daniel Preisig¹, Michael Weingartner¹, Felipe J. O. Varum², Roberto Bravo², Rainer Alles¹, Jörg Huwyler¹, Maxim Puchkov¹

¹ Department of Pharmaceutical Sciences, University of Basel, Klingelbergstrasse 50, 4056 Basel, Switzerland

² Tillotts Pharma AG, Baslerstrasse 15, 4310 Rheinfelden, Switzerland

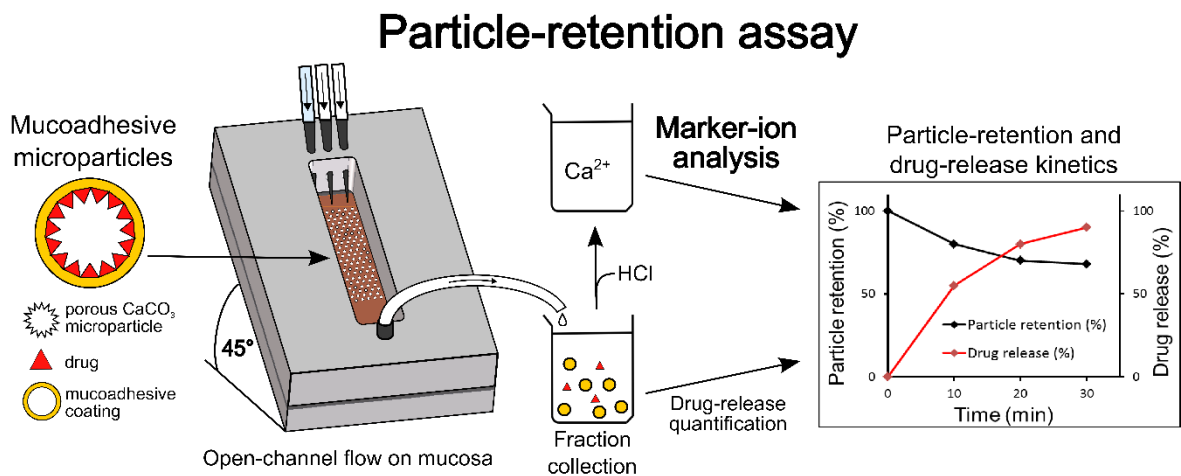
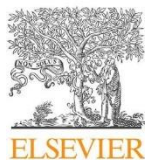


Fig. 3.2: Graphical abstract of the publication.



Contents lists available at ScienceDirect

International Journal of Pharmaceutics

journal homepage: www.elsevier.com/locate/ijpharm

Marker-ion analysis for quantification of mucoadhesivity of microparticles in particle-retention assays



Daniel Preisig^a, Michael Weingartner^a, Felipe J.O. Varum^b, Roberto Bravo^b, Rainer Alles^a, Jörg Huwyler^{a,*}, Maxim Puchkov^a

^a Department of Pharmaceutical Sciences, University of Basel, Klingelbergstrasse 50, 4056 Basel, Switzerland

^b Tillotts Pharma AG, Baslerstrasse 15, 4310 Rheinfelden, Switzerland

ARTICLE INFO

Article history:

Received 11 February 2015

Received in revised form 7 April 2015

Accepted 9 April 2015

Available online 13 April 2015

Keywords:

Mucoadhesion

Bioadhesion

Microparticles

Particle-retention assay

Marker-ion analysis

Colon delivery

ABSTRACT

The objective of the present work was to develop an improved method to quantify particle retention on mucosal tissue under dynamic flow conditions with simultaneous determination of drug dissolution. The principle was to dissolve the collected inert carrier material and quantify specific marker ions by reliable analytical methods. The mucoadhesive model particles consisted of drug-loaded porous calcium carbonate microcarriers coated with chitosan, and quantification of calcium ions by capillary electrophoresis enabled to determine particle-retention kinetics on colonic mucosal tissue. The method was validated by image analysis, and the particle-retention assay was successfully applied to granulate material (125–250 μm) and small particles (<90 μm) with mucoadhesive properties. Particle retention on colonic mucosa was improved by increasing the chitosan content, demonstrating the sensitivity and usefulness of marker-ion analysis for quantification of detached particles. Furthermore, we showed that drug dissolution from mucoadhesive microparticles followed comparable kinetics in the particle-retention assay and the standard USP IV method. Our findings are helpful for the development of micro-sized colonic drug delivery systems, in particular for optimization of mucoadhesive properties and sustained drug release kinetics of porous drug carriers.

© 2015 Elsevier B.V. All rights reserved.

1. Introduction

The physiology of the gastrointestinal tract presents innumerable challenges to drug delivery, particularly when developing modified-release dosage forms for oral administration (McConnell et al., 2008). For instance, a physiological parameter showing marked variability is gastrointestinal transit. Total transit of dosage forms through the gut can be as short as a few hours or as long as a few days (Varum et al., 2010a), highlighting wide inter- and intra-individual variabilities. Therefore, increased residence time in the target region would improve oral bioavailability. This can be achieved using the mucoadhesion approach. Mucoadhesive drug delivery systems can potentially prolong and harmonize the gastrointestinal residence time due to their adhesive interactions with the mucus covering the gastrointestinal epithelium (Ch'ng et al., 1985; Park and Robinson, 1984; Varum et al., 2008).

Modified-release dosage forms can be classified as single-unit or multiple-unit forms. The latter consist of many, often small-sized, units which are filled in a capsule or sachet, or they are compressed as tablets which disintegrate to release the individual units (Follonier and Doelker, 1992). Multiple-unit dosage forms generally have a more predictable and reproducible transit through the gut, resulting in lower inter- and intra-individual variabilities compared to single-unit dosage forms (Efentakis et al., 2000).

The design of multiparticulate drug delivery systems with a mucoadhesive functionality combines the advantages of both technologies to increase residence time, particularly in the colon (Chowdary and Rao, 2004; Varum et al., 2011). However, *in vitro* evaluation of such mucoadhesive formulations is still challenging, and standardized methods are missing. Evaluation of particles in the nano- and micro-size ranges is particularly difficult.

For *in vitro* evaluation of mucoadhesive formulations, the tensile detachment method is most commonly used due to the convenient experimental procedure and simple data reading (Woertz et al., 2013). The mucoadhesive formulation is thereby brought into contact with an appropriate gastrointestinal mucosa model (animal mucosa or artificial substrate), and the force to

* Corresponding author. Tel.: +41 0 61 267 15 13.

E-mail addresses: daniel.preisig@unibas.ch (D. Preisig), fvarum@tillotts.ch (F.J.O. Varum), rbravo@tillotts.ch (R. Bravo), rainer.alles@unibas.ch (R. Alles), joerg.huwyler@unibas.ch (J. Huwyler), maxim.puchkov@unibas.ch (M. Puchkov).

break the adhesive bond is measured (Ch'ng et al., 1985; Lejoyeux et al., 1989). This method found application also for investigation of mucoadhesive microspheres (Cao et al., 2012), but uneven particle distribution on the sticky tape and varying contact surface areas may impact on the reproducibility of the results. Furthermore, the test conditions, such as initial application force and tensile stress, do not match the shear forces *in vivo* (Laulicht et al., 2009). Therefore, other assessment methods were proposed in which multiparticulate bioadhesives were exposed to shear stress of a fluid. Examples are the rotating cylinder method performed in a USP II dissolution apparatus (Bernkop-Schnürch and Steininger, 2000; Grabovac et al., 2005), and the wash-off method for which a USP disintegration apparatus is used (Brahmaiah et al., 2013).

The falling liquid method first described by Rao and Buri (1989) has been most often used and adapted to investigate mucoadhesion of microparticles (Belgamwar and Surana, 2010; De Ascentiis et al., 1995; Déat-Lainé et al., 2013; Kockisch et al., 2003; Liu et al., 2005; Mishra and Mishra, 2012; Nielsen et al., 1998; Rastogi et al., 2007). The mucosal tissue is mounted on a channel-like device, and the particles are evenly distributed on the mucosal surface. A constant flow of medium is then applied to simulate the dynamic conditions and shear forces in the gastrointestinal tract or at any other site of intended delivery. Quantification of the remaining particles is done by visual counting (Belgamwar and Surana, 2010; Déat-Lainé et al., 2013; Kockisch et al., 2003; Liu et al., 2005), but this method is prone to human error and limited to a particle size of at least 200 μm . Gravimetric analysis of the dried washings presents a more reliable method (De Ascentiis et al., 1995; Mishra and Mishra, 2012; Rajinikanth et al., 2003; Rastogi et al., 2007), but washed-out mucus and drug released from adhering particles might significantly affect the results.

Fluorescein-labeled microspheres were also tested in a modified flow channel. Adhering particles were determined under UV light and by image analysis software, but this approach provided only semi-quantitative information about the release of the water-soluble model drug fluorescein, and not about the retention behavior of the particles on mucosal tissue (Kockisch et al., 2004).

Simultaneous determination of particle retention and drug dissolution kinetics using mucoadhesion assays with dynamic flow conditions has not yet been described in the literature. Additionally, there is still a need for improved analytical tools to quantify the detached microparticles. Such microparticles often consist of inert drug carriers, such as silicon dioxide or calcium carbonate, for example.

In previous studies, we used functionalized calcium carbonate (FCC¹, Omyapharm, Switzerland) for the development of floating gastroretentive drug delivery systems (Eberle et al., 2014) and orally dispersible tablets (Stirnemann et al., 2013). This multifunctional excipient, which is characterized by a small particle size ranging from 5 μm to 15 μm and high porosity of 70% (Stirnemann et al., 2014), was also shown to be a suitable drug carrier for oral delivery of various small molecules (Preisig et al., 2014).

The semisynthetic polymer chitosan (CS)² is well known for its mucoadhesive properties (Lehr et al., 1992), also when formulated as microparticles (He et al., 1998; Kockisch et al., 2004). Since CS is soluble at acidic pH but insoluble at pH > 6 (Sogias et al., 2010), calcium carbonate microparticles can be coated with CS layers using a precipitation method, as demonstrated by Han et al. (2012).

It can be hypothesized that carrier materials such as FCC can be brought into solution, e.g. by chemical dissolution, thus producing marker ions that can be quantified by appropriate analytical methods. This method has the advantage that very small particles

can be tested without labeling. Drug carriers based on calcium carbonate are well suited for marker-ion analysis due to fast dissolution in acidic conditions, and due to the availability of various analytical methods to quantify calcium, e.g. ion chromatography (Souter et al., 2011), flame atomic absorption spectrometry (Pohl et al., 2014), and capillary electrophoresis (Nussbaumer et al., 2010).

The objective of our study was therefore to investigate the usefulness and reliability of marker-ion analysis as a new method for particle quantification in dynamic particle-retention assays. For this purpose, visible (125–250 μm) and subvisible (<90 μm) mucoadhesive model particles based on calcium carbonate were used. Furthermore, we aimed to implement simultaneous testing of drug dissolution and particle retention on the colonic mucosa.

2. Materials and methods

2.1. Materials

FCC (Omyapharm, batch S01) was kindly provided by Omya, Switzerland. Metronidazole benzoate (MBZ)³ was purchased from Farchemia, Italy. Ammonium formate, formic acid (98%), HCl, methanol, *N*-acetylcysteine, phthalaldehyde (all HPLC-grade), and CS with medium molecular weight and 75–85% of deacetylation were purchased from Sigma-Aldrich, Switzerland. Acetone, acetic acid (99%), sodium dihydrogenphosphate dihydrate (NaH₂PO₄·2H₂O), and NaOH pellets were purchased from Häseler AG, Switzerland. Boric acid was obtained from Merck, Germany.

2.2. Preparation of mucoadhesive model microparticles

2.2.1. Drug loading

Drug loading of the porous microparticles was done by solvent evaporation as described recently by our group (Preisig et al., 2014). Briefly, MBZ-loaded FCC microparticles with a drug load of 40% (w/w) were prepared in a scale of 100 g by dissolving MBZ (40 g) in acetone (250 ml). FCC (60 g) was suspended in a round-bottom flask (31) connected to the solvent evaporator (R-114, Büchi, Switzerland). Rotation speed was set to 30 rpm, and the water bath (B-480, Büchi, Switzerland) was kept at 40° C. Pressure was initially set to 450 mbar and held for 1 h, followed by a gradual decrease to 20 mbar at a rate of 100 mbar/30 min, and maintained for 1 h at the final pressure. Total drying time was approximately 4 h. The collected solid material was ground and fractionated by sieving (Retsch, Switzerland) to generate two fractions of particle sizes: (1) <90 μm , and (2) 125–250 μm . Both fractions were used as non-mucoadhesive control in the particle-retention assay. Particles smaller than 90 μm were used for mucoadhesive coating.

2.2.2. Mucoadhesive coating

For CS coating of drug-loaded FCC, a previously reported precipitation method was adapted (Han et al., 2012). Precipitation of different amounts of CS (1.0 g, 2.0 g, and 5.0 g) on 10.0 g of drug-loaded FCC resulted in three batches with theoretical CS contents of 9.1%, 16.7%, and 33.3% (w/w), respectively. First, CS was dissolved in ultra-pure water (1000 ml) containing acetic acid (0.1%, 0.2%, and 0.5%, v/v, respectively) by stirring for 12 h. Subsequently, the solution was adjusted to pH 5.0 with NaOH (1 M). After sonication in a water bath for 1 h, the solution was paper-filtered. The MBZ-loaded FCC particles (10 g) with a drug load of 40% (w/w) and particle size smaller than 90 μm were homogeneously dispersed in the solution. Under constant stirring, the suspension was slowly adjusted to neutral pH with NaOH (0.05 M) using a peristaltic

¹ FCC: Functionalized calcium carbonate.

² CS: Chitosan.

³ MBZ: Metronidazole benzoate.

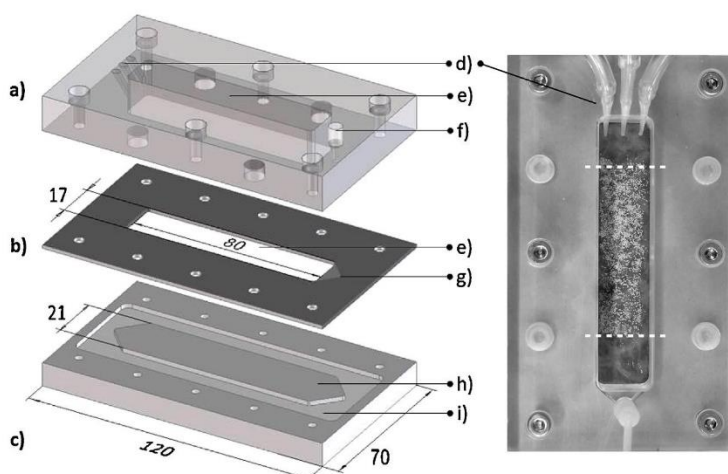


Fig. 1. Schematic drawing on the left side showing breakdown of the flow-channel assembly: (a) upper plate, (b) fixation plate, (c) support plate, (d) nozzle plugs for inlet flow, (e) open channel, (f) threaded hole for outlet flow, (g) chamfered collection region with connection to the upper plate, (h) mucosa holder, (i) excessive mucosa void space. The dimensions are in millimeters. The right side shows the top view of the flow-channel assembly with particles placed on the mucosa. The area of particle application is indicated by dashed lines.

pump (0.5 ml/min). Separation of the CS-coated microparticles from the aqueous phase was done by centrifugation at 1000 rpm for 5 min (302 K, Sigma, Germany). After removing the supernatant, the product was washed with ultra-pure water and centrifuged again. This washing and centrifugation step was repeated three times. In the final step, the particles were dried in a vacuum oven at 40°C. The dried product was sieved (Retsch, Switzerland) to generate two fractions of particle sizes: (1) particles smaller than 90 µm, and (2) granules with particle sizes ranging from 125 to 250 µm.

2.3. Particle characterization

2.3.1. Scanning electron microscopy

The outer surface of CS-coated microparticles was analyzed with a scanning electron microscope (SEM⁴; Nova NanoSEM 230, FEI Company, USA). Samples were sputtered with a 20 nm gold layer by a high-vacuum sputter coater (EM ACE600, Leica, Germany).

2.3.2. Drug quantification by HPLC

MBZ in model particles was extracted with acetone and then diluted with methanol and ultra-pure water to receive drug concentrations in the validated range of the isocratic HPLC method described previously (Preisig et al., 2014). The samples were assayed with an HPLC-UV system (Agilent 1100 series) comprising an autosampler, binary pump, and variable wavelength detector. The C18 column (Nucleosil, Marchery-Nagel, Switzerland) with 120 mm length, 3 mm inner diameter, and 5 µm particle size was kept in a column oven (PerkinElmer 200 series) set to 40°C. The mobile phase consisted of ammonium formate (10 mM, pH 4.5) and acetonitrile at a volumetric ratio of 50:50. Flow rate was 0.5 ml/min, and UV detection was performed at 320 nm.

2.3.3. Chitosan quantification by colorimetric assay

CS was quantified by a colorimetric method as described by Larionova et al. (2009). The primary amine of CS was derivatized

with phthalaldehyde, and the resulting isoindoles were measured with a UV spectrophotometer (V-630, Jasco, Japan) at 340 nm. Since MBZ also shows UV absorbance at 340 nm, the drug was first extracted with acetone, which does not dissolve CS. The CS-coated particles (100 mg) were transferred to a Falcon tube and dispersed in acetone (10 ml). After mixing for 5 min on an orbital shaker (3005, GFL, Germany) at 300 rpm, the particles were centrifuged for 5 min at 2000 rpm (302 K, Sigma, Germany), and the supernatant was decanted. The extraction step with acetone was repeated three times. After drying under reduced pressure, the Falcon tube containing FCC and CS was weighed. The solids were dissolved in 10 ml HCl (0.1 M) using an orbital shaker. When complete dissolution of FCC and CS was observed, the solution was adjusted to pH 3.0 with NaOH. The Falcon tube was weighed again to determine the precise sample volume based on a density equal to unity. The solutions were filtered using 0.45 µm syringe filters (Filtropur S, Sarstedt, Germany) and diluted (1:50) with HCl 1 mM. Equal volumes of reagent solution and diluted CS sample (1 ml) were mixed and allowed to react for 1 h. The reagent solution was freshly prepared by adding 200 µl of phthalaldehyde solution (0.11 M in ethanol) and 200 µl of *N*-acetylcysteine solution (0.071 M in ethanol) to 5 ml of borate buffer (0.2 M, pH 8.9). Absorption was measured against a reference consisting of equal volumes of reagent solution and 1 mM HCl. Calibration curve included 5 data points with CS concentrations ranging from 10 to 100 µg/ml ($R^2 > 0.999$).

2.3.4. FCC quantification by capillary electrophoresis

FCC content in mucoadhesive and non-mucoadhesive model particles was determined by capillary electrophoresis using the Cation Analysis Kit (Beckman & Coulter, USA) for quantification of calcium ions. MBZ-loaded or CS-coated FCC particles (50 mg) were decomposed to calcium ions by adjusting the pH to pH 2.5 with HCl in a 50 ml volumetric flask. The samples were diluted 1:10 with 3 mM HCl (pH 2.5), and filtered with 0.45 µm syringe filters. Ion analysis by capillary electrophoresis was done according to the Cation Analysis Kit (2013). Samples were prepared in triplicate. The area under the curves (AUCs) of calcium peaks were calculated using 32 Karat™ Software 8.0 (Beckman Coulter, Germany). The masses of FCC were calculated according to the calibration curve of

⁴ SEM: Scanning electron microscope.

FCC, which included 7 data points with FCC concentrations ranging from 1 to 80 $\mu\text{g}/\text{ml}$ ($R^2 > 0.990$). The calibration curve was re-measured every time before each test run, and each capillary electrophoresis measurement was carried out in duplicate.

2.4. Particle-retention assay

2.4.1. Flow-channel design

The flow channel for measuring particle retention was adapted from Batchelor et al. (2002) and built in-house. It consisted of three main parts, i.e. polymethyl methacrylate support plate, upper plate, and stainless steel fixation plate (Fig. 1). The mucosal tissue (porcine colonic mucosa) was spread on the mucosa holder of the support plate and immobilized with the fixation plate and four screws. The fixation plate and mucosa holder overlapped by 2 mm on the long sides allowing to clamp the mucosa in between. Excessive tissue was fitted into void space surrounding the mucosa holder. Between the fixation plate and upper plate, a silicon seal was placed to prevent leakage of flow medium. The upper plate with connections for inlet and outlet flow was fixed with six screws. The flow medium was transported with a peristaltic pump (Flocon 1B.1003-R/65, Petro Gas Germany) and distributed on the mucosa via three nozzles plugged into the designated holes. The distance between the nozzle tips and mucosa was set to 1 mm. The flow medium arriving at the chamfered collection region of the channel was removed with a second peristaltic pump through the outlet of the upper plate into the collection beakers.

2.4.2. Experimental procedure

Segments of pig proximal colon obtained from a local slaughterhouse were kept on ice and processed the same day. The colonic tube was opened longitudinally and washed with tap water. After removing the outer muscle layers, the mucosal tissue was sectioned into smaller pieces and rinsed with isotonic saline (0.9% NaCl). The mucosal sections were wrapped in aluminium foil, flash-frozen with liquid nitrogen, and stored at -20°C . Before use, the tissue was allowed to thaw in a refrigerator and equilibrate at room temperature (Varum et al., 2010b). This procedure has been shown to not affect the mucosa quality (Tobyn et al., 1995).

Prior to each experiment, the flow rate was set to 20 ml/min, which is close to the 22 ml/min recommended by Rao and Buri (1989). After a pre-hydration phase of 5 min with a constant flow of ultra-pure water (37°C), 20.0 mg of particles was evenly distributed over the center area of the mucosa ($55 \times 17\text{ mm}$) with a sieve. The flow channel was kept in horizontal position for 5 min. Subsequently, the assembly was tilted to 45° and the flow was started. The outgoing flow medium was collected in beakers which were changed every 10 min. The duration of the experiment was 30 min. Experiments with small control particles presented an exception, since in preliminary experiments a quick washout was visually observed. Therefore, the duration of the experiment was reduced to 10 min, and collection beakers were changed after 2 min and 5 min. The remaining particles were scraped off the mucosa and washed out with flow medium into separate beakers. All beakers were weighed before and after collection of flow medium to calculate the sample volume based on a density equal to unity. Samples were adjusted to pH 2.5 and analyzed according to Section 2.3.4. For each formulation, the particle-retention assay was repeated five times. As a control of calcium flux from mucosal tissue, the experiment was repeated without applying particles (in triplicate).

The percentage of detached particles, FCC_{det} , was calculated for each collected fraction using Eq. (1):

$$\text{FCC}_{\text{det}}(\%) = \frac{\text{FCC}_{\text{det}}(\text{mg})}{\text{FCC}_{\text{app}}(\text{mg})} \times 100 \quad (1)$$

where FCC_{det} (mg) is the weight of detached FCC determined by capillary electrophoresis, and FCC_{app} is the weight of FCC applied on the mucosa, i.e. the FCC content in 20 mg of tested formulations. The relative adhesion to mucosal membrane is presented as retained FCC particles (FCC_{ret}), which was calculated by Eq. (2):

$$\text{FCC}_{\text{ret}}(\%) = 100\% - \text{FCC}_{\text{det}}(\%) \quad (2)$$

Recovery of FCC was a measure for the reliability of the particle-retention assay and was determined by Eq. (3):

$$\text{Recovery}(\%) = \text{FCC}_{\text{det}}(\%) + \text{FCC}_{\text{muc}}(\%) \quad (3)$$

where FCC_{muc} is the percentage of remaining particles which were scraped off the mucus after 30 min.

2.4.3. Image analysis

The particle-retention assay was validated with mucoadhesive granules. The experiments were done as described in the standard protocol of the particle-retention assay, but the detached particles were trapped on a dark membrane filter (0.45 μm , VWR, USA) having grating lines with a defined mesh size of 3500 μm . The flow medium was passed through the filters by the aid of a vacuum filtration system and collected for further analysis of calcium content. The filters were changed every 10 min, and filters were photographed for investigation by image analysis software (ImageJ 1.48 v, National Institutes of Health, USA). The mesh size of the grating on the filter was measured in pixels and was used to set the scale in $\mu\text{m}/\text{pixel}$. The threshold was set to convert into monochrome image, and Watershed function was applied to separate adjacent particles (Rasband, 2014). For selective particle analysis, the size range was set from 0.01 mm^2 to Infinity, and circularity range was set from 0.3 to 1.0. For quantification of particles, a calibration image with 10.0 mg of particles distributed on a filter was processed, and the total area of particles (projected area in mm^2) was determined. The total projected area of 20.0 mg of mucoadhesive granules was 420.0 mm^2 corresponding to 100% of particles. Based on this calibration value, the image analysis results of each fraction were expressed as detached particles in percentage. Afterwards, the particles trapped on the filters were dissolved in a known volume of HCl and determined as described in Section 2.3.4.

Comparison with the results from image analysis can provide quantitative information about the reliability of the FCC quantification method by capillary electrophoresis. The calcium concentrations in the filtered flow medium were also quantified by capillary electrophoresis. The influence of tissue-derived calcium was investigated in three blank runs without application of FCC particles.

2.5. Drug dissolution

2.5.1. Particle-retention assay

Immediately after collecting a fraction, samples were taken to determine drug release from control and mucoadhesive particles. To prevent further drug dissolution in the collection beaker, aliquots (1.5 ml) were immediately sampled into Eppendorf tubes through a syringe filter (0.45 μm). For HPLC analysis, 800 μl of each sample was diluted with 200 μl water/methanol (50%, v/v) in HPLC vials, ensuring a constant methanol concentration of 10% (v/v). The HPLC method for MBZ quantification was used as previously described by our research group (Preisig et al., 2014).

2.5.2. USP IV

Drug release from CS-coated particles was also investigated in the USP IV closed-loop dissolution apparatus (CE 6, Sotax,

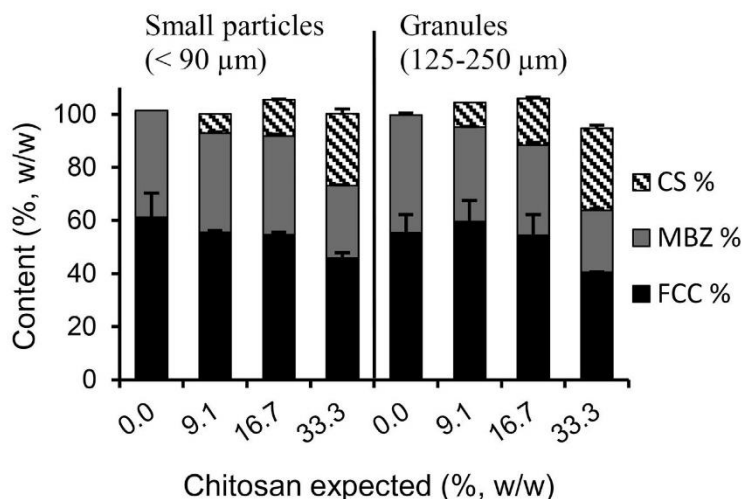


Fig. 2. Particle composition of tested mucoadhesive particles and control particles. Content of FCC (black bar), MBZ (gray bar), and CS (hatched bar) is shown for small particles (<90 μm, left side) and granules (125–250 μm, right side) with different CS contents (0.0%, 9.1%, 16.7%, and 33.3% w/w). Error bars indicate the SD ($n=3$ for all).

Switzerland). The dissolution cells with 12 mm inner diameter were filled with 1 mm glass beads and covered with a sieve insert (90 μm mesh). Sample size was 50 mg. The dissolution medium (phosphate buffer, 37° C, pH 6.8, 1000 ml) was transported through the USP IV dissolution cells and back to the reservoir vessels with a piston pump (CY 7-50, Sotax, Switzerland) at a flow rate of 16 ml/min. The UV absorbance was measured online at 320 nm with a multi-cell UV-spectrophotometer (Amersham Bioscience, Ultrospec 3100 pro).

2.6. Statistical analysis

All results were expressed as means ± standard deviations⁵ (SD). Single-factor analysis of variance (ANOVA)⁶ was performed to analyze the degree of significance for investigated parameters, e.g. particle size and CS content. For statistical analysis, we used the data analysis software (OriginPro 9.1.0, OriginLab USA).

3. Results

3.1. Particle characterization

Depending on the CS concentration, the precipitation processes lasted 30–40 min, and a total volume of 15–20 ml NaOH (0.05 M) was required to reach pH 7. The yields of the three precipitation batches (9.1%, 16.7%, and 33.3% CS, w/w) were 73.1%, 79.1%, and 61.9% (w/w), respectively.

The results of quantitative analysis of FCC, MBZ, and CS were consistent with the expected values, and total contents were close to 100% (w/w) as shown in Fig. 2. This means that the ratio (w/w) of drug-loaded FCC to CS can be controlled by their masses used for precipitation. The largest deviation from theoretical CS content was found for the small particles (expected CS content of 33.3%, versus actual content of $27.1 \pm 0.3\%$ w/w).

The CS coatings were qualitatively analyzed by SEM (see Fig. 3). After drug loading of FCC, the particles had a relatively rough surface, as shown in Fig. 3A (<90 μm) and Fig. 3B (125–250 μm).

After CS precipitation, the particles had a much smoother surface, which is an indication for successful CS coating. Typical examples of particles after precipitation with a CS content of 33.3% are shown in Fig. 3C (<90 μm) and Fig. 3D (125–250 μm). Qualitative analysis by SEM confirmed the feasibility of the precipitation method to create homogeneous CS coatings on drug-loaded FCC particles.

3.2. Particle-retention assay

3.2.1. Image analysis

Fig. 4 shows a typical example of an image for mucoadhesive granules retained on the filter. Particle-detachment profiles obtained by capillary electrophoresis and image analysis are almost superimposable as shown in Fig. 5. Cumulative detachment after 30 min was $11.8 \pm 3.0\%$ (w/w) determined by capillary electrophoresis ($n=3$), and $10.8 \pm 1.4\%$ (w/w) determined by image analysis ($n=3$). Particle recovery for image analysis was $98.5 \pm 5.3\%$ (w/w). The cumulative amount of dissolved FCC after 30 min was $7.8 \pm 1.6\%$ (w/w). Fig. 5 shows the FCC dissolution profile of mucoadhesive granules. Total recovery of FCC measured by capillary electrophoresis was $92.9 \pm 5.6\%$ (w/w), also taking into account dissolved FCC. This result indicates that calcium flux from the tissue was negligible. However, the opposite was observed for blank runs with no calcium-containing particles applied on the mucosal tissue. In this case, high amounts of calcium were detected in collected fractions and were equivalent to approximately 3 mg of FCC ($n=3$). This calcium was tissue-derived, but the calcium flux from the tissue to the flow medium was suppressed when the mucus was covered with a homogeneous layer of mucoadhesive microparticles containing calcium.

3.2.2. Particle retention and drug dissolution

Table 1 shows the results of particle retention after 30 min, demonstrating that mucoadhesion strongly depended on the extent of CS coating. Immediate washout of the control particles (<90 μm) was observed after only 2 min, whereas $64.4 \pm 9.0\%$ (w/w) of small mucoadhesive particles (<90 μm) with a CS content of 33.3% (w/w) still remained after 30 min. Mucoadhesive granules (125–250 μm) with highest CS content (33.3% w/w) showed strongest retention on colonic mucosa ($81.6 \pm 6.2\%$ w/w), which was more than three times higher than the value for control

⁵ SD: Standard deviation.

⁶ ANOVA: Analysis of variance.

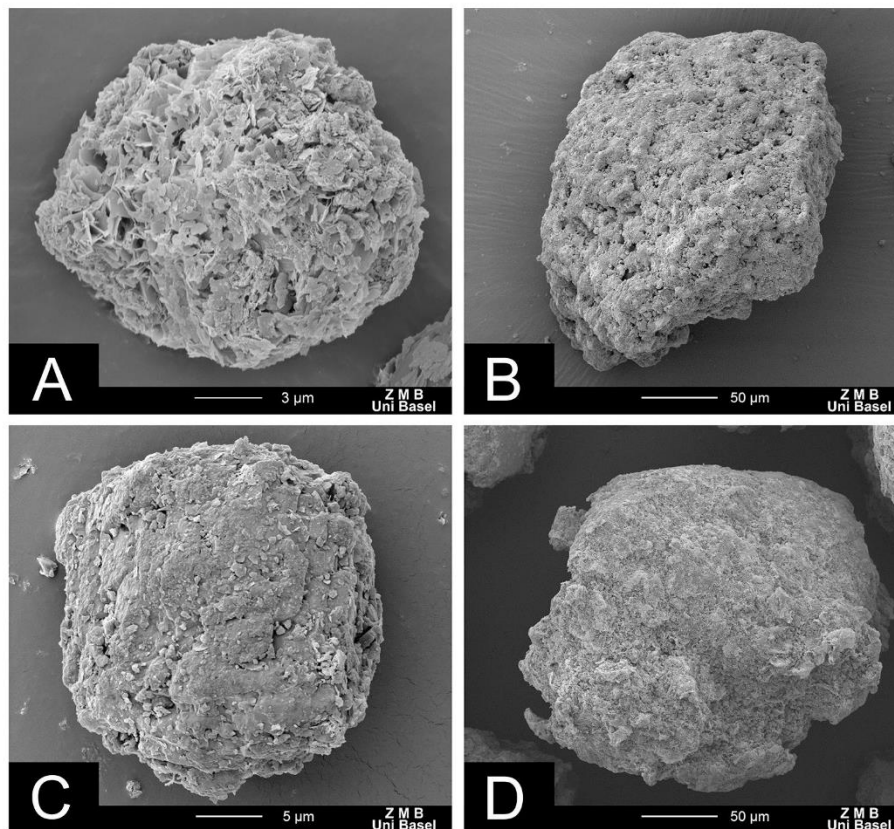


Fig. 3. Representative SEM images of model particles: (A) Non-mucoadhesive particles (<90 μm), (B) non-mucoadhesive granules (125–250 μm), (C) mucoadhesive particles (<90 μm, 33% CS, w/w), and (D) mucoadhesive granules (125–250 μm, 33% CS, w/w).

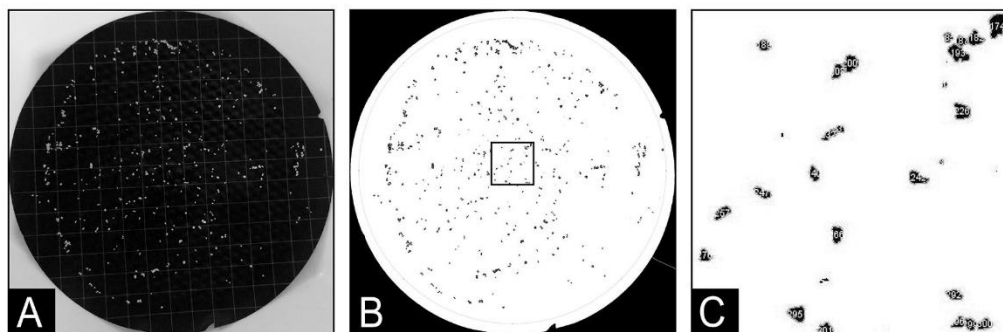


Fig. 4. Typical procedure for particle quantification by image analysis software. (A) Photo of detached mucoadhesive granules retained on the filter after 10 min, (B) particle analysis, and (C) magnification of highlighted area.

granules ($25.7 \pm 20.4\%$, w/w). ANOVA revealed no significant differences of particle retention between particles with 9.1% and 16.7% CS coatings, for both the small particles ($p > .05$) and the granules ($p > .05$). However, particles with 33.3% CS (w/w) showed significantly higher mucoadhesivity compared to particles containing 16.7% CS (w/w), for the small particles ($p < .0005$) as well as for the granules ($p < .05$). Another important aspect was the influence of particle size on particle retention. In general, the granules (125–250 μm) showed better mucoadhesive performance in the particle-retention assay than smaller particles

(<90 μm). **Table 1** shows average FCC recoveries for different model particles tested in the particle-retention assay. Most values were between 84.6% and 96.5% (w/w). Recoveries in excess of 100% (w/w) were only found for control particles without CS coating, and a poor recovery of 67.7% (w/w) was only found for the small particles with 33.3% CS (w/w).

Fig. 6 shows typical results for particle-retention and drug-dissolution kinetics for the model particles with an expected CS content of 33.3% (w/w). The retention kinetics of mucoadhesive particles were characterized by an initial burst detachment within

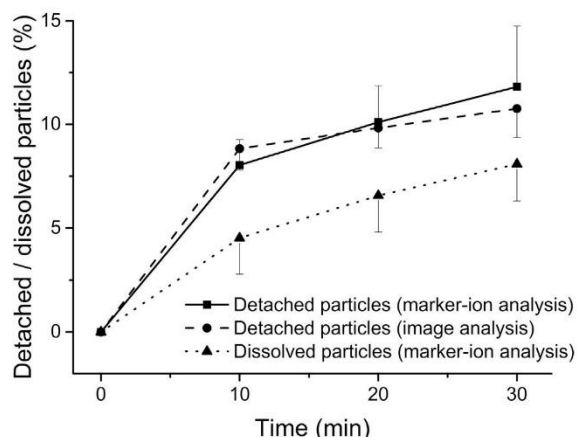


Fig. 5. Validation results of the particle-retention assay with mucoadhesive granules (125–250 μm , 33% CS, w/w). Detached particles measured by marker-ion analysis (solid line) and image analysis (dashed line) are related to the particles trapped on the filter, whereas dissolved particles (dotted line) are related to the particle-free solution after filtration. The error bars indicate the SD ($n=3$).

the first 10 min, followed by lower detachment rate for the remaining time of the experiment, which was in agreement with visual observations.

The two different dissolution methods (flow-channel and USP IV) showed comparable drug-release kinetics for tested particles. Drug-dissolution rates of CS-coated particles (33.3%, w/w) were relatively fast for both particle sizes. After 60 min in the USP IV, the small particles ($<90\ \mu\text{m}$) had released $74.0 \pm 7.3\%$ of the drug, and the granules showed almost complete drug release ($87.7 \pm 2.7\%$).

Table 1

Particle retention after 30 min ($\text{FCC}_{\text{ret},30}$) and particle recovery (% w/w) of small particles and granules with different CS contents (0.0%, 9.1%, 16.7%, and 33.3%, w/w). The results are presented as mean \pm SD ($n=5$).

CS content (% w/w)	Small particles ($<90\ \mu\text{m}$)		Granules (125–250 μm)	
	$\text{FCC}_{\text{ret},30}$ (% w/w)	Recovery (% w/w)	$\text{FCC}_{\text{ret},30}$ (% w/w)	Recovery (% w/w)
0.0	-2.6 ± 4.9	115.5 ± 6.5	25.7 ± 20.4	105.2 ± 11.1
9.1	27.6 ± 7.0	96.0 ± 5.8	62.0 ± 14.9	89.7 ± 18.0
16.7	32.3 ± 7.4	92.1 ± 11.7	69.2 ± 6.5	96.5 ± 6.8
33.3	64.4 ± 9.0	67.7 ± 7.6	81.6 ± 6.2	84.6 ± 23.1

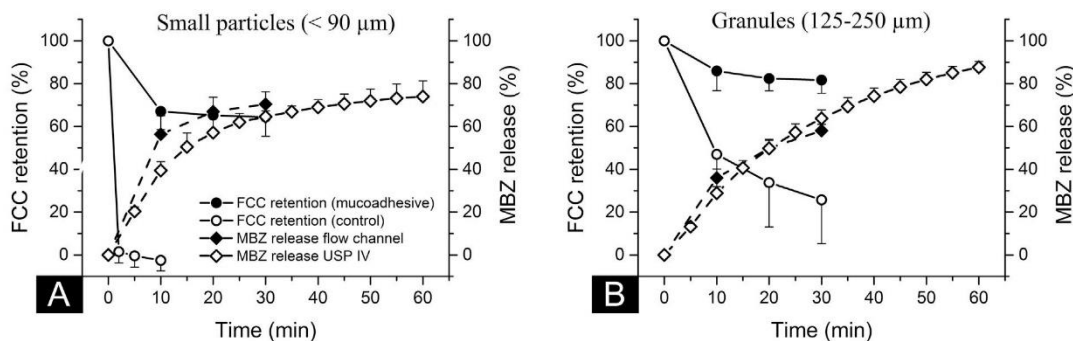


Fig. 6. Typical particle-retention and drug-dissolution kinetics of (A) small particles ($<90\ \mu\text{m}$) and (B) granules (125–250 μm), both containing 33.3% CS (w/w). The solid lines present FCC retention (left y-axis) of mucoadhesive particles (\bullet) and control particles (\circ). The dashed lines show MBZ release (right y-axis) of mucoadhesive particles measured in the flow channel (\blacklozenge) and with the USP IV method (\diamond). Error bars indicate SD for FCC retention ($n=5$), MBZ dissolution in the flow channel ($n=3$), and MBZ dissolution in USP IV ($n=3$).

4. Discussion

4.1. Design of the flow channel

A new feature of our flow channel was the mucosa holder on the support plate, on which the mucosal tissue could be placed and clamped with the fixation plate. The void space surrounding the mucosa holder was necessary to prevent excessive mucosa from squeezing into the channel. The sealing was tight enough to prevent leakage of the flow medium, and the mucosal tissue remained firmly attached to the support plate during the whole experiment without additional fixation aids such as pins (Rao and Buri, 1989) or low vacuum (Kockisch et al., 2003; Riley et al., 2002; Smart et al., 2003) described by others.

As shown in Fig. 1, the drilled holes present plugging stations for the nozzle tips. Three of them showed satisfying fluid distribution over the whole width (17 mm) of the exposed mucosa. The flow rate of 20 ml/min was close to the 22 ml/min originally described (Rao and Buri, 1989). In healthy humans, the intestinal fluid is transported from the ileum to the colon at a rate of 1.5–2 l/day, corresponding to approximately 1 ml/min (Szmulowicz and Hull, 2011). The use of a higher flow rate in the particle-retention assay than that *in vivo* is reasonable since it can compensate for the lower shear stress of water compared to the more viscous intestinal fluid. Another advantage of a high flow rate is that the duration of an experiment can be reduced, and the integrity of the mucus layer is less markedly affected.

4.2. Validation of marker-ion analysis

The lower limit of FCC quantification was 1.0 $\mu\text{g/ml}$. Thus, it was possible to quantify 0.20 mg FCC in a collected fraction of 200 ml, which corresponds to 0.33 mg of the small control particles and 0.49 mg of mucoadhesive granules. Therefore, a minimum of 1.7% of small control particles or 2.5% of mucoadhesive granules had to

be detached or dissolved in each fraction for precise calcium quantification, considering the sample size of 20 mg. Thus, the method was sensitive enough to detect small amounts of detached particles. However, it was not possible to use a physiological buffer solution as the flow medium because high sodium concentrations in isotonic saline decreased the sensitivity of the ion-quantification method, and low calcium concentrations were no longer detectable. Therefore, ultra-pure water was used to optimize the reproducibility of results. The use of an alternative method for calcium quantification could allow using physiological buffer solutions, provided that the method accuracy is not affected by sodium.

In this study, we showed that microparticles retained on a suitable filter can directly be quantified by image analysis without dye labeling (see Fig. 4). To exclude the influence of tissue-derived calcium flux, values from image-analysis experiments were compared with those obtained by the calcium-quantification method. Comparison of projected area of particles with findings from the calcium-quantification method revealed almost identical values (see Fig. 5). This finding implies that FCC quantification by capillary electrophoresis is reliable, and the influence of tissue-derived calcium flux is negligible.

Evaluation of particle retention by image analysis was already described for microparticles (Kockisch et al., 2004) and polymeric solutions (Cave et al., 2012) by incorporation of a dye. However, results from image analysis gave information about the retention of the water-soluble dye only, and not about the retention of the drug carriers. Image analysis of particles retained on filters was not possible for small particles (<90 μm), since they tend to agglomerate and hide other particles leading to inaccurate results. Another reason why the image-analysis method was only applicable to granules (>125 μm) was the requirement to exclude image artefacts, for example detached mucus retained on the filter. This was done by setting the minimum area of measured particles to 0.01 mm². Since the process of image analysis, including thresholding and particle selection, is tedious and error-prone (Cave et al., 2012), the results from image analysis were only used for validation of the calcium-quantification method. The filtration step in validation experiments also allowed estimating the dissolution of FCC during the particle-retention assay. The contribution of FCC dissolution to overall clearance of mucoadhesive granules from the mucosal tissue was 7.8% ± 1.6% (w/w), as shown in Fig. 5.

To test the reliability of the results and estimate the amount of calcium extracted from the biological matrix, recovery of FCC was determined in each particle-retention experiment. Indeed, control experiments without any particles showed relatively high amounts of tissue-derived calcium, but since validation experiments resulted in an FCC recovery of 92.9 ± 5.6% (w/w), the influence of mucosal calcium was considered to be negligible in the presence of calcium microparticles. Despite the high potential of variability associated with biological tissues (Varum et al., 2010b) and potentially non-laminar flow regime (Chanson, 2004), the proposed method showed high robustness as demonstrated by the low SD values (Fig. 6). Moreover, the particle-retention assay was highly discriminative between CS-coated particles and non-mucoadhesive control formulations, which is a prerequisite for *in vitro* evaluation of mucoadhesion.

4.3. Influence of particle size on *in vitro* particle retention

Mucoadhesion was tested using colonic tissue in view of our interests in colonic drug delivery. Retention of control formulations significantly depended on particle size, i.e. granules showed better retention than small particles. This implies that besides mucoadhesion, there are other mechanisms involved in resisting

the washout. Transport of particles in an open-channel flow is a well-known problem in sedimentology (Hsü, 2004), and it is commonly known that large particles are more difficult to be transported than the smaller ones (Chanson, 2004). Particles can be set in motion when the resulting weight \bar{F}_R is exceeded by a drag force \bar{F}_D , which is the force exerted by the fluid onto a particle due to relative differences of speed between the stream and particle. Drag force \bar{F}_D of a spherical particle is defined by Eq. (4):

$$\bar{F}_D = \frac{1}{2} \pi r^2 \rho_f v^2 C_D \tag{4}$$

where r is the radius of the particle, ρ_f is the density of the fluid, v is the speed of the object relative to the fluid, and C_D is the dimensionless drag coefficient (Chanson, 2004). The resulting weight \bar{F}_R of a particle immersed in a fluid is the vectorial sum of gravity and buoyancy force, and is defined by Eq. (5):

$$\bar{F}_R = \frac{4}{3} \pi r^3 g (\rho_p - \rho_f) \tag{5}$$

where g is the gravitational constant, and ρ_p is the density of the particle (Eberle et al., 2014).

Fig. 7 illustrates the forces acting on small and large particles. The large particle on the right is assumed to have a radius 10 times larger than that of the small particle ($R = 10r$), which approximately corresponds to the two size fractions of tested model particles (20 μm vs. 200 μm). Assuming a constant flow velocity, \bar{F}_D and \bar{F}_R are solely dependent on the particle radius. According to Eqs. (4) and (5), the ratio of \bar{F}_R to \bar{F}_D increases exponentially by increasing the particle radius. For example, \bar{F}_{D_2} of the large particle is increased by a factor of 100 compared to \bar{F}_{D_1} of the small particle, whereas \bar{F}_{R_2} is increased by a factor of 1000 compared to \bar{F}_{R_1} . This simplified theoretical consideration explains why larger particles are less readily set in motion than the smaller ones.

Our experimental data indicate that non-mucoadhesive granules reached a critical weight to resist the drag of the fluid. We also observed that the granules were not completely covered with the fluid, which decreases \bar{F}_{D_2} due to the lower cross-section area exposed to the stream, and additionally increases \bar{F}_{R_2} due to lower buoyancy force. These findings demonstrate the importance of performing control experiments on non-mucoadhesive particles of a density and particle size identical to those of the mucoadhesive particles.

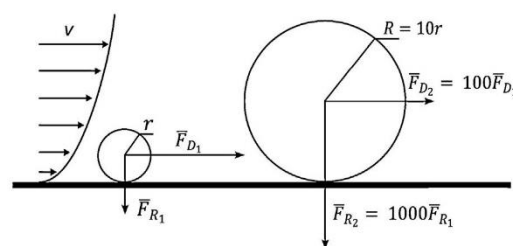


Fig. 7. Schematic presentation of two spheres with different particle sizes in an open channel flow with defined flow-velocity profile v . For the small particle with radius r , the drag force \bar{F}_{D_1} exceeds the resulting weight \bar{F}_{R_1} leading to initiation of particle motion. For the large particle with radius $R = 10r$, the ratio of \bar{F}_{R_2} to \bar{F}_{D_2} is increased by a factor of 10, which leads to better resistance to the washout of particles. The dimensions and vectors are schematic and not true to scale. Image modified from Sourani et al., 2014.

4.4. Drug release in the flow channel vs. USP IV dissolution

It was possible to simultaneously investigate drug release and particle retention of mucoadhesive formulations in the same experiment. Drug-release kinetics in the flow-channel method were similar to those obtained by the USP IV method (see Fig. 6), possibly due to the comparable flow rates which were 20 ml/min for the flow channel and 16 ml/min for the USP IV method. The two flow media (ultra-pure water and phosphate buffer) showed no differences in MBZ-dissolution kinetics when tested in the USP IV apparatus (results not shown). Therefore, the results from the flow-channel method, where ultra-pure water was used, were expected to be similar to the results from the USP IV method involving phosphate buffer. The flow rate used in the USP IV method (16 ml/min) most probably overestimated the drug dissolution rate *in vivo*. Among the different flow rates (4, 8, and 16 ml/min) described in the USP IV method (European Pharmacopoeia, 2011), a flow rate of 4 ml/min might be more biorelevant for simulation of the colonic conditions, as discussed in Section 4.1 and as indicated by *in vitro-in vivo* correlation studies (Fotaki et al., 2005). It was shown that CS is characterized by a fast water uptake of more than 100% (w/w) within 15 min (Silva et al., 2004). This implies fast water diffusion through the micrometer-thick CS layer to the inner core, where the drug is dissolved and transported out again. Introduction of sustained-release polymers may optimize sustained drug release in the targeted gastrointestinal mucosa.

5. Conclusions

Our study demonstrates the relevance of appropriate analytical methods to quantify mucoadhesive microparticles in dynamic test systems. The new approach of quantifying inert carrier particles presents a simple and more reliable alternative to the counting or weighing method, since it is not affected by drug dissolution and mucus detachment. Furthermore, the method is applicable to a wide range of particle sizes, potentially down to the nanometer size range, as well as different drugs and polymer coatings. The prerequisites for marker-ion analysis are (1) a poorly water-soluble carrier material which can be chemically decomposed to water-soluble ions, and (2) an analytical method capable of accurately quantifying the marker ions at low concentrations (1–100 µg/ml).

Reliability of the FCC quantification method was confirmed by validation experiments supported by image analysis. Calcium flux from porcine mucosal tissue was negligible when the tissue was covered with FCC particles, as indicated by the results for FCC recovery.

Investigation of mucoadhesive model particles showed increased retention on mucosal tissue for particles with increased CS content, demonstrating the sensitivity of the marker-ion analysis method. Since the particle-retention assay also allows to determine drug-release kinetics, it presents a useful tool for *in vitro* characterization of mucoadhesive microparticles for colonic drug delivery.

Acknowledgements

This project was financially supported by the Swiss Commission of Technology and Innovation (grant number: 13742.1 PFFLR-LS) and Tillotts Pharma AG. The authors thank Mr. Philip Salomon and Mrs. Evelyn Mühle from Centravo AG for providing fresh samples of porcine colonic tissue, and Dr. Silvia Rogers for editorial assistance.

References

- Batchelor, H., Banning, D., Dettmar, P., Hampson, F., Jolliffe, I., Craig, D.Q., 2002. An *in vitro* mucosal model for prediction of the bioadhesion of alginate solutions to the oesophagus. *Int. J. Pharm.* 238, 123–132. doi:[http://dx.doi.org/10.1016/S0378-5173\(02\)00062-5](http://dx.doi.org/10.1016/S0378-5173(02)00062-5).
- Belgamwar, V.S., Surana, S.J., 2010. Design and development of oral mucoadhesive multiparticulate system containing atenolol: *in vitro-in vivo* characterization. *Chem. Pharm. Bull.* 58, 1168–1175 (Tokyo).
- Bernkop-Schnürch, A., Steininger, S., 2000. Synthesis and characterisation of mucoadhesive thiolated polymers. *Int. J. Pharm.* 194, 239–247. doi:[http://dx.doi.org/10.1016/S0378-5173\(99\)00387-7](http://dx.doi.org/10.1016/S0378-5173(99)00387-7).
- Brahmaiah, B., Desu, P.K., Nama, S., Khalilullah, S., Babu, S.S., 2013. Formulation and evaluation of extended release mucoadhesive microspheres of simvastatin. *Int. J. Pharm. Biomed. Res.* 4 (1), 57–64.
- Cao, Q.-R., Liu, Y., Xu, W.-J., Lee, B.-J., Yang, M., Cui, J.-H., 2012. Enhanced oral bioavailability of novel mucoadhesive pellets containing valsartan prepared by a dry powder-coating technique. *Int. J. Pharm.* 434, 325–333. doi:<http://dx.doi.org/10.1016/j.ijpharm.2012.05.076>.
- Cation Analysis Kit <http://www.absciex.com/Documents/Products/CationAnalysisUsersGuide.pdf> (cited: 2014. Nov. 1), 2013.
- Cave, R.A., Cook, J.P., Connon, C.J., Khutoryanskiy, V.V., 2012. A flow system for the on-line quantitative measurement of the retention of dosage forms on biological surfaces using spectroscopy and image analysis. *Int. J. Pharm.* 428, 96–102. doi:<http://dx.doi.org/10.1016/j.ijpharm.2012.02.047>.
- Chanson, H., 2004. *Hydraulics of Open Channel Flow*. Butterworth-Heinemann.
- Ch'ng, H.S., Park, H., Kelly, P., Robinson, J.R., 1985. Bioadhesive polymers as platforms for oral controlled drug delivery II: synthesis and evaluation of some swelling, water-insoluble bioadhesive polymers. *J. Pharm. Sci.* 74, 399–405.
- Chowdary, K.P.R., Rao, Y.S., 2004. Mucoadhesive microspheres for controlled drug delivery. *Biol. Pharm. Bull.* 27, 1717–1724.
- De Ascentiis, A., deGrazia, J.L., Bowman, C.N., Colombo, P., Peppas, N.A., 1995. Mucoadhesion of poly(2-hydroxyethyl methacrylate) is improved when linear poly(ethylene oxide) chains are added to the polymer network. *J. Controlled Release* 33, 197–201. doi:[http://dx.doi.org/10.1016/0168-3659\(94\)00087-B](http://dx.doi.org/10.1016/0168-3659(94)00087-B).
- Déat-Lainé, E., Hoffart, V., Garrait, G., Jarrige, J.-F., Cardot, J.-M., Subirade, M., Beyssac, E., 2013. Efficacy of mucoadhesive hydrogel microparticles of whey protein and alginate for oral insulin delivery. *Pharm. Res.* 30, 721–734. doi:<http://dx.doi.org/10.1007/s11095-012-0913-3>.
- Eberle, V.A., Schoelkopf, J., Gane, P.A.C., Alles, R., Huwyler, J., Puchkov, M., 2014. Floating gastroretentive drug delivery systems: comparison of experimental and simulated dissolution profiles and floatation behavior. *Eur. J. Pharm. Sci.* 58, 34–43. doi:<http://dx.doi.org/10.1016/j.ejps.2014.03.001>.
- Efentakis, M., Koutlis, A., Vlachou, M., 2000. Development and Evaluation of oral multiple-unit and single-unit hydrophilic controlled-release systems. *AAPS PharmSciTech* 1, 62–70. doi:<http://dx.doi.org/10.1208/pt010434>.
- European Pharmacopoeia, 7th ed., 2011. Council Of Europe, Strasbourg, France.
- Follonier, N., Doelker, E., 1992. Biopharmaceutical comparison of oral multiple-unit and single-unit sustained-release dosage forms. *STP Pharm. Sci.* 2, 141–158.
- Fotaki, N., Symillides, M., Reppas, C., 2005. *In vitro* versus canine data for predicting input profiles of isosorbide-5-mononitrate from oral extended release products on a confidence interval basis. *Eur. J. Pharm. Sci.* 24, 115–122. doi:<http://dx.doi.org/10.1016/j.ejps.2004.10.003>.
- Grabovac, V., Guggi, D., Bernkop-Schnürch, A., 2005. Comparison of the mucoadhesive properties of various polymers. *Adv. Drug Deliv. Rev.* 57, 1713–1723. doi:<http://dx.doi.org/10.1016/j.addr.2005.07.006>.
- Han, Y., Tong, W., Zhang, Y., Gao, C., 2012. Fabrication of chitosan single-component microcapsules with a micrometer-thick and layered wall structure by stepwise core-mediated precipitation. *Macromol. Rapid Commun.* 33, 326–331. doi:<http://dx.doi.org/10.1002/marc.201100685>.
- He, P., Davis, S.S., Illum, L., 1998. *In vitro* evaluation of the mucoadhesive properties of chitosan microspheres. *Int. J. Pharm.* 166, 75–88. doi:[http://dx.doi.org/10.1016/S0378-5173\(98\)00027-1](http://dx.doi.org/10.1016/S0378-5173(98)00027-1).
- Hsü, K.J., 2004. *Physics of Sedimentology: Textbook and Reference*. Springer Science & Business Media.
- Kockisch, S., Rees, G.D., Young, S.A., Tsiouklis, J., Smart, J.D., 2004. *In situ* evaluation of drug-loaded microspheres on a mucosal surface under dynamic test conditions. *Int. J. Pharm.* 276, 51–58. doi:<http://dx.doi.org/10.1016/j.ijpharm.2004.02.020>.
- Kockisch, S., Rees, G.D., Young, S.A., Tsiouklis, J., Smart, J.D., 2003. Polymeric microspheres for drug delivery to the oral cavity: an *in vitro* evaluation of mucoadhesive potential. *J. Pharm. Sci.* 92, 1614–1623. doi:<http://dx.doi.org/10.1002/jps.10423>.
- Larionova, N.I., Zubaerova, D.K., Guranda, D.T., Pechyonkin, M.A., Balabushevich, N. G., 2009. Colorimetric assay of chitosan in presence of proteins and polyelectrolytes by using o-phthalaldehyde. *Carbohydr. Polym.* 75, 724–727. doi:<http://dx.doi.org/10.1016/j.carbpol.2008.10.009>.
- Laulicht, B., Cheifetz, P., Tripathi, A., Mathiowitz, E., 2009. Are *in vivo* gastric bioadhesive forces accurately reflected by *in vitro* experiments? *J. Controlled Release* 134, 103–110. doi:<http://dx.doi.org/10.1016/j.jconrel.2008.11.012>.
- Lehr, C.-M., Bouwstra, J.A., Schacht, E.H., Junginger, H.E., 1992. *In vitro* evaluation of mucoadhesive properties of chitosan and some other natural polymers. *Int. J. Pharm.* 78, 43–48. doi:[http://dx.doi.org/10.1016/0378-5173\(92\)90353-4](http://dx.doi.org/10.1016/0378-5173(92)90353-4).

- Lejoyeux, F., Ponchel, G., Wouessidjewe, D., Peppas, N.A., Duchène, D., 1989. Bioadhesive tablets influence of the testing medium composition on bioadhesion. *Drug Dev. Ind. Pharm.* 15, 2037–2048. doi:http://dx.doi.org/10.3109/03639048909052517.
- Liu, Z., Lu, W., Qian, L., Zhang, X., Zeng, P., Pan, J., 2005. In vitro and in vivo studies on mucoadhesive microspheres of amoxicillin. *J. Controlled Release* 102, 135–144. doi:http://dx.doi.org/10.1016/j.jconrel.2004.06.022.
- McConnell, E.L., Fadda, H.M., Basit, A.W., 2008. Gut instincts: explorations in intestinal physiology and drug delivery. *Int. J. Pharm.* 364, 213–226. doi:http://dx.doi.org/10.1016/j.ijpharm.2008.05.012.
- Mishra, M., Mishra, B., 2012. Mucoadhesive microparticles as potential carriers in inhalation delivery of doxycycline hydrochloride: a comparative study. *Acta Pharm. Sin. B* 2, 518–526. doi:http://dx.doi.org/10.1016/j.apsb.2012.05.001.
- Nielsen, L.S., Schubert, L., Hansen, J., 1998. Bioadhesive drug delivery systems. I. Characterisation of mucoadhesive properties of systems based on glyceryl mono-oleate and glyceryl monolinoleate. *Eur. J. Pharm. Sci.* 6, 231–239.
- Nussbaumer, S., Fleury-Souverain, S., Bouchoud, L., Rudaz, S., Bonnabry, P., Veuthey, J.-L., 2010. Determination of potassium, sodium, calcium and magnesium in total parenteral nutrition formulations by capillary electrophoresis with contactless conductivity detection. *J. Pharm. Biomed. Anal. Selected Papers from the 13th International Meeting on Recent Developments in Pharmaceutical Analysis (RDP A 2009)* 53, 130–136. doi:http://dx.doi.org/10.1016/j.jpba.2010.01.042.
- Park, K., Robinson, J.R., 1984. Bioadhesive polymers as platforms for oral-controlled drug delivery: method to study bioadhesion. *Int. J. Pharm.* 19, 107–127. doi:http://dx.doi.org/10.1016/0378-5173(84)90154-6.
- Pohl, P., Stelmach, E., Szymczycha-Madeja, A., 2014. Simplified sample treatment for the determination of total concentrations and chemical fractionation forms of Ca, Fe, Mg and Mn in soluble coffees. *Food Chem.* 163, 31–36. doi:http://dx.doi.org/10.1016/j.foodchem.2014.04.073.
- Preisig, D., Haid, D., Varum, F.J.O., Bravo, R., Alles, R., Huwyler, J., Puchkov, M., 2014. Drug loading into porous calcium carbonate microparticles by solvent evaporation. *Eur. J. Pharm. Biopharm.* 87, 548–558. doi:http://dx.doi.org/10.1016/j.ejpb.2014.02.009.
- Rajinikanth, P.S., Sankar, C., Mishra, B., 2003. Sodium alginate microspheres of metoprolol tartrate for intranasal systemic delivery: development and evaluation. *Drug Deliv.* 10, 21–28. doi:http://dx.doi.org/10.1080/713840323.
- Rao, K.V.R., Buri, P., 1989. A novel in situ method to test polymers and coated microparticles for bioadhesion. *Int. J. Pharm.* 52, 265–270. doi:http://dx.doi.org/10.1016/0378-5173(89)90229-9.
- Rasband W.S., 2014. ImageJ, U.S. Maryland, USA, imagej.nih.gov/ij/ National Institutes of Health Bethesda.
- Rastogi, R., Sultana, Y., Aqil, M., Ali, A., Kumar, S., Chuttani, K., Mishra, A.K., 2007. Alginate microspheres of isoniazid for oral sustained drug delivery. *Int. J. Pharm.* 334, 71–77. doi:http://dx.doi.org/10.1016/j.ijpharm.2006.10.024.
- Riley, R.G., Smart, J.D., Tsibouklis, J., Young, S.A., Hampson, F., Davis, A., Kelly, G., Dettmar, P.W., Wilber, W.R., 2002. An in vitro model for investigating the gastric mucosal retention of 14C-labelled poly(acrylic acid) dispersions. *Int. J. Pharm.* 236, 87–96. doi:http://dx.doi.org/10.1016/S0378-5173(02)00014-5.
- Silva, R.M., Silva, G.A., Coutinho, O.P., Mano, J.F., Reis, R.L., 2004. Preparation and characterisation in simulated body conditions of glutaraldehyde crosslinked chitosan membranes. *J. Mater. Sci. Mater. Med.* 15, 1105–1112. doi:http://dx.doi.org/10.1023/B:JMSM.0000046392.44911.46.
- Smart, J.D., Riley, R.G., Tsibouklis, J., Young, S.A., Hampson, F.C., Davis, J.A., Kelly, G., Dettmar, P.W., Wilber, W.R., 2003. The retention of 14C-labelled poly(acrylic acid) on gastric and oesophageal mucosa: an in vitro study. *Eur. J. Pharm. Sci.* 20, 83–90. doi:http://dx.doi.org/10.1016/S0928-0987(03)00175-1.
- Sogias, I.A., Khutoryanskiy, V.V., Williams, A.C., 2010. Exploring the factors affecting the solubility of chitosan in water. *Macromol. Chem. Phys.* 211, 426–433. doi:http://dx.doi.org/10.1002/macp.200900385.
- Sourani, S., Afkhami, M., Kazemzadeh, Y., Fallah, H., 2014. Effect of fluid flow characteristics on migration of nano-particles in porous media. *Geomaterials* 04, 73–81. doi:http://dx.doi.org/10.4236/gm.2014.43008.
- Souter, P., Horner, A., Cunningham, J.C., 2011. Quantification of in vitro mineralisation using ion chromatography. *Anal. Biochem.* 410, 244–247. doi:http://dx.doi.org/10.1016/j.ab.2010.11.041.
- Stirnemann, T., Atria, S., Schoelkopf, J., Gane, P.A.C., Alles, R., Huwyler, J., Puchkov, M., 2014. Compaction of functionalized calcium carbonate, a porous and crystalline microparticulate material with a lamellar surface. *Int. J. Pharm.* 466, 266–275. doi:http://dx.doi.org/10.1016/j.ijpharm.2014.03.027.
- Stirnemann, T., Maiuta, N.D., Gerard, D.E., Alles, R., Huwyler, J., Puchkov, M., 2013. Functionalized calcium carbonate as a novel pharmaceutical excipient for the preparation of orally dispersible tablets. *Pharm. Res.* 30, 1915–1925. doi:http://dx.doi.org/10.1007/s11095-013-1034-3.
- Szmulowicz, U.M., Hull, T.L., 2011. Colonic Physiology. In: Beck, D.E., Roberts, P.L., Saclarides, T.J., Senagore, A.J., Stamos, M.J., Wexner, S.D. (Eds.), *The ASCRS Textbook of Colon and Rectal Surgery*. Springer, New York, pp. 23–39.
- Tobyn, M.J., Johnson, J.R., Dettmar, P.W., 1995. Factors affecting in vitro gastric mucoadhesion. I: Test conditions and instrumental parameters. *Eur. J. Pharm. Biopharm.* 41, 235–241.
- Varum, F.J.O., McConnell, E.L., Sousa, J.J.S., Veiga, F., Basit, A.W., 2008. Mucoadhesion and the gastrointestinal tract. *Crit. Rev. Ther. Drug Carrier Syst.* 25, 207–258.
- Varum, F.J.O., Merchant, H.A., Basit, A.W., 2010a. Oral modified-release formulations in motion: the relationship between gastrointestinal transit and drug absorption. *Int. J. Pharm.* 395, 26–36. doi:http://dx.doi.org/10.1016/j.ijpharm.2010.04.046.
- Varum, F.J.O., Veiga, F., Sousa, J.J.S., Basit, A.W., 2010b. An investigation into the role of mucus thickness on mucoadhesion in the gastrointestinal tract of pig. *Eur. J. Pharm. Sci.* 40, 335–341. doi:http://dx.doi.org/10.1016/j.ejps.2010.04.007.
- Varum, F.J.O., Veiga, F., Sousa, J.J.S., Basit, A.W., 2011. Mucoadhesive platforms for targeted delivery to the colon. *Int. J. Pharm.* 420, 11–19. doi:http://dx.doi.org/10.1016/j.ijpharm.2011.08.006.
- Woertz, C., Preis, M., Breikreutz, J., Kleinebudde, P., 2013. Assessment of test methods evaluating mucoadhesive polymers and dosage forms: an overview. *Eur. J. Pharm. Biopharm.* 85, 843–853. doi:http://dx.doi.org/10.1016/j.ejpb.2013.06.023.

3.3 Preparation of optimized mucoadhesive microparticles

Mucoadhesive microparticles for local treatment of gastrointestinal diseases

Daniel Preisig¹, Roger Roth¹, Sandy Tognola¹, Felipe J. O. Varum², Roberto Bravo², Yalcin Cetinkaya², Jörg Huwlyer¹, Maxim Puchkov¹

¹ Department of Pharmaceutical Sciences, University of Basel, Klingelbergstrasse 50, 4056 Basel, Switzerland

² Tillotts Pharma AG, Baslerstrasse 15, 4310 Rheinfelden, Switzerland

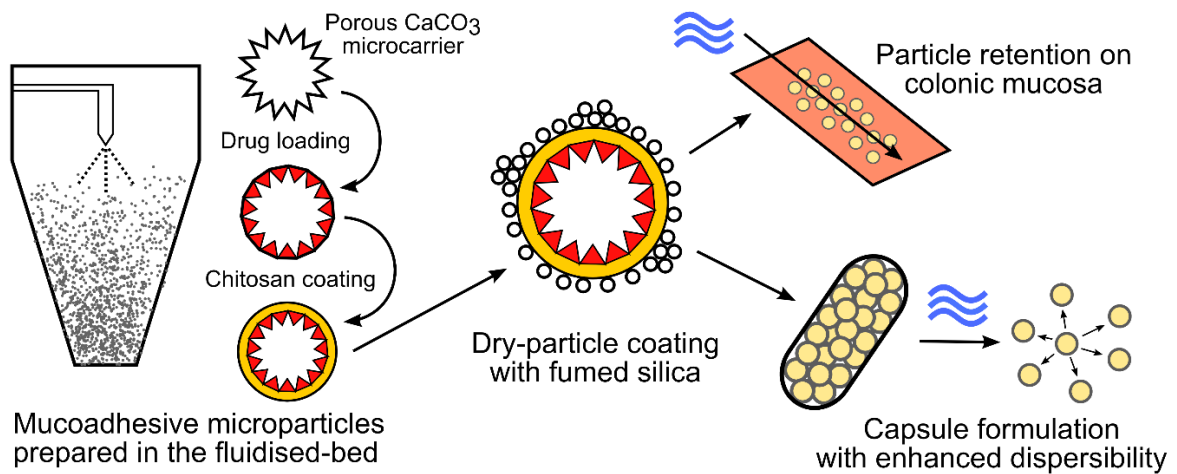


Fig. 3.3: Graphical abstract of the publication.



Contents lists available at ScienceDirect

European Journal of Pharmaceutics and Biopharmaceutics

journal homepage: www.elsevier.com/locate/ejpb

Research paper

Mucoadhesive microparticles for local treatment of gastrointestinal diseases



Daniel Preisig^a, Roger Roth^a, Sandy Tognola^a, Felipe J.O. Varum^b, Roberto Bravo^b, Yalcin Cetinkaya^b, Jörg Huwyler^{a,*}, Maxim Puchkov^a

^a Department of Pharmaceutical Sciences, University of Basel, Klingelbergstrasse 50, 4056 Basel, Switzerland

^b Tillotts Pharma AG, Baslerstrasse 15, 4310 Rheinfelden, Switzerland

ARTICLE INFO

Article history:

Received 14 December 2015

Revised 31 May 2016

Accepted in revised form 9 June 2016

Available online 11 June 2016

Keywords:

Mucoadhesion

Bioadhesion

Microparticles

Fluidized-bed

Drug loading

Porous carriers

Chitosan

Dispersibility enhancement

Colon drug delivery

ABSTRACT

Mucoadhesive microparticles formulated in a capsule and delivered to the gastrointestinal tract might be useful for local drug delivery. However, swelling and agglomeration of hydrophilic polymers in the gastrointestinal milieu can have a negative influence on particle retention of mucoadhesive microparticles. In this work, we investigated the impact of dry-coating with nano-sized hydrophilic fumed silica on dispersibility and particle retention of mucoadhesive microparticles. As a model for local treatment of gastrointestinal diseases, antibiotic therapy of *Clostridium difficile* infections with metronidazole was selected. For particle preparation, we used a two-step fluidized-bed method based on drug loading of porous microcarriers and subsequent outer coating with the mucoadhesive polymer chitosan. The prepared microparticles were analysed for drug content, and further characterized by thermal analysis, X-ray diffraction, and scanning electron microscopy. The optimal molecular weight and content of chitosan were selected by measuring particle retention on porcine colonic mucosa under dynamic flow conditions. Mucoadhesive microparticles coated with 5% (weight of chitosan coating/total weight of particles) of low molecular weight chitosan showed good *in vitro* particle retention, and were used for the investigation of dispersibility enhancement. By increasing the amount of silica, the dissolution rate measured in the USP IV apparatus was increased, which was an indirect indication for improved dispersibility due to increased surface area. Importantly, mucoadhesion was not impaired up to a silica concentration of 5% (w/w). In summary, mucoadhesive microparticles with sustained-release characteristics over several hours were manufactured at pilot scale, and dry-coating with silica nanoparticles has shown to improve the dispersibility, which is essential for better particle distribution along the intestinal mucosa in humans. Therefore, this advanced drug delivery concept bears great potential, in particular for local treatment of gastrointestinal diseases.

© 2016 Elsevier B.V. All rights reserved.

1. Introduction

Mucoadhesive drug delivery systems can be beneficial for local treatment of diseases related to mucosal membranes, such as fungal or bacterial infections [1,2]. Since the dosage form can be brought in close contact with the diseased tissue for an extended period of time, the therapeutic efficacy can be increased and lower

drug doses may be required, eventually reducing systemic adverse drug effects [3].

Colonic drug delivery is paramount for local treatment of diseases such as ulcerative colitis, Crohn's disease, or pseudomembranous colitis [4,5]. However, these diseases are often characterized by severe diarrhoea episodes [6], making it difficult to reach sufficiently high local drug concentrations for a long enough period of time, particularly in the ascending colon where the volume of fluids is higher [7]. The mucoadhesion approach can be an effective strategy to resist the wash-out of the drug. However, delivery and adhesion to the colonic mucosa still presents a great challenge [8].

In case of hard-gelatine capsules for delivery of a mucoadhesive formulation, there is a lack of strategies to prevent agglomeration after hydration. McGirr et al. [9] have observed an incomplete

Abbreviations: AUC, area under the curve; D50, median particle size; DSC, differential scanning calorimetry; FCC, functionalized calcium carbonate; LMW, low molecular weight; MBZ, metronidazole benzoate; MMW, medium molecular weight; SD, standard deviation; XRPD, X-ray powder diffraction.

* Corresponding author.

E-mail address: joerg.huwyler@unibas.ch (J. Huwyler).

<http://dx.doi.org/10.1016/j.ejpb.2016.06.009>

0939-6411/© 2016 Elsevier B.V. All rights reserved.

release of mucoadhesive polymers (carbomers) from InteliSite[®] plastic capsules administered to beagle dogs and opened in the colon by remote control. This was explained by hydration and swelling of the polymer inside the capsule before the polymer could be released.

The gastrointestinal transit of multiparticulate formulations is less variable than single-units, and transit through the colon is slower than monolithic dosage forms due to a sieving effect of multiparticulates [10,11]. Therefore, a drug delivery platform combining mucoadhesive features in multiparticulates can contribute to an overall increased gastrointestinal residence time. Procedures describing the preparation of mucoadhesive multiparticulates, nanoparticles [12–14], microparticles [15–18], and pellets in the millimetre range [19,20] have been reported.

The particle size of mucoadhesive drug carriers plays an important role in terms of mucoadhesion and manufacturability. Schmidt et al. have carried out a first *in vivo* study investigating the size-dependency of carrier uptake to inflamed rectal mucosa [21]. The most striking finding was the significantly enhanced accumulation of microparticles (3 µm) in ulcerous lesions. The authors concluded that size-tuning of drug carriers in the micrometre range offers a possibility for passive targeting of the inflamed regions in the gastrointestinal tract. Moreover, the results of *ex vivo* transport experiments let suggest that nanoparticles are not suitable for local treatment of inflammatory bowel diseases, since translocation towards the serosal compartment could enhance systemic drug absorption leading to higher risk of adverse drug effects [21].

In general, manufacturability of microcarriers is easier compared to nanocarriers due to the improved flowability of larger particles and the possibility of using standardized processes suitable for scale-up. Mucoadhesive microparticles were prepared by spray drying [22], dry powder coating [20], suspension polymerization [15], ionic gelation [23], emulsion-solvent evaporation [24], and supercritical fluid technique [25]. Our group has developed a precipitation method to coat drug-loaded microparticles with the mucoadhesive polymer chitosan [26]. These model particles showed significant retention on porcine colonic mucosa, and they have been used for the implementation and validation of a new particle-retention assay based on marker-ion analysis. However, manufacture of mucoadhesive microparticles by chitosan precipitation was done at small scale, and therefore, a method suitable for large scale is essential.

The fluidized-bed technology is an efficient and established pharmaceutical process often used for drug layering of non-porous pellets, particularly for low drug dosages, with several products in the pharmaceutical market [27,28]. The suitability for drug loading of porous microcarriers has also been demonstrated [29]. Additionally, this technology can be used to stabilize the drug as a solid dispersion leading to increased dissolution rate and bioavailability of poorly water-soluble drugs [30–32]. Scarce literature is available on the preparation of mucoadhesive microparticles using a fluidized-bed process, being a publication from Möschwitzer and Müller [17] one of the few examples. However, no mucoadhesion studies with these chitosan-layered pellets have been carried out.

In the present work, we describe a two-step fluidized-bed method for preparation of mucoadhesive microparticles with optimized drug-loading and chitosan-coating process to address local drug delivery to the colon. Metronidazole benzoate (MBZ, prodrug of metronidazole) was used as a model drug for poor aqueous solubility and local treatment of gastrointestinal diseases (*Clostridium difficile* infections). Further objectives of this work were to evaluate the feasibility of hydrophilic fumed silica to improve the dispersibility of the mucoadhesive microparticles, and to investigate its impact on the mucoadhesivity.

2. Materials and methods

2.1. Materials

Functionalized calcium carbonate (FCC, Omyapharm 500-OG) was kindly provided by Omya, Switzerland. Metronidazole benzoate (MBZ) was purchased from Farchemia, Italy. Ammonium formate, formic acid (98%), HCl, methanol (all HPLC-grade), and chitosan with low and medium molecular weight (LMW and MMW, respectively) and 75–85% of deacetylation were purchased from Sigma-Aldrich, Switzerland. Ethocel[®] Std. 10 cp was received from Colorcon, UK. Aerosil 300 was obtained from Evonik Industries AG, Germany. Acetone, acetic acid (99%), sodium dihydrogen phosphate dihydrate (NaH₂PO₄·2H₂O), and NaOH pellets were purchased from Hünslers AG, Switzerland.

2.2. Particle preparation

For preparation of mucoadhesive microparticles, we used a laboratory-scale fluidized-bed equipment (Strea-1, Aeromatic Fielder, Switzerland) with top-spray configuration. A spray nozzle with an orifice diameter of either 0.5 or 0.8 mm was used (Schlick, Germany). The spray rate was controlled using a peristaltic pump and a balance. The mucoadhesive microparticles were prepared in two steps: (1) drug loading of the porous microcarrier FCC with the model drug MBZ dissolved in a mixture of ethanol and acetone co-loaded with a binder polymer, and (2) spray coating of the drug-loaded carrier particles with a chitosan solution.

After preliminary experiments, three different mucoadhesive formulations, and one non-mucoadhesive control formulation were prepared in this study. MMW-5 and MMW-10 particles containing 5% and 10% (w/w) MMW chitosan, respectively, were prepared to evaluate the optimal chitosan content in terms of mucoadhesivity. LMW-5 particles containing 5% (w/w) LMW chitosan were the optimized formulation in terms of higher drug load and easier manufacturability. The viscosity of the spray solution is lower for LMW chitosan than for MMW chitosan (20–300 cps vs. 200–800 cps, 1% (w/w) in 1% acetic acid [33,34]), which should result in decreased droplet size and reduced risk of nozzle blocking, leading to an overall improved coating quality. The fluidized-bed process parameters of the drug-loading and chitosan-coating batches are summarized in Tables 1 and 2, respectively.

2.2.1. Drug loading

After a preliminary screening, two drug-loading batches were prepared according to Table 1. For preparation of PEG-MBZ-FCC particles, PEG 3000, MBZ, and FCC were used at a ratio of 28.6:28.6:42.8 (w/w). PVP-MBZ-FCC particles were prepared at a higher drug load using PVP K-25, MBZ, and FCC at a ratio of 37.5:37.5:25 (w/w). The drug solution consisted of 10% MBZ (w/w), and 10% polymer (w/w) dissolved in a mixture of acetone

Table 1
Fluidized-bed process parameters used for the two drug loading batches PEG-MBZ-FCC and PVP-MBZ-FCC.

	PEG-MBZ-FCC	PVP-MBZ-FCC
FCC (g)	180	96
MBZ (g)	120	144
Polymer (g)	120	144
Co-loaded polymer	PEG 3000	PVP K-25
Theoretical drug load (% w/w)	28.6	37.5
Inlet temperature (°C)	50	50
Air volume (level)	2–3	2–3
Atomization pressure (bar)	0.8	0.8
Spray rate (g/min)	5	5
Spray nozzle orifice diameter (mm)	0.8	0.8
Process time (h)	4	5

Table 2
Fluidized-bed process parameters for mucoadhesive coating with MMW and LMW chitosan on drug-loaded PEG-MBZ-FCC and PVP-MBZ-FCC particles, respectively.

	MMW-5	MMW10	LMW-5	EC-5
Drug-loading batch	PEG-MBZ-FCC	PEG-MBZ-FCC	PVP-MBZ-FCC	PVP-MBZ-FCC
MBZ-loaded FCC (g)	70	70	120	152
Chitosan coating (% w/w)	5	10	5	–
Theoretical drug load (% w/w)	27.14	25.71	35.63	32.39
Inlet temperature (°C)	50	50	50	40
Air volume (level)	2–4	2–4	2–4	2–4
Atomization pressure (bar)	0.8	0.8	0.8	0.8
Spray rate (g/min)	1–1.5	1–1.5	5	2.5
Spray nozzle orifice diameter (mm)	0.5	0.5	0.8	0.8
Process time (h)	4	8	2	1

and ethanol (60:40, v/v). The drug solutions were sprayed completely to reach the desired drug loads. The dimensions of the stainless steel chamber were as follows: cone height 330 mm, bottom diameter 100 mm, and top diameter 250 mm. The product was dried by fluidizing for 30 min at 40 °C, and by storing overnight in a vacuum oven set to 40 °C. The dried product was kept in closed jars and stored at room temperature.

2.2.2. Chitosan coating

Mucoadhesive coatings using MMW chitosan were applied on drug-loaded PEG-MBZ-FCC particles to a final chitosan content of 5% and 10% (w/w, MMW-5 and MMW-10, respectively). The coating solution was prepared by suspending 1.5% chitosan (w/v) in purified water and adding 1.5% acetic acid (w/v). After stirring for 12 h, the pH was adjusted to pH 5.8 using NaOH 1 M, and then the solution was passed through a metal sieve with a mesh size of 90 µm (Retsch, Switzerland). To reach the desired chitosan contents of 5% and 10% (w/w), the chitosan solutions (250 ml and 500 ml, respectively) were sprayed with a spray rate set to 1–1.5 g/min. The bottom diameter of the fluidizing chamber was slightly reduced to 55 mm to process smaller quantities of particles.

The optimized LMW-5 particles containing 5% (w/w) LMW chitosan were prepared using drug-loaded PVP-MBZ-FCC particles. A stainless steel chamber with 100 mm bottom diameter was used. An aqueous solution of LMW chitosan (1%, w/v) was prepared in 620 ml diluted acetic acid (10%, w/v) by stirring for 12 h and filtering through a metal sieve with a mesh size of 90 µm.

2.2.3. Granulation with ethyl cellulose

For preparation of the non-mucoadhesive control particles containing 5% (w/w) of ethyl cellulose (EC-5), 152 g of PVP-MBZ-FCC was granulated with 8 g of ethyl cellulose in a fluidized-bed process. The spray solution consisted of 16 g PVP dissolved in 124 ml of purified water, and was sprayed at a flow rate of 5 g/min. The process parameters for the EC-5 particles are summarized in Table 2.

2.2.4. Dry-coating with silica

Dry-coating of LMW-5 particles with hydrophilic fumed silica (Aerosil 300) was carried out by a simple blending procedure. The exact amounts of LMW-5 and silica particles were weighed to obtain silica concentrations of 2%, 5%, and 10% (w/w). The blends were sieved three times using a metal sieve with a mesh size of 500 µm (Retsch, Switzerland). Subsequently, the blends were processed in a laboratory-scale Turbula[®] mixer for 10 min, and sieved again (500 µm) three times.

2.3. Particle characterization

2.3.1. Particle-retention assay

Mucoadhesivity of chitosan-coated particles was characterized by measuring the relative particle retention on mucosal tissue in

a custom-built flow channel. Porcine colonic mucosal tissue was used as substrate to mimic the anatomy and mucus thickness of the human large intestine [8], which is the target tissue for local treatment of *Clostridium difficile* infections.

Segments of pig proximal colon obtained from a local slaughterhouse were kept on ice and processed the same day. The colonic tract was opened longitudinally and washed with tap water. After removing the outer muscle layers, the mucosal tissue was sectioned into smaller pieces and rinsed with isotonic saline (0.9% NaCl). The mucosal sections were wrapped in aluminium foil, flash-frozen with liquid nitrogen, and stored at –20 °C. Before use, the tissue was allowed to thaw in a refrigerator and equilibrate at room temperature [35].

Fig. 1A shows a diagram of the flow-channel assembly. The colonic mucosal tissue was spread on the mucosa holder of the support plate and immobilized with the fixation plate. The flow medium (37 °C) was transported with a peristaltic pump and distributed on the mucosa via three nozzles. The flow rate was set to 20 ml/min, and the mucosal tissue was hydrated by applying a constant flow of medium for 5 min. The dry particles (20.0 mg) were evenly distributed over the centre area of the mucosa (55 × 17 mm). After a contact time of 5 min, the flow channel was tilted to 45° and the flow was started. Ultra-pure water was used as flow medium for better sensitivity and precision of the calcium quantification by capillary electrophoresis.

The flow medium was collected in beakers, which were changed every 10 min and weighted to determine the sample volume. The duration of the experiment was 30 min. The remaining particles were scraped off the mucosa and washed out with flow medium into separate beakers. Samples were adjusted to pH 2.5 and analysed by capillary electrophoresis according to Section 2.3.2. For each formulation, the particle-retention assay was repeated three times.

The percentage of detached particles, FCC_{det} , was calculated for each collected fraction using Eq. (1):

$$FCC_{det} = \frac{FCC_{det}}{FCC_{app}} \quad (1)$$

where FCC_{det} is the mass of detached FCC determined by capillary electrophoresis, and FCC_{app} is the mass of FCC applied on the mucosa, i.e. the FCC content in 20 mg of tested formulations. The results of particle retention are the percentage of retained FCC, FCC_{ret} , which was calculated by Eq. (2):

$$FCC_{ret} = 1 - FCC_{det} \quad (2)$$

To measure the reliability of the experimental results, recovery of FCC was determined by Eq. (3):

$$Recovery = FCC_{det} + FCC_{muc} \quad (3)$$

where FCC_{muc} is the percentage of remaining particles which were scraped off the mucus after 30 min.

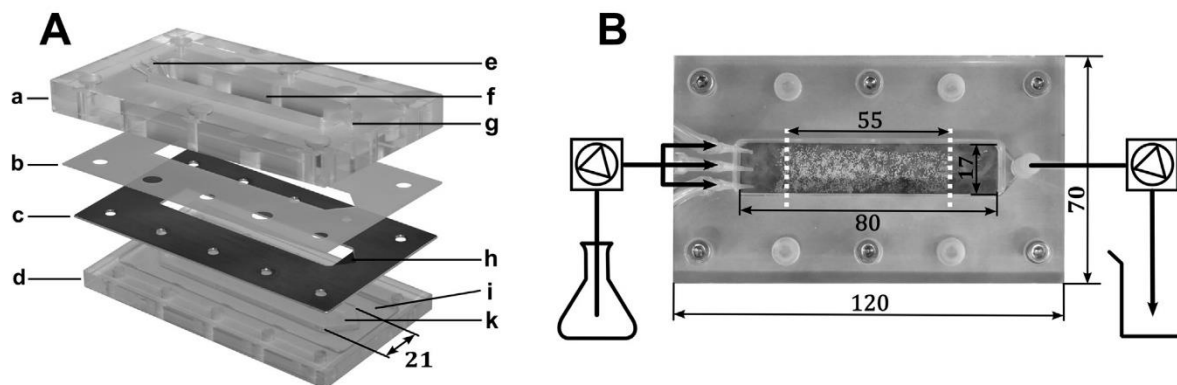


Fig. 1. Particle-retention assay for measuring mucoadhesivity under dynamic flow conditions. (A) The breakdown of the flow-channel assembly: (a) upper plate, (b) silicon seal, (c) fixation plate, (d) support plate, (e) nozzle plugs for inlet flow, (f) open channel, (g) vertical connection to collection region for outlet flow, (h) chamfered collection region, (i) excessive mucosa void space, and (k) mucosa holder. (B) The top view of the flow-channel assembly with schematic illustration of inlet and outlet flow using two peristaltic pumps. The area of particle application (55×17 mm) is indicated by dashed lines. The dimensions are in millimetres.

2.3.2. FCC quantification by capillary electrophoresis

For quantification of detached microparticles, marker-ion analysis was applied as described previously [26]. FCC content of collected samples from the particle-retention assay was determined by capillary electrophoresis using the Cation Analysis Kit (Beckman & Coulter, USA) for quantification of calcium ions [36]. FCC content in tested microparticles was also determined. The microparticles (50 mg) were decomposed to calcium ions and remaining components by adjusting the pH to pH 2.5 with HCl in a 50 ml volumetric flask. The samples were diluted (1 ml in 10 ml) with 3 mM HCl (pH 2.5), and filtered with $0.45 \mu\text{m}$ syringe filters. Samples were prepared in triplicate.

The area under the curves (AUCs) of calcium peaks was calculated using 32 Karat™ Software 8.0 (Beckman Coulter, Germany). The masses of FCC were calculated according to the calibration curve of FCC, which included 7 data points with FCC concentrations ranging from 1 to $80 \mu\text{g/ml}$ ($R^2 > 0.990$). The calibration curve was re-measured every time before each test run, and each capillary electrophoresis measurement was carried out in duplicate.

2.3.3. Drug dissolution in USP IV and particle dispersibility

Drug-loaded, chitosan-coated, and silica-coated microparticles were filled in hard-shell gelatine capsules size 2 and tested in the USP IV dissolution apparatus (CE 6, Sotax, Switzerland) using a closed-loop system. The USP IV dissolution cells with 12 mm inner diameter were filled with 1 mm glass beads and covered with a sieve insert ($90 \mu\text{m}$ mesh). Glass-microfiber filters (Whatman, GF/D, GE Healthcare Life Sciences, UK) with diameter of 25 mm and pore size of $2.7 \mu\text{m}$ were used to filter the dissolution medium prior to spectrophotometric measurement. The dissolution medium (1 l of phosphate buffer, pH 6.8, 37°C) was transported through the USP IV dissolution cells and back to the reservoir vessels with a piston pump (CY 7-50, Sotax, Switzerland) at a flow rate of 16 ml/min. The UV absorbance was measured online at 320 nm with a multi-cell UV-spectrophotometer (Amersham Bioscience, Ultro-spec 3100 pro).

The capsules were completely filled with the microparticles, and the sample size was weighted after closing of the capsule. Due to the different bulk densities, the sample size varied from 80 to 120 mg formulation per capsule, but sink conditions were provided in all experiments. Pure MBZ was filled in capsules size 3 with a sample size of 40 mg. For a qualitative comparison of particle dispersibility, the photographs of the dissolution cells were taken after opening of the capsule, and after 30 min of the experiment.

2.3.4. Particle drug content

To determine the drug content in prepared microparticles, a validated HPLC method was applied as described previously [37]. After extraction of MBZ with acetone, a first dilution (1 ml in 10 ml) with methanol, and second dilution (1 ml in 10 ml) with a mixture of ultra-pure water and methanol (90:10, v/v) were prepared. The resulting drug concentrations were in the validated range of the isocratic HPLC method. The samples were assayed with an HPLC-UV system (Agilent 1100 series) comprising an autosampler, binary pump, and variable wavelength detector. The C18 column (Nucleosil, Macherey-Nagel, Switzerland) with 120 mm length, 3 mm inner diameter, and $5 \mu\text{m}$ particle size was kept in a column oven (Perkin Elmer 200 series) set to 40°C . The mobile phase consisted of ammonium formate (10 mM, pH 4.5) and acetonitrile at a volumetric ratio of 50:50. Flow rate was 0.5 ml/min, and UV detection was performed at 320 nm.

2.3.5. Scanning electron microscopy (SEM)

The morphology of non-loaded, drug-loaded, chitosan-coated, silica-coated, and ethyl cellulose control microparticles was analysed with a scanning electron microscope (SEM; Nova Nano-SEM 230, FEI Company, USA). Samples were sputtered with a 20 nm gold layer by a high-vacuum sputter coater (EM ACE600, Leica, Germany).

2.3.6. Particle size

For measurement of particle size, a Camsizer XT (Retsch Technology, Germany) equipped with the X-Jet module for air pressure dispersion was used. A sample of 200 mg was applied via the vibrating feed chute and dispersed with a pressure of 300 kPa. The two-camera system and the included software for digital image processing allowed particle analysis in the range from $1 \mu\text{m}$ to 4.5 mm. In our study, results of particle size are presented as the longest Feret diameter, which is the longest possible distance between two parallel tangents of a projected particle. The amount of particles is presented as volume percentage (% v/v). For each formulation, five measurements were performed, and the mean volume percentage (% v/v) was calculated for each size fraction.

2.3.7. X-ray powder diffractometry (XRPD)

The crystalline state of the drug-loaded samples was investigated using a high-resolution XRPD system (SmartLab, Rigaku, Japan) equipped with Bragg-Brentano optics and a HyPix-3000 detector (Rigaku, Japan). A rotating anode X-ray source (45 kV

and 200 mA) was used for generation of the Cu K α radiation ($\lambda = 1.5406 \text{ \AA}$). The samples were measured in 1D detection mode in an angular range of $10\text{--}40^\circ$ (2θ) and with a step size of 0.01° (2θ).

For comparison purposes, co-evaporates of the drug and PVP K-25 in ratios of 50:50 and 10:90 (w/w) were prepared. The ratio of 50:50 was the same as in drug-loaded samples, and the ratio of 10:90 was for preparation of a solid dispersion. For preparation of both co-evaporates, a total mass of 1 g (MBZ and PVP) was dissolved in 20 ml of a mixture of acetone and ethanol (60:40, v/v). The solvents were removed using a rotary evaporator (R-114, Büchi, Switzerland) until a highly viscous solution was obtained which was filled into the depression of the sample holder, and dried in a vacuum oven set to 40°C and 250 mbar.

2.3.8. Differential scanning calorimetry (DSC)

Thermal analysis of the samples was carried out with a DSC 400 instrument (PerkinElmer, USA). A temperature scan from 0°C up to 150°C was performed in steps of $10^\circ\text{C}/\text{min}$. Samples size was between 4 and 9 mg.

For comparison purposes, the same co-evaporates of MBZ and PVP as described in Section 2.3.7 (drug-to-polymer ratio of 50:50 and 10:90, w/w) were analysed. One drop of the highly viscous solution was put in a DSC-analysis pan, and dried in a vacuum oven set to 40°C and 250 mbar.

2.3.9. Statistical analysis

For statistical analysis, we used the data analysis software (OriginPro 9.1.0, OriginLab, USA). All results were expressed as means \pm standard deviations (SD). A two-tailed *t*-test was performed to analyse the differences of mucoadhesivity between different mucoadhesive formulations. *P*-values < 0.05 were considered as statistically significant.

3. Results

3.1. Particle-retention assay

The results of *in vitro* particle retention for mucoadhesive microparticles (without silica) are summarized in Fig. 2A. The data showed strongest particle retention for MMW-10 particles ($74.79\% \pm 4.79\%$) being significantly higher than for MMW-5 particles ($p < 0.01$). It was possible to significantly improve the mucoadhesive performance by increasing the content of medium molecular weight chitosan coating from 5% to 10% (w/w). Interestingly, particles coated with LMW chitosan were significantly better retained than MMW-5 particles ($p < 0.01$) with identical amount of

chitosan coating. For comparison purposes, non-mucoadhesive control particles (EC-5) comprising ethyl cellulose showed almost complete detachment after 30 min ($6.67\% \pm 8.38\%$). The average recoveries ranged from 87.91% to 111.78%, which was an indication for the good reliability of the experimental data.

Typical retention kinetics for different particles are plotted in Fig. 2B. LMW-5 particles showed an initial burst detachment within the first 10 min, followed by a reduced detachment rate for the rest of the experiment. Contrarily, most of the EC-5 particles were already washed off after 10 min.

In a next step, LMW-5 microparticles, coated with various concentrations of silica nanoparticles as potential dispersing agent, were also assayed for particle-retention on colonic mucosal tissue. The results are summarized in Fig. 2C. The average recoveries were between 75.79% and 113.72%. It should be noted that the addition of 2% and 5% (w/w) silica led to an insignificant decrease in mucoadhesivity compared to LMW-5 particles without silica ($p > 0.1$), whereas 10% silica (w/w) reduced the particle retention significantly ($p < 0.005$).

3.2. Drug dissolution in USP IV and particle dispersibility

Drug-dissolution profiles of pure drug, drug loaded particles, mucoadhesive, and non-mucoadhesive microparticles are shown in Fig. 3A. The drug-loaded batches PEG-MBZ-FCC and PVP-MBZ-FCC showed a much higher dissolution rate than pure MBZ powder. Contrarily, the drug-dissolution rate of chitosan-coated particles was lower than drug-loaded particles, which can be explained by the strong agglomeration effect of mucoadhesive microparticles. Fig. 4A shows a typical agglomerate of MMW-10 particles during dissolution studies, keeping the form of the capsule. The increased dissolution rate of LMW-5 compared to MMW-10 particles can be well explained by the better dispersibility of LMW-5 as shown in Fig. 4B.

Dissolution profiles of LMW-5 particles coated with silica are also shown in Fig. 3B. For the formulations containing 0%, 2%, and 5% silica, the average time until 60% of the drug had been released was >10 , 3.6, and 2.9 h, respectively. Moreover, capsules filled with 10% silica could achieve a drug release of 80% after 4.6 h. This correlation of higher drug-dissolution rate with increasing silica concentrations can be explained by the capability of silica to disperse the particles and enlarge the surface area accessible by the dissolution medium. The improved particle dispersion was also found by visual observation as shown in Fig. 4D and F, showing LMW-5 particles coated with 5% and 10% silica, respectively, directly after disintegration of the capsule. Fig. 4E shows the LMW-5 particles

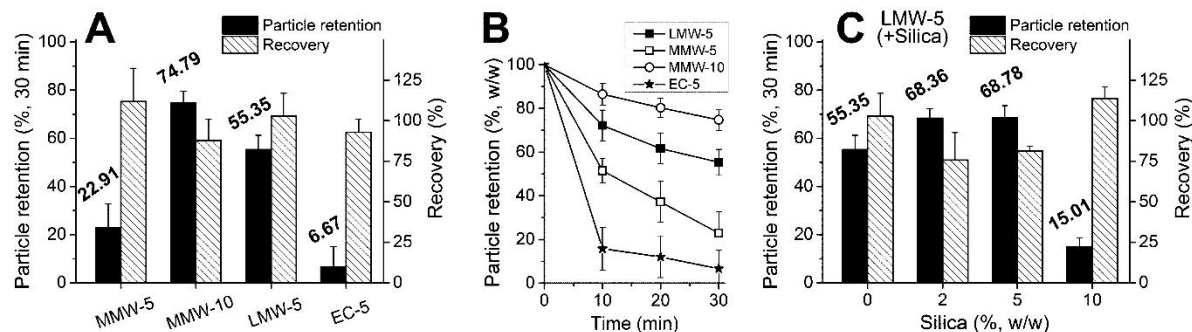


Fig. 2. Results of mucoadhesivity for chitosan-coated and silica-coated microparticles tested in the particle-retention assay. Panel A shows particle retention after 30 min for MMW-5, MMW-10, LMW-5, and EC-5 (non-mucoadhesive control). Panel B shows particle-retention kinetics for LMW-5, MMW-5, and EC-5. Panel C shows particle retention after 30 min for LMW-5 particles dry-coated with different amounts of silica. By increasing the silica concentration from 5% to 10% (w/w), the particle retention decreased significantly. The dashed bars in Panels A and C indicate the particle recovery (right y-axis). Error bars represent SD ($n = 3$ for all, except $n = 6$ for LMW-5).

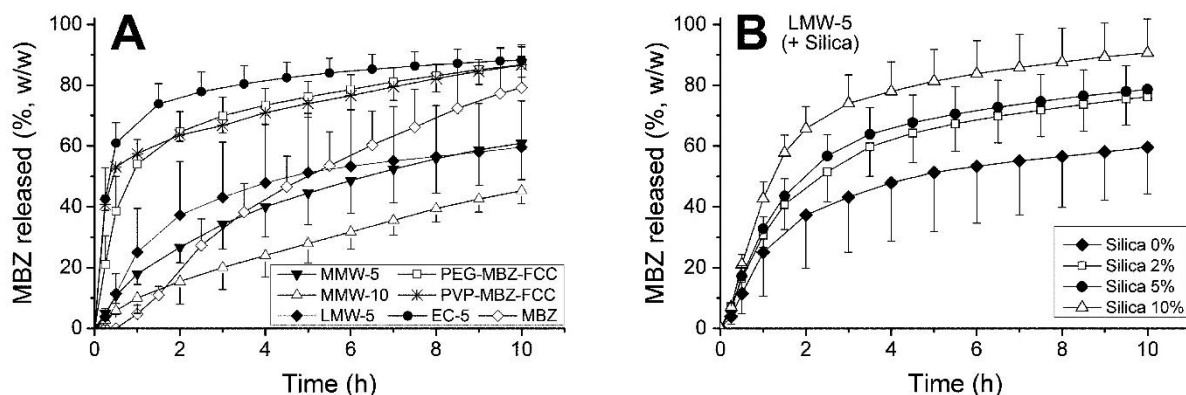


Fig. 3. USP IV drug-dissolution profiles of microparticles filled in capsules. Panel A shows results for drug-loaded, chitosan-coated, and non-mucoadhesive control particles. The slow drug release from MMW-5, MMW-10, and LMW-5 was associated with the formation of agglomerates. Panel B shows results for LMW-5 particles dry-coated with different concentrations of silica. The higher dissolution rate was an indication for improved dispersibility. Error bars represent SD ($n = 3$ for all) and are shown only for one direction (+ or -) for better presentation of the results.

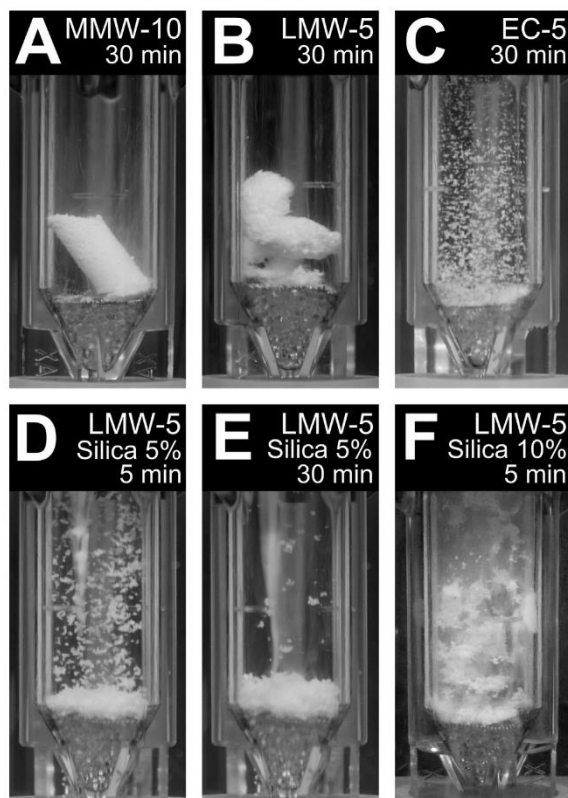


Fig. 4. Representative images of particle dispersion during USP IV dissolution studies after disintegration of the capsule shell. The photographs were taken 30 min after starting the flow, except (D) and (F) were taken after 5 min, i.e. after disintegration of the capsule. Contrary to MMW-5 and LMW-5 (A and B) showing dense agglomerates, EC-5 (C) was characterized by excellent dispersibility. The silica-coated (5%, w/w) LMW-5 particles showed good dispersion directly after capsule disintegration (D), but formation of loose agglomerates occurred after a certain period of time (E).

coated with 5% (w/w) silica after 30 min, indicating that, despite the good particle dispersion in the beginning of the dissolution run, agglomeration occurred after a certain time.

3.3. Scanning electron microscopy (SEM)

Typical SEM images of bulk FCC, drug-loaded PEG-MBZ-FCC, and drug-loaded PVP-MBZ-FCC particles are shown in Fig. 5A–C, respectively. Particles co-loaded with PEG still showed the characteristic pore structure of FCC, and they were mainly consisting of single FCC particles, whereas PVP-MBZ-FCC particles with higher drug and polymer content showed complete pore filling and bigger aggregates. In the example of PVP-MBZ-FCC, the drug can be identified as crystals embedded in the polymer layers.

Representative examples of chitosan-coated particles (MMW-5, MMW-10, and LMW-5) are shown in Fig. 5D–F, respectively, indicating a homogeneous layer of chitosan. The formation of granules was also observed, including EC-5 particles (Fig. 5G).

LMW-5 particles with different concentrations of silica nanoparticles were analysed by SEM to evaluate whether the dry-particle coating process was feasible. Fig. 5I shows a close-up view of a chitosan surface with 2% silica (w/w) revealing a homogeneous distribution of silica particles as a monolayer. However, due to the uneven surface morphology of the chitosan granules, there was a strong tendency of the silica nanoparticles to adsorb and accumulate between the gaps as shown in Fig. 5H. The same image shows that the major fraction of silica nanoparticles was present as agglomerates with sizes from 1 to 50 μm .

3.4. Particle drug content

In Table 3, the theoretical and experimental drug loads of prepared microparticles are compared. Both drug-loading batches (PEG-MBZ-FCC and PVP-MBZ-FCC) deviated less than 1% (w/w) from expected MBZ contents (28.6% and 37.5%, respectively). For mucoadhesive and control particles, the discrepancies between theoretical and experimental drug loads were also within an acceptable range (1–2.5%, w/w).

3.5. Particle size

Median particle sizes (D_{50}) of prepared microparticles are listed in Table 3, and plots of particle size distribution are shown in Fig. 6. PEG-MBZ-FCC particles were characterized by a very narrow size distribution (Fig. 6A), and median particle size was only slightly higher than for bulk FCC ($10.10 \pm 0.07 \mu\text{m}$ vs. $7.77 \pm 0.07 \mu\text{m}$). The PVP-MBZ-FCC particles, having increased drug and polymer

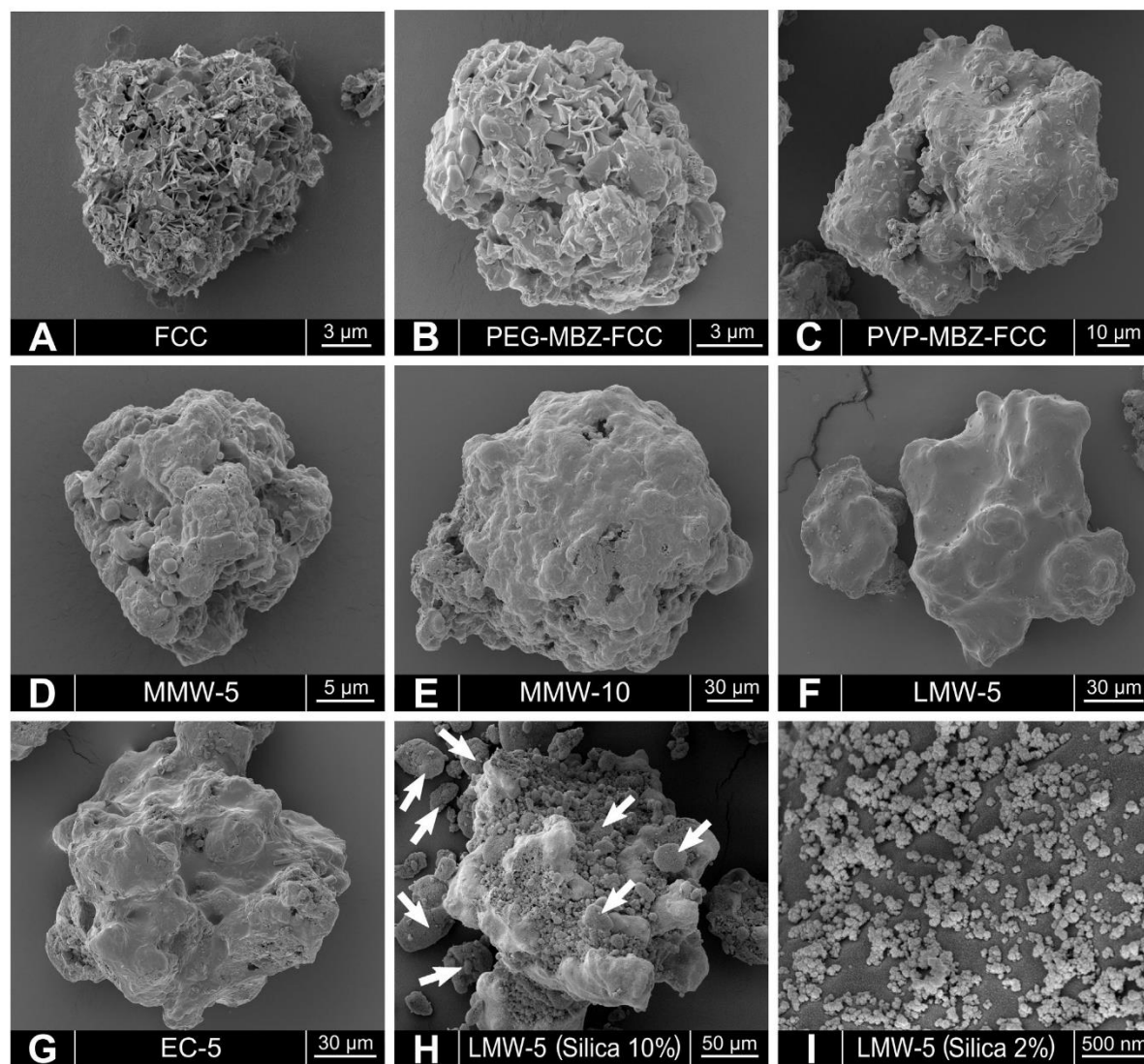


Fig. 5. Representative SEM images of bulk FCC (A), microparticles prepared in the fluidized bed (B,G), and LMW-5 particles dry-coated with fumed silica (H and I). (H) was dry-coated with 10% silica (w/w) and white arrows indicate silica agglomerates. (I) is a close-up view of a LMW-5 surface homogeneously coated with silica (2%, w/w).

content, showed a wider size distribution (Fig. 6B) and a higher median diameter ($48.48 \pm 2.83 \mu\text{m}$) as expected.

Coating of the drug-loaded microparticles with chitosan led to a further increase in median particle size as shown in Table 3. By increasing the content of MMW chitosan from 5% to 10% (w/w), particles sizes increased approximately by a factor of 3 ($54.40 \pm 2.01 \mu\text{m}$ vs. $183.48 \pm 9.98 \mu\text{m}$). The median particle size of EC-5 particles was in between $115.23 \pm 3.51 \mu\text{m}$, which was important for the use as a control formulation.

3.6. X-ray powder diffractometry XRPD

For the X-ray diffraction pattern of crystalline MBZ, we identified 2 characteristic peaks at 12.11° and 17.27° (2θ) which do not interfere with FCC and PEG. The characteristic peaks are labelled in Fig. 7B with *1 and *2, respectively, and were also detected in

samples of PEG-MBZ-FCC and PVP-MBZ-FCC. This clearly demonstrated that the major fraction of the drug was still in the crystalline state. As a reference for XRD sensitivity, mixtures of FCC and crystalline drug in low concentrations were prepared. Mixtures of 1% (w/w), 0.5% (w/w), and 0.1% (w/w) of MBZ in FCC were analysed (data not shown). It was possible to detect crystalline MBZ at the 1% concentration but no signal was detected at 0.5% concentration of drug. The characteristic peaks are labelled in Fig. 7B with *1 and *2, respectively, and were also detected in samples of PEG-MBZ-FCC and PVP-MBZ-FCC. In view of the high sensitivity and selectivity of the used method, we can assume that the major fraction of the drug was still in the crystalline state. The co-evaporate of MBZ and PVP in a ratio of 10:90 (w/w) led to stabilization of the amorphous form of MBZ as confirmed by the diffraction pattern without any peaks detected.

Table 3
Experimental drug loads (% w/w, n = 3), process yields (% w/w), and mean particle size (D50) of different batches prepared in the fluidized bed.

	Theoretical drug load (% w/w)	Experimental drug load (% w/w, n = 3)	Process yield (% w/w)	Median particle size D50 (µm, n = 5)
Bulk FCC	–	–	–	7.77 ± 0.06
PEG-MBZ-FCC	28.57	28.92 ± 2.91	98.4	10.10 ± 0.07
PVP-MBZ-FCC	37.50	38.19 ± 0.24	96.5	48.48 ± 2.83
EC-5	32.39	34.31 ± 0.13	97.5	115.23 ± 3.51
MMW-5	27.14	25.25 ± 0.36	98.2	54.40 ± 2.01
MMW-10	25.71	23.29 ± 0.08	102.0	183.48 ± 9.98
LMW-5	35.63	35.88 ± 0.20	101.1	190.88 ± 10.96

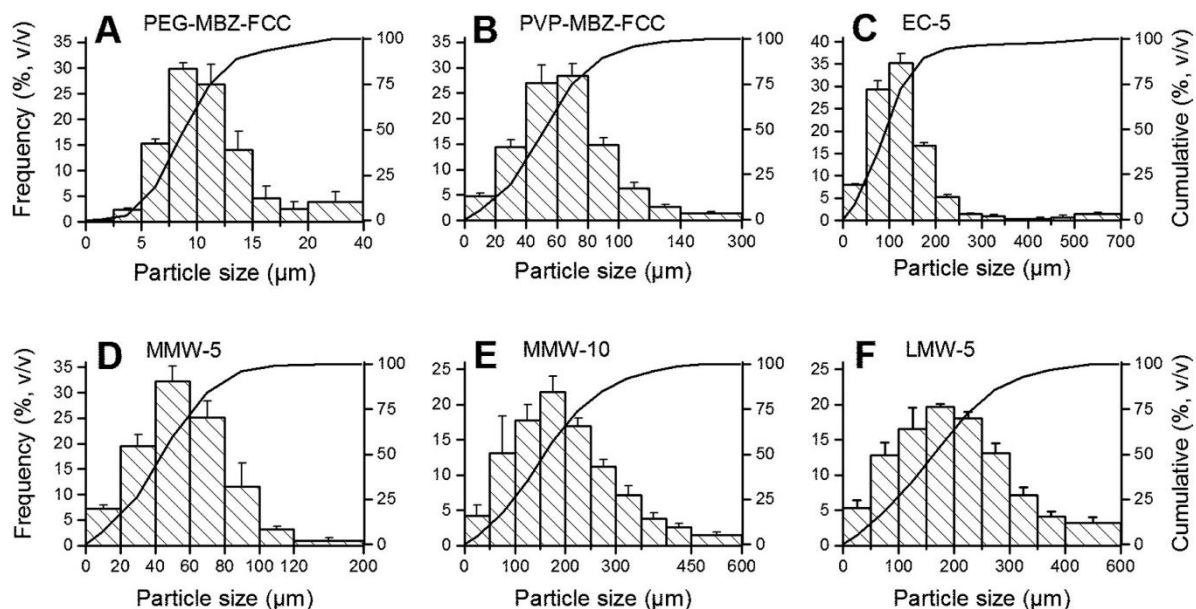


Fig. 6. Particle size distributions (largest Feret diameter) of prepared particles measured by dynamic image analysis. The bar plots indicate the frequency by volume for the measured size ranges (% v/v, left y-axis), and the curve plots are the cumulative volume percentages (% v/v, right y axis). Error bars represent SD (n = 5).

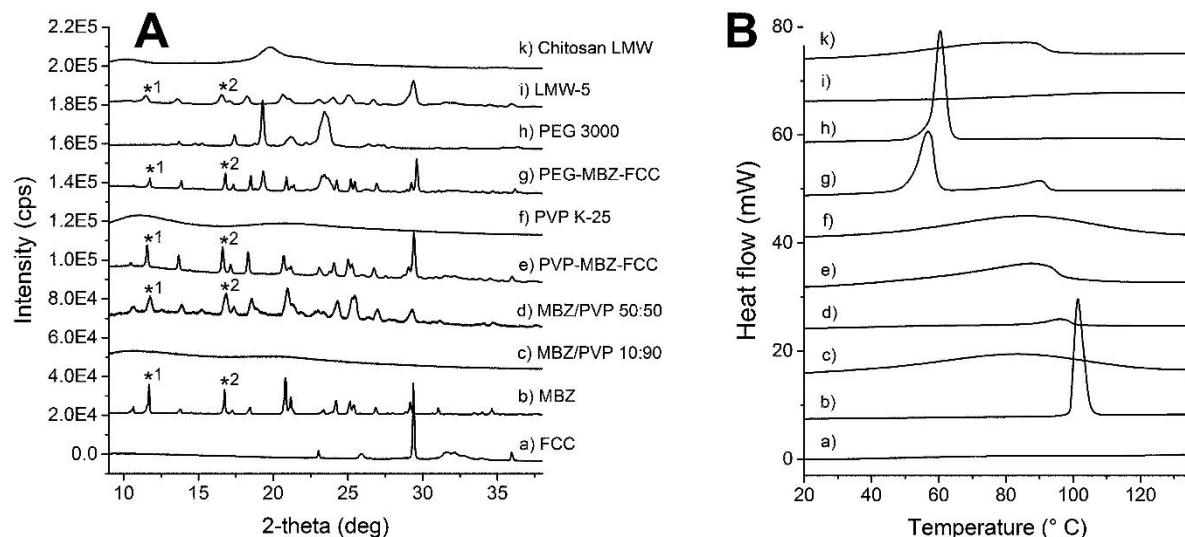


Fig. 7. Results of XRPD (A) and DSC analysis (B) of (a) FCC; (b) crystalline MBZ; (c) co-evaporate of MBZ and PVP (10:90, w/w) with all drugs in amorphous state; (d) co-evaporate of MBZ and PVP (50:50, w/w) with drug in crystalline state; (e) PVP-MBZ-FCC; (f) PVP K-25; (g) PEG-MBZ-FCC; and (h) PEG 3000. XRPD peaks labelled with *1 and *2 are characteristic for crystalline MBZ.

3.7. Differential scanning calorimetry (DSC)

Representative plots of DSC analysis are shown in Fig. 7A. For the crystalline MBZ, a sharp endothermic peak was observed at 101.5 ± 0.1 °C with a melting enthalpy of 93.0 ± 0.9 J/g. For the PEG-MBZ-FCC particles with a drug load of 28.57% (w/w), a first peak was detected close to 60 °C, which is in line with the endothermic peak from PEG alone. Therefore, the second peak at 90.3 ± 0.3 with a melting enthalpy of 13.10 ± 0.8 J/g corresponds to MBZ, even though the peak onset was shifted to lower temperatures. The melting enthalpy lower than the expected value for 28.57% of crystalline MBZ (26.6 J/g), and the peak onset shifted to lower temperatures were already observed previously in drug-loaded FCC samples [37]. It is also likely that MBZ has partially dissolved in liquid PEG resulting in an apparently reduced melting enthalpy. In case of PVP-MBZ-FCC particles, determination of melting enthalpy of MBZ was not possible due to the strongly interfering heat-flow curve of amorphous PVP.

4. Discussions

In this study, we present for the first time data on particle retention of chitosan-coated microparticles prepared in a fluidized-bed process. MMW-10 particles showed a 3-fold increase in particle retention compared to MMW-5 (see Fig. 2A). The LMW-5 particles also showed good *in vitro* particle retention ($55.35\% \pm 5.94\%$) in comparison with non-mucoadhesive EC-5 particles. The use of LMW chitosan with lower concentration in the spray solution had a big advantage compared to MMW chitosan in terms of manufacturability, since the shorter chain length of chitosan and the lower concentration in the spray solution (1% vs. 1.5%) decreased the viscosity which was important to reduce the risk of nozzle blocking. Further optimizations of the LMW-5 formulation led to a higher drug load (see Table 1), i.e. higher dose, and a reduced process time due to increased spray rate of the chitosan coating solution (see Table 2).

Dissolution studies were performed using the USP IV apparatus since the resulting drug-release profiles were found to be similar to the results measured in the flow channel [26]. However, mucoadhesive microparticles tested in the USP IV apparatus have shown a strong agglomeration tendency, potentially affecting particle retention. To overcome this issue, we investigated the dispersibility-enhancing effect of dry-particle coating with nano-sized colloidal silica. A silica concentration in the range of 0.10.5% (w/w) is often used as a lubricant or glidant in tablets, and higher concentrations of 24% (w/w) were reported to act as a disintegrant [38]. In our study, we used relatively high silica concentrations (110%, w/w) to achieve the desired disintegration properties. From a toxicological point of view, it was reported that oral intake of colloidal silica up to 1500 mg/day is of no safety concern [39]. The simple blending and sieving process led to homogeneous silica monolayers adsorbed to the chitosan surfaces as shown in a typical example of an SEM image with high magnification (see Fig. 5I). However, the main fraction of silica was agglomerated and not adsorbed as shown by the arrows in Fig. 5H. These silica agglomerates were considered to be the main mechanism of improved dispersibility. Measuring drug dissolution in the USP IV apparatus presented a feasible method for indirect quantitative measurement of dispersibility. According to Noyes-Whitney and Nernst-Brunner equation (Eq. (4)), the surface area at the interface of the dissolution medium (A), and the thickness of the diffusion layer to the interface of the dissolution medium (d) are the two factors which influence the dissolution rate (dm/dt) when agglomerates are formed.

$$\frac{dm}{dt} = A \frac{D}{d} (C_s - C_b) \quad (4)$$

where D is the diffusion coefficient, C_s is the drug solubility, and C_b is the drug concentration in the bulk medium [40]. Dispersibility enhancement means smaller agglomerates and more individual particles, i.e. a larger surface area and a shorter thickness of the diffusion layer, both of which increase the dissolution rate. This hypothesis was confirmed by the experimental data shown in Fig. 3B, where the dissolution rate and drug release after 10 h were increased with higher silica concentrations. All silica-coated mucoadhesive formulations showed a controlled release over several hours, which is desired for local treatment of colonic diseases directly at the site of action for prolonged period of time.

The mucoadhesion of LMW-5 particles coated with 2% and 5% (w/w) silica was marginally improved in comparison with non-coated LMW-5 particles, however, without significant difference ($p > 0.1$). This is explained by the hydrophilic nature of the silica nanoparticles which allows them to diffuse into the hydrated chitosan coating and mucin meshwork, and interpenetration of the chitosan polymer chains into the mucin meshwork is not hindered. This assumption has to be further investigated with cryo-SEM or cryo-TEM imaging techniques to confirm an entanglement of the polymer and mucin chains. Contrarily, coating with 10% (w/w) silica decreased the mucoadhesivity significantly ($p < 0.005$) as shown in Fig. 2C, probably due to an oversaturation with silica agglomerates, preventing a close contact of the chitosan polymer chains with the mucus. Thus, silica nanoparticles used as a dispersant aid may reduce drug-mucosa contact, thus affecting mucoadhesivity.

In addition to the chitosan coating, the fluidized-bed process was also shown to be feasible for drug loading of porous microcarriers with particle sizes from 5 to 12 µm and outer-pore sizes of approximately 0.1–1 µm. Qualitative SEM analysis confirmed that the outer pores were filled as shown in Fig. 5A–C. Since the fluidized-bed method is well suited for scale-up, it is preferable to the previously reported solvent-evaporation method [37]. Drug dissolution rates of PVP-MBZ-FCC and PEG-MBZ-FCC particles were much higher than those of pure MBZ powder as shown in Fig. 3. This increased dissolution rate was associated with the enlarged surface area of the inert microcarrier (FCC) as demonstrated recently [37], and probably also due to the solubility-enhancing effect given by the polymers. In both drug-loaded batches, MBZ was present in a crystalline state as demonstrated by XRPD and DSC analysis (see Fig. 7A and B), which could be an indicator for long shelf-life of the drug product [32]. It was not possible to distinguish between different crystal polymorphs based on registered diffraction patterns. However, a distinction between the amorphous and the crystalline state was possible. In case of PVP-MBZ-FCC particles, analysis of SEM images made it possible to identify drug crystals embedded in the polymer matrix. XRPD analysis of the co-evaporates with a drug-to-polymer ratio of 50:50 (w/w) showed that MBZ was not in an amorphous phase, hence, cannot contribute to increased dissolution rates. As a reference for solid dispersions, co-evaporation of PVP and MBZ in a high ratio of 90:10 (w/w) was performed, resulting in a glassy material. The absence of characteristic peaks in the X-ray diffraction pattern indicated that MBZ was present in amorphous form. This indicates a usability of the fluidized-bed process for preparation of mucoadhesive microparticles containing the drug as a solid dispersion. However, a higher drug-to-polymer ratio is required, which is decreasing the drug load, and potentially leading to drug stability issues [32].

5. Conclusions

The fluidized-bed process is a suitable method for preparation of mucoadhesive microparticles by applying a two-step method, i.e. drug loading and chitosan coating. The optimized LMW-5 particles showed good manufacturability, high drug load, and a good *in vitro* particle retention on porcine colonic mucosa. Dry coating of the chitosan-coated microparticles with hydrophilic fumed silica improved the dispersibility as indicated by visual observation and dissolution studies. Moreover, mucoadhesion was not negatively influenced by colloidal silica particles up to 5% (w/w) concentration. Since the formulation approach described here is applicable to other drugs, the results of this study present a basis for further development and optimization of mucoadhesive dosage forms for local treatment of gastrointestinal diseases.

Acknowledgements

This project was financially supported by the Swiss Commission of Technology and Innovation (grant number: 13742.1 PFFLR-LS) and Tillotts Pharma AG. The authors thank Dr. Markus Dürrenberger at the microscopy centre (University of Basel) for the assistance in using the SEM, Mrs. Evelyn Mühle from Centravo AG for providing fresh samples of porcine colonic tissue, Dr. Gabriela Québatte for her support with XRPD analysis, and Darryl Borland for editorial assistance.

References

- G.P. Andrews, T.P. Laverty, D.S. Jones, Mucoadhesive polymeric platforms for controlled drug delivery, *Eur. J. Pharm. Biopharm.* 71 (2009) 505–518, <http://dx.doi.org/10.1016/j.ejpb.2008.09.028>.
- V. Hearnden, V. Sankar, K. Hull, D.V. Juras, M. Greenberg, A.R. Kerr, et al., New developments and opportunities in oral mucosal drug delivery for local and systemic disease, *Adv. Drug Deliv. Rev.* 64 (2012) 16–28, <http://dx.doi.org/10.1016/j.addr.2011.02.008>.
- J.F. Pinto, Site-specific drug delivery systems within the gastro-intestinal tract: from the mouth to the colon, *Int. J. Pharm.* 395 (2010) 44–52, <http://dx.doi.org/10.1016/j.ijpharm.2010.05.003>.
- G. Van den Mooter, Colon drug delivery, *Expert Opin. Drug Deliv.* 3 (2005) 111–125, <http://dx.doi.org/10.1517/17425247.3.1.111>.
- A.K. Philip, B. Philip, Colon targeted drug delivery systems: a review on primary and novel approaches, *Oman Med. J.* 25 (2010) 79–87, <http://dx.doi.org/10.5001/omj.2010.24>.
- E.F. Stange, S.P.L. Travis, The European consensus on ulcerative colitis: new horizons?, *Gut* 57 (2008) 1029–1031, <http://dx.doi.org/10.1136/gut.2007.146761>.
- C. Schiller, C.-P. Fröhlich, T. Giessmann, W. Siegmund, H. Mönnikes, N. Hosten, et al., Intestinal fluid volumes and transit of dosage forms as assessed by magnetic resonance imaging, *Aliment. Pharmacol. Ther.* 22 (2005) 971–979, <http://dx.doi.org/10.1111/j.1365-2036.2005.02683.x>.
- F.J.O. Varum, E.L. McConnell, J.S. Sousa, F. Veiga, A.W. Basit, Mucoadhesion and the gastrointestinal tract, *Crit. Rev. Ther. Drug Carrier Syst.* 25 (2008) 207–258.
- M.E.A. McGirr, S.M. McAllister, E.E. Peters, A.W. Vickers, A.F. Parr, A.W. Basit, The use of the IntelliSite® Companion device to deliver mucoadhesive polymers to the dog colon, *Eur. J. Pharm. Sci.* 36 (2009) 386–391, <http://dx.doi.org/10.1016/j.ejps.2008.11.007>.
- B. Abrahamsson, M. Alpstén, U.E. Jonsson, P.J. Lundberg, A. Sandberg, M. Sundgren, et al., Gastro-intestinal transit of a multiple-unit formulation (metoprolol CR/ZOK) and a non-disintegrating tablet with the emphasis on colon, *Int. J. Pharm.* 140 (1996) 229–235, [http://dx.doi.org/10.1016/0378-5173\(96\)04604-2](http://dx.doi.org/10.1016/0378-5173(96)04604-2).
- F.J.O. Varum, H.A. Merchant, A.W. Basit, Oral modified-release formulations in motion: the relationship between gastrointestinal transit and drug absorption, *Int. J. Pharm.* 395 (2010) 26–36, <http://dx.doi.org/10.1016/j.ijpharm.2010.04.046>.
- H. Takeuchi, H. Yamamoto, Y. Kawashima, Mucoadhesive nanoparticulate systems for peptide drug delivery, *Adv. Drug Deliv. Rev.* 47 (2001) 39–54, [http://dx.doi.org/10.1016/S0169-409X\(00\)00120-4](http://dx.doi.org/10.1016/S0169-409X(00)00120-4).
- S. Sakuma, R. Sudo, N. Suzuki, H. Kikuchi, M. Akashi, Y. Ishida, et al., Behavior of mucoadhesive nanoparticles having hydrophilic polymeric chains in the intestine, *J. Control. Release* 81 (2002) 281–290, [http://dx.doi.org/10.1016/S0168-3659\(02\)00072-X](http://dx.doi.org/10.1016/S0168-3659(02)00072-X).
- A. Sosnik, J. das Neves, B. Sarmiento, Mucoadhesive polymers in the design of nano-drug delivery systems for administration by non-parenteral routes: a review, *Prog. Polym. Sci.* 39 (2014) 2030–2075, <http://dx.doi.org/10.1016/j.progpolymsci.2014.07.010>.
- A. De Ascentiis, J.L. deGrazia, C.N. Bowman, P. Colombo, N.A. Peppas, Mucoadhesion of poly(2-hydroxyethyl methacrylate) is improved when linear poly(ethylene oxide) chains are added to the polymer network, *J. Control. Release* 33 (1995) 197–201, [http://dx.doi.org/10.1016/0168-3659\(94\)00087-B](http://dx.doi.org/10.1016/0168-3659(94)00087-B).
- K.P.R. Chowdary, Y.S. Rao, Mucoadhesive microspheres for controlled drug delivery, *Biol. Pharm. Bull.* 27 (2004) 1717–1724.
- J. Möschwitzer, R.H. Müller, Spray coated pellets as carrier system for mucoadhesive drug nanocrystals, *Eur. J. Pharm. Biopharm.* 62 (2006) 282–287, <http://dx.doi.org/10.1016/j.ejpb.2005.09.005>.
- T. Pengpong, P. Sangvanich, K. Sirilertmukul, N. Muangsin, Design, synthesis and *in vitro* evaluation of mucoadhesive p-coumarate-thiolated-chitosan as a hydrophobic drug carriers, *Eur. J. Pharm. Biopharm.* 86 (2014) 487–497, <http://dx.doi.org/10.1016/j.ejpb.2013.11.009>.
- F.J.O. Varum, F. Veiga, J.S. Sousa, A.W. Basit, Mucoadhesive platforms for targeted delivery to the colon, *Int. J. Pharm.* 420 (2011) 11–19, <http://dx.doi.org/10.1016/j.ijpharm.2011.08.006>.
- Q.-R. Cao, Y. Liu, W.-J. Xu, B.-J. Lee, M. Yang, J.-H. Cui, Enhanced oral bioavailability of novel mucoadhesive pellets containing valsartan prepared by a dry powder-coating technique, *Int. J. Pharm.* 434 (2012) 325–333, <http://dx.doi.org/10.1016/j.ijpharm.2012.05.076>.
- C. Schmidt, C. Lautenschlaeger, E.-M. Collnot, M. Schumann, C. Bojarski, J.-D. Schulzke, et al., Nano- and microscaled particles for drug targeting to inflamed intestinal mucosa—a first *in vivo* study in human patients, *J. Control. Release* 165 (2013) 139–145, <http://dx.doi.org/10.1016/j.jconrel.2012.10.019>.
- P. He, S.S. Davis, L. Illum, *In vitro* evaluation of the mucoadhesive properties of chitosan microspheres, *Int. J. Pharm.* 166 (1998) 75–88, [http://dx.doi.org/10.1016/S0378-5173\(98\)00027-1](http://dx.doi.org/10.1016/S0378-5173(98)00027-1).
- V.S. Belgamwar, S.J. Surana, Design and development of oral mucoadhesive multiparticulate system containing atenolol: *in vitro*-*in vivo* characterization, *Chem. Pharm. Bull. (Tokyo)* 58 (2010) 1168–1175.
- Z. Liu, W. Lu, L. Qian, X. Zhang, P. Zeng, J. Pan, *In vitro* and *in vivo* studies on mucoadhesive microspheres of amoxicillin, *J. Control. Release* 102 (2005) 135–144, <http://dx.doi.org/10.1016/j.jconrel.2004.06.022>.
- J.K. Patel, P.S. Patil, V.B. Sutariya, Formulation and characterization of mucoadhesive microparticles of cinnarizine hydrochloride using supercritical fluid technique, *Curr. Drug Deliv.* 10 (2013) 317–325.
- D. Preisig, M. Weingartner, F.J.O. Varum, R. Bravo, R. Alles, J. Huwyler, et al., Marker-ion analysis for quantification of mucoadhesivity of microparticles in particle-retention assays, *Int. J. Pharm.* 487 (2015) 157–166, <http://dx.doi.org/10.1016/j.ijpharm.2015.04.020>.
- D.B. Beten, K. Amighi, A.J. Moës, Preparation of controlled-release coevaporates of dipyrnidamole by loading neutral pellets in a fluidized-bed coating system, *Pharm. Res.* 12 (1995) 1269–1272.
- S. Muschert, F. Siepmann, B. Leclercq, B. Carlin, J. Siepmann, Drug release mechanisms from ethylcellulose: PVA-PEG graft copolymer-coated pellets, *Eur. J. Pharm. Biopharm.* 72 (2009) 130–137, <http://dx.doi.org/10.1016/j.ejpb.2008.12.007>.
- T. Linnell, H.A. Santos, E. Mäkilä, T. Heikkilä, J. Salonen, D.Y. Murzin, et al., Drug delivery formulations of ordered and nonordered mesoporous silica: comparison of three drug loading methods, *J. Pharm. Sci.* 100 (2011) 3294–3306, <http://dx.doi.org/10.1002/jps.22577>.
- H.-O. Ho, H.-L. Su, T. Tsai, M.-T. Sheu, The preparation and characterization of solid dispersions on pellets using a fluidized-bed system, *Int. J. Pharm.* 139 (1996) 223–229, [http://dx.doi.org/10.1016/0378-5173\(96\)04594-2](http://dx.doi.org/10.1016/0378-5173(96)04594-2).
- N. Sun, X. Zhang, Y. Lu, W. Wu, *In vitro* evaluation and pharmacokinetics in dogs of solid dispersion pellets containing *Silybum marianum* extract prepared by fluidized-bed coating, *Planta Med.* 74 (2008) 126–132, <http://dx.doi.org/10.1055/s-2008-1034294>.
- C. Leuner, J. Dressman, Improving drug solubility for oral delivery using solid dispersions, *Eur. J. Pharm. Biopharm.* 50 (2000) 47–60, [http://dx.doi.org/10.1016/S0939-6411\(00\)00076-X](http://dx.doi.org/10.1016/S0939-6411(00)00076-X).
- Sigma-Aldrich specification sheet of medium molecular weight chitosan, <http://www.sigmaaldrich.com/Graphics/COFAInfo/SigmaSAPQM/SPEC/44/448877/448877-BULK_____ALDRICH_.pdf>, 2015.
- Sigma-Aldrich specification sheet of medium molecular weight chitosan, <http://www.sigmaaldrich.com/Graphics/COFAInfo/SigmaSAPQM/SPEC/44/448877/448877-BULK_____ALDRICH_.pdf>, 2015.
- F.J.O. Varum, F. Veiga, J.S. Sousa, A.W. Basit, An investigation into the role of mucus thickness on mucoadhesion in the gastrointestinal tract of pig, *Eur. J. Pharm. Sci.* 40 (2010) 335–341, <http://dx.doi.org/10.1016/j.ejps.2010.04.007>.
- Cation Analysis Kit <<http://www.absciex.com/Documents/Products/CationAnalysisUsersGuide.pdf>> 2013 (accessed November 1, 2014).
- D. Preisig, D. Haid, F.J.O. Varum, R. Bravo, R. Alles, J. Huwyler, et al., Drug loading into porous calcium carbonate microparticles by solvent evaporation, *Eur. J. Pharm. Biopharm.* 87 (2014) 548–558, <http://dx.doi.org/10.1016/j.ejpb.2014.02.009>.
- C. Hunnius, *Hunnius Pharmazeutisches Wörterbuch*, De Gruyter, 1998.
- U. Charoniere, D. Gott, Calcium silicate and silicon dioxide/silicic acid gel added for nutritional purposes to food supplements, *EFSA ANS* 1132 (2009) 1–24, <http://dx.doi.org/10.2903/j.efsa.2009.1132>.
- P. Macheras, A. Iliadis, Modeling in Biopharmaceutics, Pharmacokinetics and Pharmacodynamics: Homogeneous and Heterogeneous Approaches, Springer Science & Business Media, 2006.

4 Clinical study protocol

To investigate the gastrointestinal transit times of two different multiparticulate formulations (mucoadhesive vs. non-mucoadhesive), a pharmaco scintigraphy study on human subjects was designed in the scope of this collaboration project. The preparation of the Phase-1 clinical trial was managed and performed by Tillotts Pharma and the University Hospital. In the context of the global project, the study protocol is here briefly described

Formulation A consists of mucoadhesive microparticles and is expected to show increased colonic transit time in comparison to Formulation B which consists of non-mucoadhesive microparticles. Both formulations contain the antibiotic drug metronidazole benzoate (100 mg/capsule) and samarium oxide (5 mg/capsule) as radioactive marker. Both formulations are filled into hard-shell capsules coated with a novel and patented colonic targeting coating system, which disintegrate upon arrival in the colon.

Each formulation will be tested in 9 fasted, healthy volunteers, i.e. 18 subjects are recruited in total. Each subject receives one capsule by oral administration. The radiolabeling of the microparticles is based on neutron activation of the incorporated samarium oxide. In this process, the stable isotope Sm-152 contained in samarium oxide is converted to Sm-153, and the activated capsules are stored in radiation protection containers till administration. Before administration to the volunteers, the capsules are tested at the site of clinical investigation to ensure a radioactivity of ≤ 1 MBq, corresponding to 0.8 mSv (effective dose of radiation), which is considered to be harmless [235]. As a comparison, the annual radiation exposure of the average population in Switzerland is 3.2 mSv [236].

On day 1 of the study, pre-dose PK sampling and pre-dose scintigraphy of the fasted subjects will be done before capsule intake to measure the baseline. After capsule intake (at 8:00), PK sampling and scintigraphy will be done at following time points (in hours): 1, 2, 3, 4, 4.5, 5, 5.5, 6, 6.5, 7, 7.5, 8, 9, 10, 11, 12, 13, 14, 15, 16, 24, 48 h post dose. The last sampling on day 1 is done at midnight (16 h post dose). The subjects can stay overnight or go home. On day 2 and day 3, there will be one sampling in the morning (24 h and 48 h post dose). On day 7, a follow-up investigation is done to finish the study.

For determination of standard PK parameters, concentrations of metronidazole and its metabolites are analyzed in blood. Among others, following PK parameters will be determined: Maximum plasma concentration (C_{\max}); time to reach C_{\max} (T_{\max}); area under the concentration-time curve from dosing to 48 h post-dose (AUC_{0-t}); elimination rate constant

(k); and lag time (T_{lag}) which is defined as the time (post-dose) of the last blood sample with a non-quantifiable metronidazole plasma concentration.

Localization of initial capsule disintegration is mainly assessed by comparison of scintigraphy images (T_{lag} not only reflects the capsule disintegration and drug dissolution, but also hydrolysis of MBZ to metronidazole). The released granules are recognizable as a scintigraphic cloud, and their colonic residence time can be determined visually by comparison of a series of scintigraphy images taken over time after capsule rupture. In addition, gastric emptying time, small intestinal transit time, ileocecal junction residence time, and colonic arrival time are determined using the same method. Furthermore, the scintigraphic images will be quantitatively analyzed by dividing into two regions of interest (ROI), i.e. right side (ROI 1) and left side (ROI 2) as shown in Fig. 4.1. ROI 1 covers the ileocecal junction, ascending colon, and the right half of the transverse colon, whereas ROI 2 covers the left half of the transverse colon, the descending colon, and the rectum. For each ROI, mean values of signal intensity from anterior and posterior images are calculated. The ratio of ROI 1 to ROI 2 will be used as quantitative parameter to compare colonic residence time from both formulations. For each time point, average ROI values of all nine subjects tested with mucoadhesive formulation can be calculated and compared to average ROI of the nine subjects tested with non-mucoadhesive formulation.

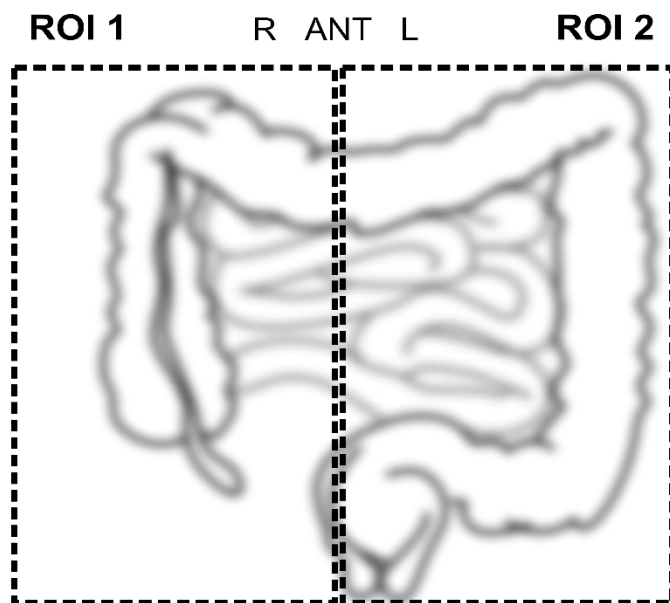


Fig. 4.1: The two ROIs for quantitative analysis of scintigraphy images.
R = right; L = left, ANT = anterior

5 Discussions

The development of the presented multiparticulate and mucoadhesive formulation platform for colon delivery consisted of three steps. The different solvent-evaporation methods for drug loading into FCC and the underlying mechanisms are discussed in Chapter 5.1. Technical aspects of mucoadhesive coating and *in vitro* particle retention of microparticles are discussed in Chapter 5.2 and 5.3, respectively. The *in vivo* potential of mucoadhesive colon drug delivery systems is discussed in Chapter 5.4. The development of the colonic-targeted capsule coating was carried out by Tillotts Pharma based on their patented technology and internal know-how and is not part of this thesis.

5.1 Drug loading into FCC

The novel pharmaceutical excipient FCC was demonstrated to be a feasible carrier material for various types of drugs, and drug loading was performed in a rotary evaporator [231], or a fluidized-bed process [237]. For both methods, the drug-loading mechanism is based on solvent evaporation and drug crystallization in the outer-porous domain of FCC. This is in contrast to immersion methods which are based on drug adsorption to the porous carriers [238–244], and which were often used for drug loading of mesoporous nanomaterials. The advantages of the presented solvent-evaporation methods are higher loading efficiencies and precise control of the loaded drug content.

A drawback of the solvent-evaporation method is that loading efficiency (which has to be differentiated from the drug load) has to be determined qualitatively by SEM analysis, since non-loaded drug crystals cannot be separated from the drug-loaded particles to perform quantitative analysis of loading efficiency. Agglomerates are formed by drug crystals growing in the interparticle voids, and thus, agglomerates were also a sign of inefficient drug loading. Loading efficiencies of the tested drugs were excellent up to a drug load of 35-40%, which was defined as the drug-loading capacity. The excellent loading efficiencies can be explained by heterogeneous nucleation on the outer lamellas of FCC [245]. Heterogeneous nucleation is the formation of critical drug clusters (nuclei) on a pre-existing surface, which requires less energy in comparison to nucleation without pre-existing surfaces (homogeneous nucleation). Hence, the drug preferably crystallizes on the large lamellar surface of FCC.

The high drug-loading capacities, up to 40% (w/w), were possible due the macroporous characteristics (0.05-1 μm pore size) of the outer stratum of FCC. Measurement of pore-size distribution by mercury intrusion revealed that most drug was deposited in the outer-porous

domain of FCC, and not in the mesoporous inner core. This was possibly due to higher crystallization pressures occurring in mesoporous systems [246]. The possibility to increase the drug-loading capacity by slowing down the evaporation process was exploited (decreasing the pressure by 50 mbar instead of 100 mbar per 0.5 hour), but no improvement of drug-loading efficiency could be achieved at high drug loads of 45% (results not shown). Hence, the drug was preferably crystallizing in the outer pores with diameters up to 1 μm [231]. Accordingly, drug-loading by solvent evaporation might not be suitable for mesoporous drug carriers, as the crystals preferably grow outside the particles [246]. Therefore, comparative studies with mesoporous microparticles, such as AEROPERL® or Neusilin US2, have not been carried out.

Despite a deposition of mainly crystalline drug (not amorphous), drug dissolution rates were increased for MBZ- and nifedipine-loaded FCC in comparison to drug powder. This effect was explained by the increased surface area associated with the high porosity of FCC and its small particle size (5-15 μm). Therefore, drug loading into FCC presents an effective strategy for oral delivery of poorly water-soluble drugs. Based on these mechanistic investigations, further developments were carried out to improve the drug-loading method in terms of manufacturability and increased drug-release rates.

The fluidized-bed process was evaluated for drug loading into FCC using MBZ as model drug for treatment of colonic diseases. Preliminary trials with a drug load of 40% (w/w) showed excellent loading efficiency and similar pore-size distribution data as for particles obtained by the rotary-evaporation method. This is not surprising, as the mechanism of drug loading in the fluidized-bed process is very similar to the solvent-evaporation method using the rotary evaporator, meaning that drug crystallization occurs on the large surface area of the outer pores of FCC. The main difference is that drying is not based on reduced pressures, but on heat and moisture transfer by applying an air flow at elevated temperature. However, it was important to adjust the parameters as such that no spray drying effect occurred, i.e. that the spray solution did not dry before it got in contact with FCC particles. Linnell *et al.* [247] have already demonstrated the feasibility of the fluidized-bed process for drug loading of indomethacin into two different types of mesoporous silica. However, the advantage of FCC is the macroporous outer stratum allowing higher drug loads than for mesoporous materials.

The fluidized-bed process offered the possibility of co-spraying solubility-enhancing polymers. In the performed drug-loading experiments, PVP K-25 and PEG 3000 were used in a drug-to-polymer ratio of 50:50 (w/w). Based on SEM and XRPD analysis, it was found that the loaded drug was present in a crystalline state, embedded in the polymer matrix [237]. Stabilization of the drug in amorphous form is possible by increasing the amount of polymer,

and could be a strategy to increase the drug dissolution rate. However, this would reduce the drug loading capacity.

Co-loading with hydrophilic polymers was also hypothesized to be useful to improve the homogeneity of the subsequent chitosan coating. MBZ-loaded FCC without co-loaded polymer has a hydrophobic surface due to the hydrophobicity of MBZ, and hence, a poor wettability of the spray solution is expected [248]. Hydrophilization of the particle surface by co-loading with PVP or PEG should lead to better wettability [249] of the chitosan spray solution on the particle surface.

To improve the flowability of FCC, granulation by roller compaction could be performed prior to drug loading [228], provided that the macroporous characteristics of the outer stratum is not lost after granulation. Such a larger particle size of the FCC granules (e.g. around 100 μm) would also be beneficial for the subsequent chitosan-coating step to avoid further granulation, and to improve the reproducibility of the chitosan-coated particles in terms of particle size distribution and mucoadhesivity. It should be noted that the mean particle sizes (D50) of the three different chitosan-coating batches MMW-5, MMW-10, and LMW-5 were highly variable, i.e. $54.4 \pm 2.0 \mu\text{m}$, $183.5 \pm 10.0 \mu\text{m}$, and $190.9 \pm 11.0 \mu\text{m}$, respectively [237].

5.2 Mucoadhesive coating of microparticles

For mucoadhesive coating of microparticles, a pH-dependent precipitation method [86] and a fluidized-bed method [237] were developed. In both methods, the semi-synthetic polymer chitosan was used for mucoadhesive coating. Chitosan is well known for its biodegradability, biocompatibility, and excellent mucoadhesivity. The relatively low viscosity of dilute chitosan solutions was an additional important property for the feasibility of the reported methods.

The development of a precipitation method was possible due to the pH-dependent solubility of chitosan which is insoluble at $\text{pH} > 6$. The method was modified from Han *et al.* [250] who prepared hollow chitosan capsules by repeated incubation of calcium carbonate particles in buffered chitosan solutions. For the preparation of the presented mucoadhesive microparticles, dissolution of the core particles was not desired, and the micrometer thick chitosan coating was obtained in one precipitation cycle. For titration of the chitosan solution, highly diluted NaOH was used (0.05 M) in order to prevent fast and locally increased precipitation. It can be assumed that chitosan precipitated directly on the surface of FCC particles due to heterogeneous nucleation [245] and the ionic interactions with calcium carbonate [250]. A critical step in the method was the initial suspension of the drug-loaded

FCC in the slightly acidic chitosan solution (pH 5), leading to partial decomposition of calcium carbonate and dissolution of MBZ. However, the amount of decomposed FCC during the whole precipitation process was only 3% (w/w) as measured by calcium-ion analysis of the remaining solution. The fraction of dissolved drug was calculated to be very similar (3.5%, w/w) based on the solubility of MBZ. Eventually, FCC, MBZ and chitosan contents were all close to the expected values. Nevertheless, for development of a delivery platform also applicable to water soluble drugs, alternative methods had to be evaluated to achieve reproducible mucoadhesive coatings on microparticles.

Established pharmaceutical processes have been evaluated in preliminary trials, e.g. lyophilization and spray drying. However, only the fluidized-bed process was feasible for mucoadhesive coating of microparticles. The drug-loaded FCC particles were spray-coated with a chitosan solution. This approach had several advantages compared to the precipitation method, such as larger batch size, higher production yields, and better suitability for scale-up. Furthermore, the absence of a milling step was of great importance in terms of mucoadhesive performance since there was no destruction of the chitosan coating. As a consequence, a lower amount of chitosan coating was required compared to the precipitation method to obtain particles with similar mucoadhesivity. Regarding the manufacturability, low molecular weight (LMW) chitosan was superior to medium molecular weight (MMW) chitosan due to the reduced viscosity of the spray solution minimizing the risk of nozzle blocking. In the optimized formulation method, a higher spray rate was used (5 g/min vs. 1.5 g/min) to reduce the process time. However, it has to be mentioned that this high spray rate resulted in larger granules ($D_{50} \approx 190 \mu\text{m}$), even though only 5% (w/w) of LMW chitosan was applied. Hence, the spray rate presents a critical process parameter that could be optimized to obtain smaller particles.

In addition, the development of non-mucoadhesive microparticles with similar mean particle size was required as control in the *in vitro* flow-detachment experiments, and as comparison to the mucoadhesive microparticles in the planned *in vivo* gamma-scintigraphy studies. For this purpose, MBZ-loaded FCC was granulated with ethylcellulose in a fluidized-bed process by spraying an aqueous binder solution containing PVP K-25. The prepared control particles had a median particle size of $115.2 \pm 3.5 \mu\text{m}$, and practically no mucoadhesive interactions on colonic mucosa was measured (mean particle retention was $6.7\% \pm 8.4\%$, $n=3$). Therefore, these ethylcellulose particles are suited to be used as non-mucoadhesive control in the gamma-scintigraphy studies in humans.

5.3 Investigation of *in vitro* particle-retention

For evaluation of mucoadhesive properties of prepared microparticles, a suitable *in vitro* mucoadhesion test was developed. To simulate the drag forces acting on the particles in the gastrointestinal tract, a flow-detachment method was preferred to the commonly used tensile-detachment method. A flow-channel device with an improved design was built in-house, and marker-ion analysis (calcium) was applied for reliable quantification of microparticles [86].

The development of the flow-channel device required several preliminary tests to evaluate the optimal channel geometry. In a closed channel with laminar flow regime, the flow velocity at the solid-fluid interface was too low to set the particles in motion, regardless of their mucoadhesive interactions. The problem observed in the semi-cylindrical channel was that the fluid formed a thin stream with an unreproducible (eddy) flow pattern. Therefore, the flat open channel was evaluated as the most suitable channel geometry. The use of multiple nozzles for inlet flow, as proposed by Batchelor *et al.* [76], was found to be an important feature to ensure homogeneous flow distribution throughout the channel area.

A new feature of our design was the mucosa holder on the support plate, on which the mucosal tissue could be clamped with the fixation plate. To prevent excessive mucosa from squeezing into the channel, a void space surrounding the mucosa holder was necessary. The sealing was tight enough to prevent leakage of the flow medium. Furthermore, the mucosal tissue remained firmly attached to the support plate during the whole experiment without additional fixation aids such as pins [84] or low vacuum [88,94,251]. To simulate the targeted tissue of our formulations, porcine colonic mucosa was used as substrate in the particle-retention assay, as it shows similarities to the human colonic mucosa in terms of anatomy and mucin structure [252].

Direct quantification of the inert carrier particle theoretically presents a more precise and reliable method compared to usual methods such as visual counting, which is limited to a certain particle size, and weighing of collected solids, which is biased by detached mucus and dissolved drug. The high sensitivity of the marker-ion analysis allowed for the first time precise characterization of mucoadhesive microparticles without additional labeling. However, the feasibility of using calcium ions as a marker to quantify the detached particles had to be evaluated first, since calcium ions are abundant in biological tissues. Indeed, control experiments without any microparticles showed relatively high amount of tissue-derived calcium. However, validation of the marker-ion analysis by image analysis of detached particles retained on a black filter showed a different picture. The projected area of photographed particles was in good correlation with the calcium concentration measured by capillary electrophoresis. Hence, the influence of tissue-derived calcium flux was found to be

negligible when the mucosa was covered with FCC particles. Therefore, marker-ion analysis was routinely applied for particle quantification in collected fractions. The obtained results usually showed low standard deviations, and FCC recoveries close to 100%, indicating a good precision and accuracy of the method. As an alternative to capillary electrophoresis, other methods for quantification of calcium ions could be used, such as flame atomic absorption spectrometry or ion chromatography. The applicability of marker-ion analysis to other carrier materials such as silica or alumina has to be assessed individually.

Investigation of two size fractions of microparticles (<90 μm and 125-250 μm) revealed a size-dependent *in vitro* retention behavior. It was shown that bigger particles were significantly better retained on mucosal tissue than the smaller ones, which was consistent for all four chitosan concentrations (0%, 9.1%, 16.7%, and 33.3%, w/w). This finding is contradictory to generally accepted mucoadhesion theories. Since this size-dependency was also observed for non-mucoadhesive control particles, additional retention mechanisms other than mucoadhesive interactions were involved. This can be explained by the forces acting on a particle in an open channel flow [86].

To set a particle in motion, the resulting weight of the particle has to be exceeded by the drag force, which is exerted by the fluid onto the particle. However, the ratio of resulting weight to drag force increases exponentially with increasing particle size. Hence, bigger particles can resist better the washout, and control experiments with particles of similar size and density would be ideal for correct data interpretation. However, particles prepared in the fluidized-bed had wide particle size distributions and varying median diameters (D50). Mucoadhesive microparticles coated with 5% of MMW chitosan (MMW-5, w/w) were the smallest (D50 \approx 55 μm) and the ones coated with 5% of LMW chitosan (LMW-5, w/w) were the largest (D50 \approx 190 μm), as measured by a Camsizer XT instrument. Since grinding would destroy the mucoadhesive coating, and size fractionation was not possible due to insufficient batch sizes, it was very difficult to prepare non-mucoadhesive control particles with similar D50 and size distribution. Therefore, the D50 of the non-mucoadhesive ethylcellulose control particles should be in between the MMW-5 and LMW-5 particles. This was well achieved since the control particles had a D50 of 115 μm .

All chitosan formulations prepared in the fluidized-bed showed significantly improved particle retention compared to the ethylcellulose control particles. The optimized mucoadhesive formulation coated with 5% LMW chitosan was selected as a prototype for the pharmaco-scintigraphy study in humans due to the good *in vitro* particle retention and manufacturability.

5.4 *In vitro* assessment of colonic mucoadhesion and *in vivo* considerations

The particle-retention assay was a useful indicative tool to characterize and optimize the mucoadhesive microparticles *in vitro* during the development stage. To simulate the *in vivo* conditions in the human large intestine, fresh porcine colonic tissue was used and the particles were exposed to drag forces of a constant flow of fluid. However, many *in vivo* parameters are difficult to simulate in this standardized *in vitro* assay, such as pre-hydration and dispersion of the dosage form, motility of the colonic content, and turnover of the mucus gel layer. The mucoadhesive microparticles must overcome various hurdles to establish a successful bioadhesive contact with the colonic mucus layer as illustrated in Fig. 5.1.

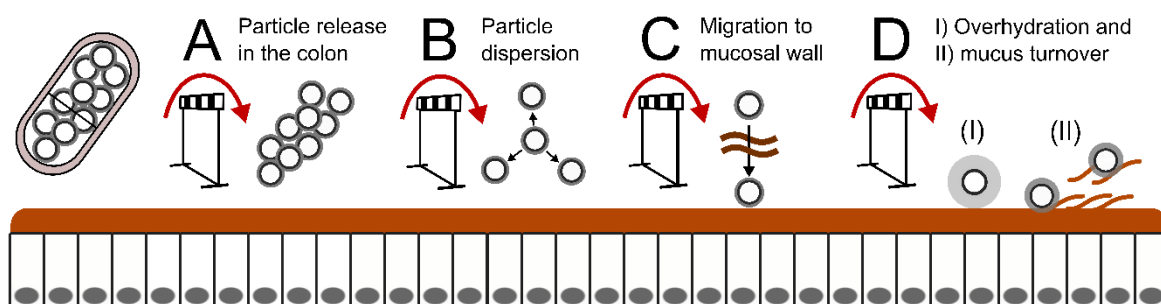


Fig. 5.1: The hurdles that a mucoadhesive and multiparticulate capsule formulation must overcome for optimal mucoadhesive performance in the colon. A) Dissolution of the capsule coating in the ileocolonic region, B) dispersion of the microparticles to improve the therapeutic effect, C) migration through the colonic content to reach the mucus layer, D) overhydration of the mucoadhesive microparticles and the mucus turnover eventually present limiting factors of mucoadhesion in the colon.

Once the colonic-targeted capsule is dissolved or disintegrated at the desired site, i.e. in the ileocolonic region, the released mucoadhesive microparticles have to disperse and spread along the colonic wall. However, hydration and swelling of the mucoadhesive microparticles in the capsule can lead to agglomerates as observed in USP II and IV dissolution studies. When no dispersibility-enhancing excipient was used, the agglomerates remained in the shape of the dissolved capsule as shown in Fig. 4 of Chapter 3.3 [232]. A similar issue was observed by McGirr *et al.* [234] when they administered radiolabeled carbomers to beagle dogs. After remotely-controlled opening of the capsule (Intelisite®), only little dispersion of radioactivity was observed. Furthermore, the capsule recovered from the stool showed incomplete release of the polymer, probably due to hydration and swelling of the polymer inside the capsule before the polymer could be released. Therefore, we evaluated different

excipients to improve the dispersibility of mucoadhesive microparticles. In preliminary trials, hydrophilic fumed silica (colloidal silica) showed the most promising results and further investigations on dry-particle coating of mucoadhesive microparticles with colloidal silica were performed. The influence of silica concentrations on particle retention and dispersibility were of particular interest.

In the study presented in Chapter 3.3 [232], it was found that colloidal silica can be added in concentrations up to 5% (w/w) without reducing the mucoadhesive properties *in vitro*. Indeed, a promising effect on particle dispersion was found by visual observation and also by increased dissolution rates of silica-coated particles. The latter can be explained by larger surface areas due to size reduction of the agglomerates, i.e. improved particle dispersion. At such high concentrations, silica nanoparticles were mainly present as secondary agglomerates with sizes ranging from 0.1-1 μm . These silica agglomerates were found to form an effective “shield” around the mucoadhesive particles, preventing a direct contact between the mucoadhesive surfaces. It is assumed that the silica monolayers, i.e. individual silica particles adsorbed to the chitosan surface, have a much lower dispersibility-enhancing effect than the silica agglomerates.

Despite the promising results indicating a dispersibility-enhancing effect of silica, an *in vitro* - *in vivo* correlation is disputable. The higher viscosity of the colonic content compared to the *in vitro* test medium is clearly a factor which negatively affects the particle dispersion *in vivo*. On the other hand, the peristalsis of the colon, which is important for mixing and transporting of the colonic content, might lead to better particle dispersion than observed *in vitro*. Therefore, gamma-scintigraphy studies of radio-labelled mucoadhesive microparticles would be also relevant for the investigation of particle dispersion in the colon once rupture of the coating and the capsule shell

For evaluation of *in vitro* particle retention on mucosal tissues, the microparticles were usually applied in dry state [68,90,91,253,254]. During a contact phase of 5 min [86], the particles had time for swelling, interpenetration into the mucin network, and formation of adhesive bonds. However, in reality the particles are hydrated before they can get in contact with the mucosal tissue, which already starts during dissolution of the capsule. Several tensile-detachment studies have shown that pre-hydration of mucoadhesive dosage forms leads to significantly reduced adhesive strength [255–257]. To measure particle retention of pre-hydrated particles, we used a special application method, and it was found that pre-hydration of the optimized formulation (5% LMW chitosan) significantly reduced the particle retention from $55.4\% \pm 5.9\%$ to $21.0\% \pm 9.2\%$ (method and results of pre-hydration not published).

These findings were in agreement with the results of Albrecht *et al.* [258] who tested the influence of pre-hydration on retention of the microparticles in a flow channel. They showed that particle retention of dry particles was increased more than 2-fold compared to pre-hydrated particles. They argued that dry polymeric particles show better interpenetration into the mucin network due to smaller sizes and increased surface area available for adhesive bonds in comparison to hydrated (swollen) particles. Other researchers explained the loss of mucoadhesive properties after pre-hydration by dissolution of the polymers and formation of a slippery mucilage [256,259]. Excessive accumulation of water molecules around the hydrophilic functional groups of mucoadhesive polymers also increases the diffusion path length, making it difficult for the polymer to get in close contact with the mucin molecule, and eventually reducing hydrogen bonding or ionic interactions.

Therefore, a formulation system capable of delivering the mucoadhesive particles in a non-hydrated state to the gastrointestinal mucosa would be of great benefit. In an interesting study, Albrecht *et al.* [260] proposed a special capsule device consisting of latex (impermeable to water), which is under tension and closed by a pH-sensitive twine made of Eudragit L100 55 (pH 5.5). When the twine is dissolved, relaxation of the stretched latex leads to immediate opening of the capsule, and the microparticles are released in dry state. In an *in vivo* study in rats, they demonstrated that mucoadhesive particles, which were delivered in non-hydrated state by such a latex capsule, had significantly prolonged residence time compared to hydrated particles delivered in a standard capsule. However, manufacturing of such a complex capsule device is very challenging at an industrial scale.

The flow rate in the particle-retention assay was chosen much higher than expected in the colon to simulate harsher conditions. The purpose was to trigger a forced detachment of the mucoadhesive microparticles and to measure their resistance to the washout in a short time. Therefore, a fast flow of water was applied to simulate the drag forces acting on the particles. The parameters influencing the drag force are the speed and density of the flow medium, and the projected surface area exposed to the flow (see Eq. 4 in Chapter 3.2) The *in vitro* flow rate of 20 ml/min was much higher than the *in vivo* flow rate of approximately 1 ml/min to increase the height of the stream and ensure a full immersion of the particles. The speed of flow applied by the inlet nozzles was already high due to the small nozzle orifice diameter and the high flow rate. The average speed of flow along the channel (positioned at an angle of 45°) was approximately 50 mm/s as measured by the time until the initial water front arrived at the end of the channel. Hence, it can be assumed that the flow conditions in the colon are milder as simulated in the particle-retention assay and that mucoadhesive microparticles with good *in vitro* particle retention might increase the residence time *in vivo*, despite the negative influence of other factors such as pre-hydration or mucus turnover.

Assuming that the mucoadhesive particles can reach the intestinal wall and form a strong adhesive bond with the mucus layer, the retention is limited to a certain time since the mucus layer is constantly being renewed. Therefore, the mucus turnover rate is the time-limiting factor of particle retention (see Fig. 5.1). As an indication of colonic mucus turnover rate in humans, rat experiments have been performed, showing a colonic mucus turnover rate of around five hours [29]. In case of diarrhea, when the gastrointestinal transit time is significantly reduced, a transit time prolongation of five hours would be of clinical importance. However, in such a condition the mucus might be washed away quicker and it is very likely that shedding of the loose outer mucus layer already leads to particle detachment. Hence, the time of adhesion might be much less than the five hours required for complete renewal. Another factor to consider is the change of mucus integrity in a diseased state. For example, patients with ulcerative colitis were found to have a depletion of goblet cells and a lower rate of mucus secretion [261], i.e. the effect of mucoadhesion could be more pronounced in ulcerative colitis patients than in healthy humans due to a lower rate of mucus turnover. However, there is no data in literature clearly showing the influence of the mucus condition in diseased state on mucoadhesive potential.

6 Conclusions and outlook

The focus in this work was the development of a multiparticulate formulation based on FCC microparticles. In this chapter, the successful development of the mucoadhesive and multiparticulate drug delivery system is summarized, and an outlook is given on other possible applications of FCC as oral drug carrier.

The formulation concept proposed in Chapter 2 (Aims) was successfully achieved. Porous FCC microparticles were used as drug carriers, and the fluidized-bed process was suitable for drug loading and mucoadhesive coating. The antibiotic MBZ was used as model drug for local treatment of colonic diseases (*Chlostridium difficile* infections). The use of LMW chitosan spray solutions reduced the risk of nozzle blocking compared to MMW chitosan, improving the manufacturability of the mucoadhesive microparticles. The optimized formulations had a high drug load, and showed good *in vitro* particle retention on porcine colonic mucosa.

By using FCC as the drug carrier, various types and high amounts of drug can be loaded into the porous calcium carbonate skeleton. Both presented drug-loading methods, i.e. the rotary-evaporation and fluidized-bed method, were based on the principle of solvent evaporation and crystallization. The rationale of using porous drug carriers for preparation of mucoadhesive microparticles is to have a stable skeleton for loading the drug and for further functionalization with a mucoadhesive coating which remains intact until the drug is released. Furthermore, the spherical shape of porous carrier particles should improve the coating quality compared to non-spherical particles, such as micronized drug crystals, which are usually characterized by poor flowability and higher agglomeration tendency during fluidized-bed coating.

For evaluation of the mucoadhesive properties of the chitosan-coated microparticles, a particle-retention assay was developed featuring a novel and reliable method for particle quantification (marker-ion analysis), and a modified flow-channel design for easier clamping of the mucosal tissue.

To prevent agglomeration of mucoadhesive microparticles due to swelling in the capsule, dry-particle coating with hydrophilic fumed silica was investigated. Promising results were obtained by visual observation and dissolution studies, indicating a dispersibility-enhancing effect of silica. Importantly, mucoadhesion was not negatively influenced by silica up to a concentration of 5% (w/w).

The application dossier of the pharmaco-scintigraphy study was approved by Swissmedic and the Ethics committee. The clinical batches were manufactured by Tillotts Pharma AG under GMP conditions, and the pharmaco-scintigraphy will be carried out at the University Hospital Basel. The results of the study is of great relevance, as it is the first-in-human investigation (from the best of our knowledge) of mucoadhesive microparticles delivered to the colon. A positive outcome, i.e. a prolonged residence time of mucoadhesive microparticles in the colon compared to the non-mucoadhesive control particles, would be an indication that the drug delivery strategy of mucoadhesion could also be applied to the harsh conditions in the large intestine, and that further research in this field would be promising. Since the preparation method allows exchange of the drug without affecting the manufacturability and mucoadhesivity of the outer chitosan layer, this formulation platform has great potential for local treatment of other colonic diseases. The presented formulation concept was subject to a patent application [262].

Drug-loaded FCC could also be used for other applications in oral drug delivery, such as immediate release formulations, orally dispersible tablets (ODTs), and as carrier of highly potent substances requiring low and precise dosing. Since the drug-loading approach was shown to result in enhanced drug dissolution, drug-loaded FCC might be beneficial for the development of immediate release formulations, in particular for poorly water-soluble drugs. The good compaction properties of FCC have already been demonstrated by Stirnimann et al. [228]. However, the use of a superdisintegrant would be essential to promote immediate disintegration into smaller particles, providing a large surface area for fast and complete drug dissolution. For better manufacturability of such tablets, granulation of drug-loaded FCC and superdisintegrants can be performed by roller compaction. It was shown that roller compaction of FCC had little impact on the compactibility of the obtained granules. The suitability of FCC for development of orally dispersible tablets (ODTs) has recently been reported [227]. Drug loading into FCC prior to roller compaction could be a promising strategy to prevent segregation of drug and excipients during manufacturing. Furthermore, improved dissolution of poorly water-soluble drugs in the saliva could lead to a large fraction of drug absorbed via the buccal mucosa, and hence, leading to a rapid onset of the pharmacological effect.

The use of FCC as a drug carrier is also encouraged for formulation of drugs with a narrow therapeutic window requiring low and precise dosing, since drug loading into FCC leads to a uniform drug distribution, even at very low drug loads. Since no segregation of drug and excipients can occur, an increased uniformity of drug content is expected. However, the usefulness of drug-loaded FCC for tablet formulations has not been investigated thus far, and further research is required to exploit the full potential of FCC as an oral drug carrier.

7 Bibliography

- [1] S.V. Sastry, J.R. Nyshadham, J.A. Fix, Recent technological advances in oral drug delivery – a review, *Pharm. Sci. Technol. Today*. 3 (2000) 138–145.
- [2] E.L. McConnell, H.M. Fadda, A.W. Basit, Gut instincts: explorations in intestinal physiology and drug delivery, *Int. J. Pharm.* 364 (2008) 213–226.
- [3] A.T. Serajuddin, Solid dispersion of poorly water-soluble drugs: early promises, subsequent problems, and recent breakthroughs, *J. Pharm. Sci.* 88 (1999) 1058–1066.
- [4] C.W. Pouton, Formulation of poorly water-soluble drugs for oral administration: Physicochemical and physiological issues and the lipid formulation classification system, *Eur. J. Pharm. Sci.* 29 (2006) 278–287.
- [5] H.A. Santos, L. Peltonen, T. Linnell, J. Hirvonen, Mesoporous materials and nanocrystals for enhancing the dissolution behavior of poorly water-soluble drugs, *Curr. Pharm. Biotechnol.* 14 (2013) 926–938.
- [6] M. Schäfer-Korting, *Drug Delivery*, Springer, 2010.
- [7] F.J.O. Varum, E.L. McConnell, J.J.S. Sousa, F. Veiga, A.W. Basit, Mucoadhesion and the gastrointestinal tract, *Crit. Rev. Ther. Drug Carrier Syst.* 25 (2008) 207–258.
- [8] H. Aoki, Y. Iwao, M. Mizoguchi, S. Noguchi, S. Itai, Clarithromycin highly-loaded gastro-floating fine granules prepared by high-shear melt granulation can enhance the efficacy of *Helicobacter pylori* eradication, *Eur. J. Pharm. Biopharm.* 92 (2015) 22–27.
- [9] M.S. Ali, V. Pandit, M. Jain, K.L. Dhar, Mucoadhesive microparticulate drug delivery system of curcumin against *Helicobacter pylori* infection: Design, development and optimization, *J. Adv. Pharm. Technol. Res.* 5 (2014) 48–56.
- [10] A. Rubinstein, B. Tirosh, M. Baluom, T. Nassar, A. David, R. Radai, I. Gliko-Kabir, M. Friedman, The rationale for peptide drug delivery to the colon and the potential of polymeric carriers as effective tools, *J. Controlled Release*. 46 (1997) 59–73.
- [11] G. Englund, F. Rorsman, A. Rönblom, U. Karlbom, L. Lazorova, J. Gråsjö, A. Kindmark, P. Artursson, Regional levels of drug transporters along the human intestinal tract: Co-expression of ABC and SLC transporters and comparison with Caco-2 cells, *Eur. J. Pharm. Sci.* 29 (2006) 269–277.
- [12] V.V. Khutoryanskiy, Advances in Mucoadhesion and Mucoadhesive Polymers, *Macromol. Biosci.* 11 (2011) 748–764.
- [13] N. Langoth, J. Kalbe, A. Bernkop-Schnürch, Development of buccal drug delivery systems based on a thiolated polymer, *Int. J. Pharm.* 252 (2003) 141–148.
- [14] M.I. Ugwoke, N. Verbeke, R. Kinget, The biopharmaceutical aspects of nasal mucoadhesive drug delivery, *J. Pharm. Pharmacol.* 53 (2001) 3–21.
- [15] T. Nagai, Adhesive topical drug delivery system, *J. Controlled Release*. 2 (1985) 121–134.

- [16] N.A. Peppas, J.R. Robinson, Bioadhesives for Optimization of Drug Delivery, *J. Drug Target.* 3 (1995) 183–184.
- [17] V.V. Khutoryanskiy, *Mucoadhesive Materials and Drug Delivery Systems*, Wiley, 2014.
- [18] Buccastem Patient Information, (2015). <http://www.drugs.com/uk/buccastem-m-buccal-tablets-leaflet.html> (accessed November 9, 2015).
- [19] N. Washington, C. Washington, C.G. Wilson, Cell Membranes, Epithelial Barriers and Drug Absorption, in: *Physiol. Pharm. Barriers Drug Absorpt.*, Taylor & Francis, 2001: pp. 1–18.
- [20] L.R. Johnson, ed., Gastroduodenal Mucosal Defense, in: *Physiol. Gastrointest. Tract*, Academic Press, 2006: pp. 1259–1290.
- [21] K. Takeuchi, Bicarbonate secretion in the mucosal defensive mechanism of the duodenum. Acid neutralization with HCO₃⁻ in the lumen and mucus gel, *Yakugaku Zasshi.* 110 (1990) 85–104.
- [22] G. Flemström, E. Kivilaakso, Demonstration of a pH gradient at the luminal surface of rat duodenum in vivo and its dependence on mucosal alkaline secretion, *Gastroenterology.* 84 (1983) 787–794.
- [23] H. Tlaskalová-Hogenová, R. Štěpánková, H. Kozáková, T. Hudcovic, L. Vannucci, L. Tučková, P. Rossmann, T. Hrnčář, M. Kverka, Z. Zákostelská, K. Klimešová, J. Příbylová, J. Bártová, D. Sanchez, P. Fundová, D. Borovská, D. Šrůtková, Z. Zidek, M. Schwarzer, P. Drastich, D.P. Funda, The role of gut microbiota (commensal bacteria) and the mucosal barrier in the pathogenesis of inflammatory and autoimmune diseases and cancer: contribution of germ-free and gnotobiotic animal models of human diseases, *Cell. Mol. Immunol.* 8 (2011) 110–120.
- [24] W.-L. Hao, Y.-K. Lee, Microflora of the gastrointestinal tract: a review, *Methods Mol. Biol. Clifton NJ.* 268 (2004) 491–502.
- [25] M.D. Kappelman, K.R. Moore, J.K. Allen, S.F. Cook, Recent Trends in the Prevalence of Crohn’s Disease and Ulcerative Colitis in a Commercially Insured US Population, *Dig. Dis. Sci.* 58 (2013) 519–525.
- [26] E. Bianconi, A. Piovesan, F. Facchin, A. Beraudi, R. Casadei, F. Frabetti, L. Vitale, M.C. Pelleri, S. Tassani, F. Piva, S. Perez-Amodio, P. Strippoli, S. Canaider, An estimation of the number of cells in the human body, *Ann. Hum. Biol.* 40 (2013) 463–471.
- [27] M.E.V. Johansson, M. Phillipson, J. Petersson, A. Velcich, L. Holm, G.C. Hansson, The inner of the two Muc2 mucin-dependent mucus layers in colon is devoid of bacteria, *Proc. Natl. Acad. Sci. U. S. A.* 105 (2008) 15064–15069.
- [28] M.E.V. Johansson, J.K. Gustafsson, K.E. Sjöberg, J. Petersson, L. Holm, H. Sjövall, G.C. Hansson, Bacteria Penetrate the Inner Mucus Layer before Inflammation in the Dextran Sulfate Colitis Model, *PLoS ONE.* 5 (2010) e12238.
- [29] C.-M. Lehr, F.G.J. Poelma, H.E. Junginger, J.J. Tukker, An estimate of turnover time of intestinal mucus gel layer in the rat in situ loop, *Int. J. Pharm.* 70 (1991) 235–240.

-
- [30] F.J.O. Varum, F. Veiga, J.S. Sousa, A.W. Basit, An investigation into the role of mucus thickness on mucoadhesion in the gastrointestinal tract of pig, *Eur. J. Pharm. Sci.* 40 (2010) 335–341.
- [31] N. Jordan, J. Newton, J. Pearson, A. Allen, A novel method for the visualization of the in situ mucus layer in rat and man, *Clin. Sci. Lond. Engl.* 95 (1998) 97–106.
- [32] V. Strugala, A. Allen, P.W. Dettmar, J.P. Pearson, Colonic mucin: methods of measuring mucus thickness, *Proc. Nutr. Soc.* 62 (2003) 237–243.
- [33] C. Atuma, V. Strugala, A. Allen, L. Holm, The adherent gastrointestinal mucus gel layer: thickness and physical state in vivo, *Am. J. Physiol. - Gastrointest. Liver Physiol.* 280 (2001) G922–G929.
- [34] R.D. Pullan, G.A. Thomas, M. Rhodes, R.G. Newcombe, G.T. Williams, A. Allen, J. Rhodes, Thickness of adherent mucus gel on colonic mucosa in humans and its relevance to colitis., *Gut.* 35 (1994) 353–359.
- [35] R. Bansil, B.S. Turner, Mucin structure, aggregation, physiological functions and biomedical applications, *Curr. Opin. Colloid Interface Sci.* 11 (2006) 164–170.
- [36] L. Serra, J. Doménech, N. Peppas, Engineering Design and Molecular Dynamics of Mucoadhesive Drug Delivery Systems as Targeting Agents, *Eur. J. Pharm. Biopharm.* 71 (2009) 519–528.
- [37] D.T. Tran, K.G.T. Hagen, Mucin-Type O-Glycosylation During Development, *J. Biol. Chem.* (2013) jbc.R112.418558.
- [38] A.P. Corfield, D. Carroll, N. Myerscough, C.S. Probert, Mucins in the gastrointestinal tract in health and disease, *Front. Biosci. J. Virtual Libr.* 6 (2001) D1321-1357.
- [39] A.P. Corfield, S.A. Wagner, J.R. Clamp, M.S. Kriaris, L.C. Hoskins, Mucin degradation in the human colon: production of sialidase, sialate O-acetyl esterase, N-acetylneuraminidase, arylesterase, and glycosulfatase activities by strains of fecal bacteria., *Infect. Immun.* 60 (1992) 3971–3978.
- [40] A.P. Corfield, S.A. Wagner, L.J. O'Donnell, P. Durdey, R.A. Mountford, J.R. Clamp, The roles of enteric bacterial sialidase, sialate O-acetyl esterase and glycosulfatase in the degradation of human colonic mucin, *Glycoconj. J.* 10 (1993) 72–81.
- [41] K. Godl, M.E.V. Johansson, M.E. Lidell, M. Mörgelin, H. Karlsson, F.J. Olson, J.R. Gum Jr, Y.S. Kim, G.C. Hansson, The N terminus of the MUC2 mucin forms trimers that are held together within a trypsin-resistant core fragment, *J. Biol. Chem.* 277 (2002) 47248–47256.
- [42] M.E.V. Johansson, D. Ambort, T. Pelaseyed, A. Schütte, J.K. Gustafsson, A. Ermund, D.B. Subramani, J.M. Holmén-Larsson, K.A. Thomsson, J.H. Bergström, S. van der Post, A.M. Rodriguez-Piñero, H. Sjövall, M. Bäckström, G.C. Hansson, Composition and functional role of the mucus layers in the intestine, *Cell. Mol. Life Sci. CMLS.* 68 (2011) 3635–3641.
- [43] X. Yang, K. Forier, L. Steukers, S. Van Vlierberghe, P. Dubruel, K. Braeckmans, S. Glorieux, H.J. Nauwynck, Immobilization of Pseudorabies Virus in Porcine Tracheal
-

- Respiratory Mucus Revealed by Single Particle Tracking, *PLoS ONE*. 7 (2012) e51054.
- [44] S. Rossi, M.C. Bonferoni, F. Ferrari, C. Caramella, Drug release and washability of mucoadhesive gels based on sodium carboxymethylcellulose and polyacrylic acid, *Pharm. Dev. Technol.* 4 (1999) 55–63.
- [45] M. Malmsten, I. Ljusegren, I. Carlstedt, Ellipsometry studies of the mucoadhesion of cellulose derivatives, *Colloids Surf. B Biointerfaces*. 2 (1994) 463–470.
- [46] A. Fini, V. Bergamante, G.C. Ceschel, Mucoadhesive Gels Designed for the Controlled Release of Chlorhexidine in the Oral Cavity, *Pharmaceutics*. 3 (2011) 665–679.
- [47] P. He, S.S. Davis, L. Illum, In vitro evaluation of the mucoadhesive properties of chitosan microspheres, *Int. J. Pharm.* 166 (1998) 75–88.
- [48] A.F. Eftaiha, N. Qinna, I.S. Rashid, M.M. Al Remawi, M.R. Al Shami, T.A. Arafat, A.A. Badwan, Bioadhesive Controlled Metronidazole Release Matrix Based on Chitosan and Xanthan Gum, *Mar. Drugs*. 8 (2010) 1716–1730.
- [49] O. Gåserød, I.G. Jolliffe, F.C. Hampson, P.W. Dettmar, G. Skjåk-Bræk, The enhancement of the bioadhesive properties of calcium alginate gel beads by coating with chitosan, *Int. J. Pharm.* 175 (1998) 237–246.
- [50] I. Henriksen, K.L. Green, J.D. Smart, G. Smistad, J. Karlsen, Bioadhesion of hydrated chitosans: An in vitro and in vivo study, *Int. J. Pharm.* 145 (1996) 231–240.
- [51] M.N.V. Ravi Kumar, A review of chitin and chitosan applications, *React. Funct. Polym.* 46 (2000) 1–27.
- [52] I.A. Sogias, A.C. Williams, V.V. Khutoryanskiy, Why is chitosan mucoadhesive?, *Biomacromolecules*. 9 (2008) 1837–1842.
- [53] A. Bernkop-Schnürch, Thiomers: A new generation of mucoadhesive polymers, *Adv. Drug Deliv. Rev.* 57 (2005) 1569–1582.
- [54] C.-M. Lehr, Lectin-mediated drug delivery: The second generation of bioadhesives, *J. Controlled Release*. 65 (2000) 19–29.
- [55] J.D. Smart, The basics and underlying mechanisms of mucoadhesion, *Adv. Drug Deliv. Rev.* 57 (2005) 1556–1568.
- [56] N. Salamat-Miller, M. Chittchang, T.P. Johnston, The use of mucoadhesive polymers in buccal drug delivery, *Adv. Drug Deliv. Rev.* 57 (2005) 1666–1691.
- [57] A. Ludwig, The use of mucoadhesive polymers in ocular drug delivery, *Adv. Drug Deliv. Rev.* 57 (2005) 1595–1639.
- [58] C. Valenta, The use of mucoadhesive polymers in vaginal delivery, *Adv. Drug Deliv. Rev.* 57 (2005) 1692–1712.
- [59] N. Nagahara, Y. Akiyama, M. Nakao, M. Tada, M. Kitano, Y. Ogawa, Mucoadhesive Microspheres Containing Amoxicillin for Clearance of *Helicobacter pylori*, *Antimicrob. Agents Chemother.* 42 (1998) 2492–2494.

-
- [60] M. Säkkinen, T. Tuononen, H. Jürjenson, P. Veski, M. Marvola, Evaluation of microcrystalline chitosans for gastro-retentive drug delivery, *Eur. J. Pharm. Sci. Off. J. Eur. Fed. Pharm. Sci.* 19 (2003) 345–353.
- [61] F.J.O. Varum, F. Veiga, J.S. Sousa, A.W. Basit, Mucoadhesive platforms for targeted delivery to the colon, *Int. J. Pharm.* 420 (2011) 11–19.
- [62] R.A. Bader, D.A. Putnam, *Engineering Polymer Systems for Improved Drug Delivery*, John Wiley & Sons, 2014.
- [63] B. Abrahamsson, M. Alpsten, U.E. Jonsson, P.J. Lundberg, A. Sandberg, M. Sundgren, A. Svenheden, J. Tölli, Gastro-intestinal transit of a multiple-unit formulation (metoprolol CR/ZOK) and a non-disintegrating tablet with the emphasis on colon, *Int. J. Pharm.* 140 (1996) 229–235.
- [64] F.J.O. Varum, H.A. Merchant, A.W. Basit, Oral modified-release formulations in motion: The relationship between gastrointestinal transit and drug absorption, *Int. J. Pharm.* 395 (2010) 26–36.
- [65] H. Takeuchi, H. Yamamoto, Y. Kawashima, Mucoadhesive nanoparticulate systems for peptide drug delivery, *Adv. Drug Deliv. Rev.* 47 (2001) 39–54.
- [66] S. Sakuma, R. Sudo, N. Suzuki, H. Kikuchi, M. Akashi, Y. Ishida, M. Hayashi, Behavior of mucoadhesive nanoparticles having hydrophilic polymeric chains in the intestine, *J. Controlled Release.* 81 (2002) 281–290.
- [67] A. Sosnik, J. das Neves, B. Sarmiento, Mucoadhesive polymers in the design of nano-drug delivery systems for administration by non-parenteral routes: A review, *Prog. Polym. Sci.* 39 (2014) 2030–2075.
- [68] A. De Ascentiis, J.L. deGrazia, C.N. Bowman, P. Colombo, N.A. Peppas, Mucoadhesion of poly(2-hydroxyethyl methacrylate) is improved when linear poly(ethylene oxide) chains are added to the polymer network, *J. Controlled Release.* 33 (1995) 197–201.
- [69] K.P.R. Chowdary, Y.S. Rao, Mucoadhesive microspheres for controlled drug delivery, *Biol. Pharm. Bull.* 27 (2004) 1717–1724.
- [70] J. Möschwitzer, R.H. Müller, Spray coated pellets as carrier system for mucoadhesive drug nanocrystals, *Eur. J. Pharm. Biopharm.* 62 (2006) 282–287.
- [71] T. Pengpong, P. Sangvanich, K. Sirilertmukul, N. Muangsin, Design, synthesis and in vitro evaluation of mucoadhesive p-coumarate-thiolated-chitosan as a hydrophobic drug carriers, *Eur. J. Pharm. Biopharm.* 86 (2014) 487–497.
- [72] Q.-R. Cao, Y. Liu, W.-J. Xu, B.-J. Lee, M. Yang, J.-H. Cui, Enhanced oral bioavailability of novel mucoadhesive pellets containing valsartan prepared by a dry powder-coating technique, *Int. J. Pharm.* 434 (2012) 325–333.
- [73] M. Davidovich-Pinhas, H. Bianco-Peled, Mucoadhesion: a review of characterization techniques, *Expert Opin. Drug Deliv.* 7 (2010) 259–271.
-

- [74] H.S. Ch'ng, H. Park, P. Kelly, J.R. Robinson, Bioadhesive polymers as platforms for oral controlled drug delivery II: synthesis and evaluation of some swelling, water-insoluble bioadhesive polymers, *J. Pharm. Sci.* 74 (1985) 399–405.
- [75] M.P. Deacon, S. McGurk, C.J. Roberts, P.M. Williams, S.J. Tendler, M.C. Davies, S.S. Davis, S.E. Harding, Atomic force microscopy of gastric mucin and chitosan mucoadhesive systems., *Biochem. J.* 348 (2000) 557–563.
- [76] H.. Batchelor, D. Banning, P.. Dettmar, F.. Hampson, I.. Jolliffe, D.Q.. Craig, An in vitro mucosal model for prediction of the bioadhesion of alginate solutions to the oesophagus, *Int. J. Pharm.* 238 (2002) 123–132.
- [77] A. Bernkop-Schnürch, S. Steininger, Synthesis and characterisation of mucoadhesive thiolated polymers, *Int. J. Pharm.* 194 (2000) 239–247.
- [78] D.J. Hall, O.V. Khutoryanskaya, V.V. Khutoryanskiy, Developing synthetic mucosa-mimetic hydrogels to replace animal experimentation in characterisation of mucoadhesive drug delivery systems, *Soft Matter.* 7 (2011) 9620–9623.
- [79] F. Madsen, K. Eberth, J.D. Smart, A rheological assessment of the nature of interactions between mucoadhesive polymers and a homogenised mucus gel, *Biomaterials.* 19 (1998) 1083–1092.
- [80] H. Park, J.R. Robinson, Mechanisms of mucoadhesion of poly(acrylic acid) hydrogels, *Pharm. Res.* 4 (1987) 457–464.
- [81] S.-H.S. Leung, J.R. Robinson, Polymer structure features contributing to mucoadhesion. II, *J. Controlled Release.* 12 (1990) 187–194.
- [82] K. Satoh, K. Takayama, Y. Machida, Y. Suzuki, M. Nakagaki, T. Nagai, Factors affecting the bioadhesive property of tablets consisting of hydroxypropyl cellulose and carboxyvinyl polymer, *Chem. Pharm. Bull. (Tokyo).* 37 (1989) 1366–1368.
- [83] F. Lejoyeux, G. Ponchel, D. Wouessidjewe, N.A. Peppas, D. Duchêne, Bioadhesive Tablets Influence of the Testing Medium Composition on Bioadhesion, *Drug Dev. Ind. Pharm.* 15 (1989) 2037–2048.
- [84] K.V.R. Rao, P. Buri, A novel in situ method to test polymers and coated microparticles for bioadhesion, *Int. J. Pharm.* 52 (1989) 265–270.
- [85] A.M. Le Ray, P. Iooss, A. Gouyette, V. Vonarx, T. Patrice, C. Merle, Development of a “continuous-flow adhesion cell” for the assessment of hydrogel adhesion, *Drug Dev. Ind. Pharm.* 25 (1999) 897–904.
- [86] D. Preisig, M. Weingartner, F.J.O. Varum, R. Bravo, R. Alles, J. Huwyler, M. Puchkov, Marker-ion analysis for quantification of mucoadhesivity of microparticles in particle-retention assays, *Int. J. Pharm.* 487 (2015) 157–166.
- [87] L.S. Nielsen, L. Schubert, J. Hansen, Bioadhesive drug delivery systems. I. Characterisation of mucoadhesive properties of systems based on glyceryl mono-oleate and glyceryl monolinoleate, *Eur. J. Pharm. Sci. Off. J. Eur. Fed. Pharm. Sci.* 6 (1998) 231–239.

-
- [88] S. Kockisch, G.D. Rees, S.A. Young, J. Tsibouklis, J.D. Smart, Polymeric microspheres for drug delivery to the oral cavity: An in vitro evaluation of mucoadhesive potential, *J. Pharm. Sci.* 92 (2003) 1614–1623.
- [89] Z. Liu, W. Lu, L. Qian, X. Zhang, P. Zeng, J. Pan, In vitro and in vivo studies on mucoadhesive microspheres of amoxicillin, *J. Controlled Release.* 102 (2005) 135–144.
- [90] R. Rastogi, Y. Sultana, M. Aqil, A. Ali, S. Kumar, K. Chuttani, A.K. Mishra, Alginate microspheres of isoniazid for oral sustained drug delivery, *Int. J. Pharm.* 334 (2007) 71–77.
- [91] V.S. Belgamwar, S.J. Surana, Design and development of oral mucoadhesive multiparticulate system containing atenolol: in vitro-in vivo characterization, *Chem. Pharm. Bull. (Tokyo).* 58 (2010) 1168–1175.
- [92] T. Nakanishi, F. Kaiho, M. Hayashi, Use of sodium salt of Carbopol 934P in oral peptide delivery, *Int. J. Pharm.* 171 (1998) 177–183.
- [93] S.A. Young, J.D. Smart, A novel in-vitro apparatus for evaluating the mucoadhesion of liquid and semi-solid formulations, *J. Pharm. Pharmacol.* 50 (1998) 167–167.
- [94] R.G. Riley, J.D. Smart, J. Tsibouklis, S.A. Young, F. Hampson, A. Davis, G. Kelly, P.W. Dettmar, W.R. Wilber, An in vitro model for investigating the gastric mucosal retention of ¹⁴C-labelled poly(acrylic acid) dispersions, *Int. J. Pharm.* 236 (2002) 87–96.
- [95] M.D. Abd El-Hameed, H.J. Baker, I.W. Kellaway, The transport of polymeric microspheres across the ciliated epithelia of the bullfrog, *Int. J. Pharm.* 180 (1999) 59–67.
- [96] R.A. Cave, J.P. Cook, C.J. Connon, V.V. Khutoryanskiy, A flow system for the on-line quantitative measurement of the retention of dosage forms on biological surfaces using spectroscopy and image analysis, *Int. J. Pharm.* 428 (2012) 96–102.
- [97] A.G. Mikos, N.A. Peppas, Bioadhesive analysis of controlled-release systems. IV. An experimental method for testing the adhesion of microparticles with mucus, *J. Controlled Release.* 12 (1990) 31–37.
- [98] V. Belgamwar, V. Shah, S.J. Surana, Formulation and evaluation of oral mucoadhesive multiparticulate system containing metoprolol tartarate: an in vitro-ex vivo characterization, *Curr. Drug Deliv.* 6 (2009) 113–121.
- [99] R.G. Riley, J.D. Smart, J. Tsibouklis, P.W. Dettmar, F. Hampson, J.A. Davis, G. Kelly, W.R. Wilber, An investigation of mucus/polymer rheological synergism using synthesised and characterised poly(acrylic acid)s, *Int. J. Pharm.* 217 (2001) 87–100.
- [100] H. Hägerström, K. Edsman, Limitations of the rheological mucoadhesion method: the effect of the choice of conditions and the rheological synergism parameter, *Eur. J. Pharm. Sci. Off. J. Eur. Fed. Pharm. Sci.* 18 (2003) 349–357.
- [101] Y. Miyazaki, K. Ogihara, S. Yakou, T. Nagai, K. Takayama, In vitro and in vivo evaluation of mucoadhesive microspheres consisting of dextran derivatives and cellulose acetate butyrate, *Int. J. Pharm.* 258 (2003) 21–29.
-

- [102] D.. Chickering III, J.. Jacob, T.. Desai, M. Harrison, W.. Harris, C.. Morrell, P. Chaturvedi, E. Mathiowitz, Bioadhesive microspheres: III. An in vivo transit and bioavailability study of drug-loaded alginate and poly(fumaric-co-sebacic anhydride) microspheres, *J. Controlled Release*. 48 (1997) 35–46.
- [103] G.A. Digenis, E.P. Sandefer, A.F. Parr, R. Beihn, C. McClain, B.M. Scheinthal, I. Ghebre-Sellassie, U. Iyer, R.U. Nesbitt, E. Randinitis, Gastrointestinal behavior of orally administered radiolabeled erythromycin pellets in man as determined by gamma scintigraphy, *J. Clin. Pharmacol.* 30 (1990) 621–631.
- [104] A.W. Basit, F. Podczeck, J. Michael Newton, W.A. Waddington, P.J. Ell, L.F. Lacey, The use of formulation technology to assess regional gastrointestinal drug absorption in humans, *Eur. J. Pharm. Sci.* 21 (2004) 179–189.
- [105] R. Khosla, S.S. Davis, The effect of polycarbophil on the gastric emptying of pellets, *J. Pharm. Pharmacol.* 39 (1987) 47–49.
- [106] D. Harris, J.T. Fell, H.L. Sharma, D.C. Taylor, GI transit of potential bioadhesive formulations in man: A scintigraphic study, *J. Controlled Release*. 12 (1990) 45–53.
- [107] M. Säkkinen, J. Marvola, H. Kanerva, K. Lindevall, A. Ahonen, M. Marvola, Are chitosan formulations mucoadhesive in the human small intestine? An evaluation based on gamma scintigraphy, *Int. J. Pharm.* 307 (2006) 285–291.
- [108] S.F. Ahrabi, S.A. Sande, T. Waaler, C. Graffner, Influence of neutron activation factors on the physico-chemical properties of suppositories and their excipients, *Eur. J. Pharm. Sci.* 8 (1999) 193–201.
- [109] M. Frier, A.C. Perkins, *Nuclear Medicine in Pharmaceutical Research*, CRC Press, 1999.
- [110] Y. Akiyama, N. Nagahara, E. Nara, M. Kitano, S. Iwasa, I. Yamamoto, J. Azuma, Y. Ogawa, Evaluation of oral mucoadhesive microspheres in man on the basis of the pharmacokinetics of furosemide and riboflavin, compounds with limited gastrointestinal absorption sites, *J. Pharm. Pharmacol.* 50 (1998) 159–166.
- [111] G. Van den Mooter, Colon drug delivery, *Expert Opin. Drug Deliv.* 3 (2005) 111–125.
- [112] A.K. Philip, B. Philip, Colon Targeted Drug Delivery Systems: A Review on Primary and Novel Approaches, *Oman Med. J.* 25 (2010) 79–87.
- [113] C. Schiller, C.-P. Fröhlich, T. Giessmann, W. Siegmund, H. Mönnikes, N. Hosten, W. Weitschies, Intestinal fluid volumes and transit of dosage forms as assessed by magnetic resonance imaging, *Aliment. Pharmacol. Ther.* 22 (2005) 971–979.
- [114] K.E. Barrett, F.K. Ghishan, J.L. Merchant, H.M. Said, J.D. Wood, *Physiology of the Gastrointestinal Tract*, Academic Press, 2006.
- [115] G. Hounnou, C. Destrieux, J. Desmé, P. Bertrand, S. Velut, Anatomical study of the length of the human intestine, *Surg. Radiol. Anat.* 24 (2002) 290–294.
- [116] S.S. Davis, J.G. Hardy, J.W. Fara, Transit of pharmaceutical dosage forms through the small intestine., *Gut*. 27 (1986) 886–892.

-
- [117] J.R. Malagelada, J.S. Robertson, M.L. Brown, M. Remington, J.A. Duenes, G.M. Thomforde, P.W. Carryer, Intestinal transit of solid and liquid components of a meal in health, *Gastroenterology*. 87 (1984) 1255–1263.
- [118] I.R. Wilding, A.J. Coupe, S.S. Davis, The role of γ -scintigraphy in oral drug delivery, *Adv. Drug Deliv. Rev.* 46 (2001) 103–124.
- [119] W.Y. Chey, T.-M. Chang, Secretin, 100 years later, *J. Gastroenterol.* 38 (2003) 1025–1035.
- [120] M.Z.I. Khan, Ž. Prebeg, N. Kurjaković, A pH-dependent colon targeted oral drug delivery system using methacrylic acid copolymers: I. Manipulation of drug release using Eudragit® L100-55 and Eudragit® S100 combinations, *J. Controlled Release*. 58 (1999) 215–222.
- [121] D.F. Evans, G. Pye, R. Bramley, A.G. Clark, T.J. Dyson, J.D. Hardcastle, Measurement of gastrointestinal pH profiles in normal ambulant human subjects., *Gut*. 29 (1988) 1035–1041.
- [122] A.G. Press, I.A. Hauptmann, L. Hauptmann, B. Fuchs, M. Fuchs, K. Ewe, G. Ramadori, Gastrointestinal pH profiles in patients with inflammatory bowel disease, *Aliment. Pharmacol. Ther.* 12 (1998) 673–678.
- [123] J.H. Cummings, G.T. Macfarlane, H.N. Englyst, Prebiotic digestion and fermentation, *Am. J. Clin. Nutr.* 73 (2001) 415S–420S.
- [124] N. Huda-Faujan, A.S. Abdulmir, A.B. Fatimah, O.M. Anas, M. Shuhaimi, A.M. Yazid, Y.Y. Loong, The Impact of the Level of the Intestinal Short Chain Fatty Acids in Inflammatory Bowel Disease Patients Versus Healthy Subjects, *Open Biochem. J.* 4 (2010) 53–58.
- [125] C.L. Sears, A dynamic partnership: Celebrating our gut flora, *Anaerobe*. 11 (2005) 247–251.
- [126] M.J. Hill, B.S. Drasar, The normal colonic bacterial flora., *Gut*. 16 (1975) 318–323.
- [127] R.R. Scheline, Metabolism of foreign compounds by gastrointestinal microorganisms, *Pharmacol. Rev.* 25 (1973) 451–523.
- [128] L.V. Hooper, J.I. Gordon, Commensal Host-Bacterial Relationships in the Gut, *Science*. 292 (2001) 1115–1118.
- [129] E.V. Loftus, Clinical epidemiology of inflammatory bowel disease: Incidence, prevalence, and environmental influences, *Gastroenterology*. 126 (2004) 1504–1517.
- [130] E.F. Stange, S.P.L. Travis, The European Consensus on Ulcerative Colitis: New Horizons?, *Gut*. 57 (2008) 1029–1031.
- [131] A. Kornbluth, D.B. Sachar, Practice Parameters Committee of the American College of Gastroenterology, Ulcerative colitis practice guidelines in adults: American College Of Gastroenterology, Practice Parameters Committee, *Am. J. Gastroenterol.* 105 (2010) 501–523; quiz 524.
- [132] C.S.J. Probert, A.U. Dignass, S. Lindgren, M. Oudkerk Pool, P. Marteau, Combined oral and rectal mesalazine for the treatment of mild-to-moderately active ulcerative
-

- colitis: Rapid symptom resolution and improvements in quality of life, *J. Crohns Colitis*. 8 (2014) 200–207.
- [133] S. Danese, C. Fiocchi, Ulcerative Colitis, *N. Engl. J. Med.* 365 (2011) 1713–1725.
- [134] R.D. Cohen, *Inflammatory Bowel Disease: Diagnosis and Therapeutics*, Springer Science & Business Media, 2011.
- [135] R.N. Cunliffe, B.B. Scott, Review article: monitoring for drug side-effects in inflammatory bowel disease, *Aliment. Pharmacol. Ther.* 16 (2002) 647–662.
- [136] C. Lautenschläger, C. Schmidt, D. Fischer, A. Stallmach, Drug delivery strategies in the therapy of inflammatory bowel disease, *Adv. Drug Deliv. Rev.* 71 (2014) 58–76.
- [137] C.M. Surawicz, L.V. McFarland, Pseudomembranous colitis: causes and cures, *Digestion*. 60 (1999) 91–100.
- [138] R. Siegel, C. DeSantis, A. Jemal, Colorectal cancer statistics, 2014, *CA. Cancer J. Clin.* 64 (2014) 104–117.
- [139] R. Labianca, L. Milesi, S. Mosconi, M.A. Pessi, G.D. Beretta, A. Quadri, The role of adjuvant chemotherapy in colon cancer, *Surg. Oncol.* 16, Supplement (2007) 93–96.
- [140] W.J. Sandborn, S.B. Hanauer, The pharmacokinetic profiles of oral mesalazine formulations and mesalazine pro-drugs used in the management of ulcerative colitis, *Aliment. Pharmacol. Ther.* 17 (2003) 29–42.
- [141] Product Monograph Salazopyrin (Salfasalazine Tablets), (2013). http://www.pfizer.ca/sites/g/files/g10017036/f/201410/Salazopyrin_0.pdf (accessed December 10, 2015).
- [142] J.P. Brown, G.V. McGarraugh, T.M. Parkinson, R.E. Wingard, A.B. Onderdonk, A polymeric drug for treatment of inflammatory bowel disease, *J. Med. Chem.* 26 (1983) 1300–1307.
- [143] B. Říhová, R.C. Rathi, P. Kopečková, J. Kopeček, In vitro bioadhesion of carbohydrate-containing N-(2-hydroxypropyl) methacrylamide copolymers to the GI tract of guinea pigs, *Int. J. Pharm.* 87 (1992) 105–116.
- [144] P. Kopečková, R. Rathi, S. Takada, B. Říhová, M.M. Berenson, J. Kopeček, Bioadhesive N-(2-hydroxypropyl) methacrylamide copolymers for colon-specific drug delivery, *J. Controlled Release*. 28 (1994) 211–222.
- [145] D.R. Friend, G.W. Chang, A colon-specific drug-delivery system based on drug glycosides and the glycosidases of colonic bacteria, *J. Med. Chem.* 27 (1984) 261–266.
- [146] D.R. Friend, G.W. Chang, Drug glycosides: potential prodrugs for colon-specific drug delivery, *J. Med. Chem.* 28 (1985) 51–57.
- [147] M.E. McNeill, A. Rashid, H.N.E. Stevens, Dispensing device, US5342624 A, 1994. <http://www.google.com/patents/US5342624> (accessed September 25, 2015).
- [148] J. Binns, H.N.E. Stevens, J. McEwen, G. Pritchard, F.M. Brewer, A. Clarke, E.S. Johnson, I. McMillan, The tolerability of multiple oral doses of Pulsincap™ capsules in healthy volunteers, *J. Controlled Release*. 38 (1996) 151–158.

-
- [149] H.N.E. Stevens, C.G. Wilson, P.G. Welling, M. Bakhshae, J.S. Binns, A.C. Perkins, M. Frier, E.P. Blackshaw, M.W. Frame, D.J. Nichols, M.J. Humphrey, S.R. Wicks, Evaluation of PulsincapTM to provide regional delivery of dofetilide to the human GI tract, *Int. J. Pharm.* 236 (2002) 27–34.
- [150] L. Yang, J.S. Chu, J.A. Fix, Colon-specific drug delivery: new approaches and in vitro/in vivo evaluation, *Int. J. Pharm.* 235 (2002) 1–15.
- [151] K.P. Steed, G. Hooper, N. Monti, M. Strolin Benedetti, G. Fornasini, I.R. Wilding, The use of pharmacoscintigraphy to focus the development strategy for a novel 5-ASA colon targeting system (“TIME CLOCK®” system), *J. Controlled Release.* 49 (1997) 115–122.
- [152] H.A. Mardini, D.C. Lindsay, C.M. Deighton, C.O. Record, Effect of polymer coating on faecal recovery of ingested 5-amino salicylic acid in patients with ulcerative colitis., *Gut.* 28 (1987) 1084–1089.
- [153] D.S. Levine, V.A. Raisys, V. Ainardi, Coating of Oral Beclomethasone Dipropionate Capsules With Cellulose Acetate Phthalate Enhances Delivery of Topically Active Antinflammatory Drug to the Terminal Ileum, *Gastroenterology.* 92 (1987) 1037–1044.
- [154] N. Madhu, P. Shanker, L. Prabakaran, K.N. Jayveera, Novel Colon Specific Drug Delivery System: A Review, *IJPSR.* 2 (2011) 2545–2561.
- [155] M. Ashford, J.T. Fell, D. Attwood, H. Sharma, P.J. Woodhead, An in vivo investigation into the suitability of pH dependent polymers for colonic targeting, *Int. J. Pharm.* 95 (1993) 193–199.
- [156] M. Saffran, G.S. Kumar, C. Savariar, J.C. Burnham, F. Williams, D.C. Neckers, A new approach to the oral administration of insulin and other peptide drugs, *Science.* 233 (1986) 1081–1084.
- [157] C.L. Cheng, S.H. Gehrke, W.A. Ritschel, Development of an azopolymer based colonic release capsule for delivering proteins/macromolecules, *Methods Find. Exp. Clin. Pharmacol.* 16 (1994) 271–278.
- [158] E. Schacht, A. Gevaert, E.R. Kenawy, K. Molly, W. Verstraete, P. Adriaensens, R. Carleer, J. Gelan, Polymers for colon specific drug delivery, *J. Controlled Release.* 39 (1996) 327–338.
- [159] H. Tozaki, T. Fujita, J. Komoike, S.I. Kim, H. Terashima, S. Muranishi, S. Okabe, A. Yamamoto, Colon-specific delivery of budesonide with azopolymer-coated pellets: therapeutic effects of budesonide with a novel dosage form against 2,4,6-trinitrobenzenesulphonic acid-induced colitis in rats, *J. Pharm. Pharmacol.* 51 (1999) 257–261.
- [160] S. Milojevic, J.M. Newton, J.H. Cummings, G.R. Gibson, R. Louise Botham, S.G. Ring, M. Stockham, M.C. Allwood, Amylose as a coating for drug delivery to the colon: Preparation and in vitro evaluation using 5-aminosalicylic acid pellets, *J. Controlled Release.* 38 (1996) 75–84.
-

- [161] F. Bigucci, B. Luppi, L. Monaco, T. Cerchiara, V. Zecchi, Pectin-based microspheres for colon-specific delivery of vancomycin, *J. Pharm. Pharmacol.* 61 (2009) 41–46.
- [162] H. Tozaki, J. Komoike, C. Tada, T. Maruyama, A. Terabe, T. Suzuki, A. Yamamoto, S. Muranishi, Chitosan capsules for colon-specific drug delivery: Improvement of insulin absorption from the rat colon, *J. Pharm. Sci.* 86 (1997) 1016–1021.
- [163] D. López-Molina, S. Chazarra, C.W. How, N. Pruidze, E. Navarro-Perán, F. García-Cánovas, P.A. García-Ruiz, F. Rojas-Melgarejo, J.N. Rodríguez-López, Cinnamate of inulin as a vehicle for delivery of colonic drugs, *Int. J. Pharm.* 479 (2015) 96–102.
- [164] L. Hovgaard, H. Brøndsted, Dextran hydrogels for colon-specific drug delivery, *J. Controlled Release.* 36 (1995) 159–166.
- [165] K. Molly, M.V. Woestyne, W. Verstraete, Development of a 5-step multi-chamber reactor as a simulation of the human intestinal microbial ecosystem, *Appl. Microbiol. Biotechnol.* 39 (1993) 254–258.
- [166] M. Saffran, J.B. Field, J. Peña, R.H. Jones, Y. Okuda, Oral insulin in diabetic dogs, *J. Endocrinol.* 131 (1991) 267–278.
- [167] M. Katsuma, S. Watanabe, S. Takemura, K. Sako, T. Sawada, Y. Masuda, K. Nakamura, M. Fukui, A.L. Connor, I.R. Wilding, Scintigraphic evaluation of a novel colon-targeted delivery system (CODES™) in healthy volunteers, *J. Pharm. Sci.* 93 (2004) 1287–1299.
- [168] V.C. Ibekwe, M.K. Khela, D.F. Evans, A.W. Basit, A new concept in colonic drug targeting: a combined pH-responsive and bacterially-triggered drug delivery technology, *Aliment. Pharmacol. Ther.* 28 (2008) 911–916.
- [169] T. Bautzová, M. Rabišková, A. Lamprecht, Multiparticulate systems containing 5-aminosalicylic acid for the treatment of inflammatory bowel disease, *Drug Dev. Ind. Pharm.* 37 (2011) 1100–1109.
- [170] T.W. Wong, G. Colombo, F. Sonvico, Pectin matrix as oral drug delivery vehicle for colon cancer treatment, *AAPS PharmSciTech.* 12 (2011) 201–214.
- [171] K. Krogars, J. Heinämäki, J. Vesalahti, M. Marvola, O. Antikainen, J. Yliruusi, Extrusion-spheronization of pH-sensitive polymeric matrix pellets for possible colonic drug delivery, *Int. J. Pharm.* 199 (2000) 187–194.
- [172] H. Steckel, F. Mindermann-Nogly, Production of chitosan pellets by extrusion/spheronization, *Eur. J. Pharm. Biopharm.* 57 (2004) 107–114.
- [173] I. Tho, P. Kleinebudde, S.A. Sande, Extrusion/spheronization of pectin-based formulations. I. Screening of important factors, *AAPS PharmSciTech.* 2 (2001) 54–62.
- [174] M.W. Rudolph, S. Klein, T.E. Beckert, H. Petereit, J.B. Dressman, A new 5-aminosalicylic acid multi-unit dosage form for the therapy of ulcerative colitis, *Eur. J. Pharm. Biopharm.* 51 (2001) 183–190.
- [175] G. Cheng, F. An, M.-J. Zou, J. Sun, X.-H. Hao, Y.-X. He, Time- and pH-dependent colon-specific drug delivery for orally administered diclofenac sodium and 5-aminosalicylic acid, *World J. Gastroenterol. WJG.* 10 (2004) 1769–1774.

-
- [176] W. He, Q. Du, D.-Y. Cao, B. Xiang, L.-F. Fan, Study on colon-specific pectin/ethylcellulose film-coated 5-fluorouracil pellets in rats, *Int. J. Pharm.* 348 (2008) 35–45.
- [177] Y. Karrout, C. Neut, D. Wils, F. Siepmann, L. Deremaux, M.-P. Flament, L. Dubreuil, P. Desreumaux, J. Siepmann, Novel polymeric film coatings for colon targeting: Drug release from coated pellets, *Eur. J. Pharm. Sci.* 37 (2009) 427–433.
- [178] J. Varshosaz, J. Emami, N. Tavakoli, M. Minaiyan, N. Rahmani, F. Dorkoosh, P. Mahzouni, Colon specific delivery of budesonide based on triple coated pellets: in vitro/in vivo evaluation, *Acta Pharm. Zagreb Croat.* 62 (2012) 341–356.
- [179] A. Akhgari, H. Afrasiabi Garekani, F. Sadeghi, M. Azimaie, Statistical optimization of indomethacin pellets coated with pH-dependent methacrylic polymers for possible colonic drug delivery, *Int. J. Pharm.* 305 (2005) 22–30.
- [180] H.H. Gangurde, M.A. Chordiya, S. Tamizharas, T. Sivakumar, Optimization of Budesonide pH Dependent Coated Pellets for Potential Colon Targeted Drug Delivery, *Insight Pharm. Sci.* 3 (2013) 1–13.
- [181] O. Chambin, G. Dupuis, D. Champion, A. Voilley, Y. Pourcelot, Colon-specific drug delivery: Influence of solution reticulation properties upon pectin beads performance, *Int. J. Pharm.* 321 (2006) 86–93.
- [182] G. Dupuis, O. Chambin, C. G nelot, D. Champion, Y. Pourcelot, Colonic Drug Delivery: Influence of Cross-linking Agent on Pectin Beads Properties and Role of the Shell Capsule type, *Drug Dev. Ind. Pharm.* 32 (2006) 847–855.
- [183] S. Bourgeois, M. Gernet, D. Pradeau, A. Andremont, E. Fattal, Evaluation of critical formulation parameters influencing the bioactivity of β -lactamases entrapped in pectin beads, *Int. J. Pharm.* 324 (2006) 2–9.
- [184] K.L.B. Chang, J. Lin, Swelling behavior and the release of protein from chitosan–pectin composite particles, *Carbohydr. Polym.* 43 (2000) 163–169.
- [185] W.A. Chan, C.D. Boswell, Z. Zhang, Comparison of the release profiles of a water soluble drug carried by Eudragit-coated capsules in different in-vitro dissolution liquids, *Powder Technol.* 119 (2001) 26–32.
- [186] M. Hiorth, T. Versland, J. Heikkil , I. Tho, S.A. Sande, Immersion coating of pellets with calcium pectinate and chitosan, *Int. J. Pharm.* 308 (2006) 25–32.
- [187] C.T. Musabayane, O. Munjeri, P. Bwititi, E.E. Osim, Orally administered, insulin-loaded amidated pectin hydrogel beads sustain plasma concentrations of insulin in streptozotocin-diabetic rats, *J. Endocrinol.* 164 (2000) 1–6.
- [188] K. Kaur, K. Kim, Studies of chitosan/organic acid/Eudragit® RS/RL-coated system for colonic delivery, *Int. J. Pharm.* 366 (2009) 140–148.
- [189] S. Das, A. Chaudhury, K.-Y. Ng, Preparation and evaluation of zinc–pectin–chitosan composite particles for drug delivery to the colon: Role of chitosan in modifying in vitro and in vivo drug release, *Int. J. Pharm.* 406 (2011) 11–20.
-

- [190] M. Rabišková, T. Bautzová, J. Gajdziok, K. Dvořáčková, A. Lamprecht, Y. Pellequer, J. Spilková, Coated chitosan pellets containing rutin intended for the treatment of inflammatory bowel disease: In vitro characteristics and in vivo evaluation, *Int. J. Pharm.* 422 (2012) 151–159.
- [191] T. Bautzová, M. Rabišková, A. Béduneau, Y. Pellequer, A. Lamprecht, Bioadhesive pellets increase local 5-aminosalicylic acid concentration in experimental colitis, *Eur. J. Pharm. Biopharm.* 81 (2012) 379–385.
- [192] G. Prudhviraaj, Y. Vaidya, S.K. Singh, A.K. Yadav, P. Kaur, M. Gulati, K. Gowthamarajan, Effect of co-administration of probiotics with polysaccharide based colon targeted delivery systems to optimize site specific drug release, *Eur. J. Pharm. Biopharm.* 97, Part A (2015) 164-172.
- [193] Y. Karrouit, L. Dubuquoy, C. Piveteau, F. Siepmann, E. Moussa, D. Wils, T. Beghyn, C. Neut, M.-P. Flament, L. Guerin-Deremaux, L. Dubreuil, B. Deprez, P. Desreumaux, J. Siepmann, In vivo efficacy of microbiota-sensitive coatings for colon targeting: A promising tool for IBD therapy, *J. Controlled Release.* 197 (2015) 121–130.
- [194] M.S. Nieto-Bobadilla, F. Siepmann, M. Djouina, L. Dubuquoy, N. Tesse, J.-F. Willart, L. Dubreuil, J. Siepmann, C. Neut, Controlled delivery of a new broad spectrum antibacterial agent against colitis: In vitro and in vivo performance, *Eur. J. Pharm. Biopharm.* 96 (2015) 152–161
- [195] C. Freire, F. Podczeczek, D. Ferreira, F. Veiga, J. Sousa, A. Pena, Assessment of the in-vivo drug release from pellets film-coated with a dispersion of high amylose starch and ethylcellulose for potential colon delivery, *J. Pharm. Pharmacol.* 62 (2010) 55–61.
- [196] C. Gao, J. Huang, Y. Jiao, L. Shan, Y. Liu, Y. Li, X. Mei, In vitro release and in vivo absorption in beagle dogs of meloxicam from Eudragit® FS 30 D-coated pellets, *Int. J. Pharm.* 322 (2006) 104–112.
- [197] J.H. Cummings, S. Milojevic, M. Harding, W.A. Coward, G.R. Gibson, R. Louise Botham, S.G. Ring, E.P. Wraight, M.A. Stockham, M.C. Allwood, J.M. Newton, In vivo studies of amylose- and ethylcellulose-coated [¹³C]glucose microspheres as a model for drug delivery to the colon, *J. Controlled Release.* 40 (1996) 123–131.
- [198] L. Zimová, D. Vetchý, J. Muselík, J. Štembírek, The development and in vivo evaluation of a colon drug delivery system using human volunteers, *Drug Deliv.* 19 (2012) 81–89.
- [199] K. Cheng, L.-Y. Lim, Insulin-loaded calcium pectinate nanoparticles: Effects of pectin molecular weight and formulation pH, *Drug Dev. Ind. Pharm.* 30 (2004) 359–367.
- [200] S. Hua, E. Marks, J.J. Schneider, S. Keely, Advances in oral nano-delivery systems for colon targeted drug delivery in inflammatory bowel disease: Selective targeting to diseased versus healthy tissue, *Nanomedicine Nanotechnol. Biol. Med.* 11 (2015)
- [201] L.B. Vong, J. Mo, B. Abrahamsson, Y. Nagasaki, Specific accumulation of orally administered redox nanotherapeutics in the inflamed colon reducing inflammation with dose–response efficacy, *J. Controlled Release.* 210 (2015) 19–25.

-
- [202] A. Bayat, F.A. Dorkoosh, A.R. Dehpour, L. Moezi, B. Larijani, H.E. Junginger, M. Rafiee-Tehrani, Nanoparticles of quaternized chitosan derivatives as a carrier for colon delivery of insulin: Ex vivo and in vivo studies, *Int. J. Pharm.* 356 (2008) 259–266.
- [203] H. Laroui, G. Dalmaso, H.T.T. Nguyen, Y. Yan, S.V. Sitaraman, D. Merlin, Drug-Loaded Nanoparticles Targeted to the Colon With Polysaccharide Hydrogel Reduce Colitis in a Mouse Model, *Gastroenterology*. 138 (2010) 843–853.e2.
- [204] A. Makhlof, Y. Tozuka, H. Takeuchi, pH-Sensitive nanospheres for colon-specific drug delivery in experimentally induced colitis rat model, *Eur. J. Pharm. Biopharm.* 72 (2009) 1–8.
- [205] A. Beloqui, R. Coco, P.B. Memvanga, B. Ucar, A. des Rieux, V. Pr at, pH-sensitive nanoparticles for colonic delivery of curcumin in inflammatory bowel disease, *Int. J. Pharm.* 473 (2014) 203–212.
- [206] H. Ali, B. Weigmann, M.F. Neurath, E.M. Collnot, M. Windbergs, C.-M. Lehr, Budesonide loaded nanoparticles with pH-sensitive coating for improved mucosal targeting in mouse models of inflammatory bowel diseases, *J. Control. Release Off. J. Control. Release Soc.* 183 (2014) 167–177.
- [207] Y. Ma, A.V. Fuchs, N.R.B. Boase, B.E. Rolfe, A.G.A. Coombes, K.J. Thurecht, The in vivo fate of nanoparticles and nanoparticle-loaded microcapsules after oral administration in mice: Evaluation of their potential for colon-specific delivery, *Eur. J. Pharm. Biopharm.* 94 (2015) 393–403.
- [208] M. Naeem, W. Kim, J. Cao, Y. Jung, J.-W. Yoo, Enzyme/pH dual sensitive polymeric nanoparticles for targeted drug delivery to the inflamed colon, *Colloids Surf. B Biointerfaces*. 123 (2014) 271–278.
- [209] M.L. Lorenzo-Lamosa, C. Remu an-L pez, J.L. Vila-Jato, M.J. Alonso, Design of microencapsulated chitosan microspheres for colonic drug delivery, *J. Control. Release Off. J. Control. Release Soc.* 52 (1998) 109–118.
- [210] L. Gan, Y.-P. Gao, C.-L. Zhu, X.-X. Zhang, Y. Gan, Novel pH-sensitive lipid-polymer composite microspheres of 10-hydroxycamptothecin exhibiting colon-specific biodistribution and reduced systemic absorption, *J. Pharm. Sci.* 102 (2013) 1752–1759.
- [211] K. Ganguly, A.R. Kulkarni, T.M. Aminabhavi, In vitro cytotoxicity and in vivo efficacy of 5-fluorouracil-loaded enteric-coated PEG-crosslinked chitosan microspheres in colorectal cancer therapy in rats, *Drug Deliv.* (2015) 1–14.
- [212] Y. Liu, H. Zhou, Budesonide-loaded guar gum microspheres for colon delivery: preparation, characterization and in vitro/in vivo evaluation, *Int. J. Mol. Sci.* 16 (2015) 2693–2704.
- [213] G. Rai, A.K. Yadav, N.K. Jain, G.P. Agrawal, Enteric-coated epichlorohydrin crosslinked dextran microspheres for site-specific delivery to colon, *Drug Dev. Ind. Pharm.* (2015) 1–11.
- [214] L. Jin, Y. Ding, M. Feng, Q. Cao, Preparation oral levofloxacin colon-specific microspheres delivery: in vitro and in vivo studies, *Drug Deliv.* (2015) 1–7.
-

- [215] M.Z. Ahmad, S. Akhter, I. Ahmad, A. Singh, M. Anwar, M. Shamim, F.J. Ahmad, In vitro and in vivo evaluation of Assam Bora rice starch-based bioadhesive microsphere as a drug carrier for colon targeting, *Expert Opin. Drug Deliv.* 9 (2012) 141–149.
- [216] C. Mura, A. Nácher, V. Merino, M. Merino-Sanjuan, C. Carda, A. Ruiz, M. Manconi, G. Loy, A.M. Fadda, O. Diez-Sales, N-Succinyl-chitosan systems for 5-aminosalicylic acid colon delivery: In vivo study with TNBS-induced colitis model in rats, *Int. J. Pharm.* 416 (2011) 145–154.
- [217] M.S. Crcarevska, M.G. Dodov, G. Petrusevska, I. Gjorgoski, K. Goracinova, Bioefficacy of budesonide loaded crosslinked polyelectrolyte microparticles in rat model of induced colitis, *J. Drug Target.* 17 (2009) 788–802.
- [218] R. Dubey, R. Dubey, P. Omrey, S.P. Vyas, S.K. Jain, Development and characterization of colon specific drug delivery system bearing 5-ASA and Camylofine dihydrochloride for the treatment of ulcerative colitis, *J. Drug Target.* 18 (2010) 589–601.
- [219] D. Jain, A.K. Panda, D.K. Majumdar, Eudragit S100 entrapped insulin microspheres for oral delivery, *AAPS PharmSciTech.* 6 (2005) E100–E107.
- [220] D. Kietzmann, B. Moulari, A. Béduneau, Y. Pellequer, A. Lamprecht, Colonic delivery of carboxyfluorescein by pH-sensitive microspheres in experimental colitis, *Eur. J. Pharm. Biopharm.* 76 (2010) 290–295.
- [221] A. Lamprecht, H. Yamamoto, H. Takeuchi, Y. Kawashima, pH-sensitive microsphere delivery increases oral bioavailability of calcitonin, *J. Controlled Release.* 98 (2004) 1–9.
- [222] R.A. Kendall, M.A. Alhnan, S. Nilkumhang, S. Murdan, A.W. Basit, Fabrication and in vivo evaluation of highly pH-responsive acrylic microparticles for targeted gastrointestinal delivery, *Eur. J. Pharm. Sci.* 37 (2009) 284–290.
- [223] G.P. Andrews, T.P. Laverty, D.S. Jones, Mucoadhesive polymeric platforms for controlled drug delivery, *Eur. J. Pharm. Biopharm.* 71 (2009) 505–518.
- [224] M. Capece, K.R. Silva, D. Sunkara, J. Strong, P. Gao, On the relationship of inter-particle cohesiveness and bulk powder behavior: Flowability of pharmaceutical powders, *Int. J. Pharm.* 511 (2016) 178–189.
- [225] X. Yang, T.C. Ong, V.K. Michaelis, S. Heng, J. Huang, R.G. Griffin, A.S. Myerson, Formation of Organic Molecular Nanocrystals under Rigid Confinement with Analysis by Solid State NMR, *CrystEngComm RSC.* 16 (2014) 9345–9352.
- [226] J. Knapik, Z. Wojnarowska, K. Grzybowska, K. Jurkiewicz, A. Stankiewicz, M. Paluch, Stabilization of the Amorphous Ezetimibe Drug by Confining Its Dimension, *Mol. Pharm.* 13 (2016) 1308–1316.
- [227] T. Stirnimann, N.D. Maiuta, D.E. Gerard, R. Alles, J. Huwyler, M. Puchkov, Functionalized calcium carbonate as a novel pharmaceutical excipient for the preparation of orally dispersible tablets, *Pharm. Res.* 30 (2013) 1915–1925.

-
- [228] T. Stirnimann, S. Atria, J. Schoelkopf, P.A.C. Gane, R. Alles, J. Huwyler, M. Puchkov, Compaction of functionalized calcium carbonate, a porous and crystalline microparticulate material with a lamellar surface, *Int. J. Pharm.* 466 (2014) 266–275.
- [229] V.A. Eberle, J. Schoelkopf, P.A.C. Gane, R. Alles, J. Huwyler, M. Puchkov, Floating gastroretentive drug delivery systems: Comparison of experimental and simulated dissolution profiles and floatation behavior, *Eur. J. Pharm. Sci.* 58 (2014) 34–43.
- [230] V.A. Eberle, A. Häring, J. Schoelkopf, P.A.C. Gane, J. Huwyler, M. Puchkov, In silico and in vitro methods to optimize the performance of experimental gastroretentive floating mini-tablets, *Drug Dev. Ind. Pharm.* 42 (2016) 808–817.
- [231] D. Preisig, D. Haid, F.J.O. Varum, R. Bravo, R. Alles, J. Huwyler, M. Puchkov, Drug loading into porous calcium carbonate microparticles by solvent evaporation, *Eur. J. Pharm. Biopharm.* 87 (2014) 548–558.
- [232] E.T. Cole, R.A. Scott, A.L. Connor, I.R. Wilding, H.U. Petereit, C. Schminke, T. Beckert, D. Cadé, Enteric coated HPMC capsules designed to achieve intestinal targeting, *Int. J. Pharm.* 231 (2002) 83–95.
- [233] M.E. Pina, A.T. Sousa, A.P. Brojo, Enteric coating of hard gelatin capsules. Part 1. Application of hydroalcoholic solutions of formaldehyde in preparation of gastro-resistant capsules, *Int. J. Pharm.* 133 (1996) 139–148.
- [234] M.E.A. McGirr, S.M. McAllister, E.E. Peters, A.W. Vickers, A.F. Parr, A.W. Basit, The use of the InteliSite® Companion device to deliver mucoadhesive polymers to the dog colon, *Eur. J. Pharm. Sci.* 36 (2009) 386–391.
- [235] C.H. Yeong, P.E. Blackshaw, K.H. Ng, B.J.J. Abdullah, M. Blaauw, R.J. Dansereau, A.C. Perkins, Reproducibility of neutron activated Sm-153 in tablets intended for human volunteer studies, in: O. Dössel, W.C. Schlegel (Eds.), *World Congr. Med. Phys. Biomed. Eng. Sept. 7 - 12 2009 Munich Ger.*, Springer Berlin Heidelberg, 2009: pp. 1027–1030.
- [236] P. Steinmann, S. Estier, *Umweltradioaktivität und Strahlendosen in der Schweiz 2014*, (2014). <http://www.bag.admin.ch/themen/strahlung/12128/12242/index.html?lang=de>.
- [237] D. Preisig, R. Roth, S. Tognola, F.J.O. Varum, R. Bravo, Y. Cetinkaya, J. Huwyler, M. Puchkov, Mucoadhesive microparticles for local treatment of gastrointestinal diseases, *Eur. J. Pharm. Biopharm.* 105 (2016) 156–165.
- [238] M. Vallet-Regi, A. Rámila, R.P. del Real, J. Pérez-Pariente, A new property of MCM-41: Drug delivery system, *Chem. Mater.* 13 (2001) 308–311.
- [239] M. Itokazu, T. Sugiyama, T. Ohno, E. Wada, Y. Katagiri, Development of porous apatite ceramic for local delivery of chemotherapeutic agents, *J. Biomed. Mater. Res.* 39 (1998) 536–538.
- [240] G. Cavallaro, P. Pierro, F.S. Palumbo, F. Testa, L. Pasqua, R. Aiello, Drug delivery devices based on mesoporous silicate, *Drug Deliv.* 11 (2004) 41–46.
- [241] C. Charnay, S. Bégu, C. Tourné-Péteilh, L. Nicole, D.A. Lerner, J.M. Devoisselle, Inclusion of ibuprofen in mesoporous templated silica: drug loading and release property, *Eur. J. Pharm. Biopharm.* 57 (2004) 533–540.
-

- [242] S.-W. Song, K. Hidajat, S. Kawi, Functionalized SBA-15 materials as carriers for controlled drug delivery: influence of surface properties on matrix-drug interactions, *Langmuir ACS J. Surf. Colloids.* 21 (2005) 9568–9575.
- [243] A.A. Ayon, M. Cantu, K. Chava, C.M. Agrawal, M.D. Feldman, D. Johnson, D. Patel, D. Marton, E. Shi, Drug loading of nanoporous TiO₂ films, *Biomed. Mater.* 1 (2006) L11–L15.
- [244] L. Gao, J. Sun, L. Zhang, J. Wang, B. Ren, Influence of different structured channels of mesoporous silicate on the controlled ibuprofen delivery, *Mater. Chem. Phys.* 135 (2012) 786–797.
- [245] H. Vehkamäki, *Classical nucleation theory in multicomponent systems*, Springer, 2006.
- [246] L.A. Rijniens, H.P. Huinink, L. Pel, K. Kopinga, Experimental Evidence of Crystallization Pressure inside Porous Media, *Phys. Rev. Lett.* 94 (2005) 075503.
- [247] T. Limnell, H.A. Santos, E. Mäkilä, T. Heikkilä, J. Salonen, D.Y. Murzin, N. Kumar, T. Laaksonen, L. Peltonen, J. Hirvonen, Drug delivery formulations of ordered and nonordered mesoporous silica: comparison of three drug loading methods, *J. Pharm. Sci.* 100 (2011) 3294–3306.
- [248] K.L. Mittal, *Contact Angle, Wettability and Adhesion*, BRILL, 2009.
- [249] N. Verplanck, Y. Coffinier, V. Thomy, R. Boukherroub, Wettability Switching Techniques on Superhydrophobic Surfaces, *Nanoscale Res. Lett.* 2 (2007) 577.
- [250] Y. Han, W. Tong, Y. Zhang, C. Gao, Fabrication of chitosan single-component microcapsules with a micrometer-thick and layered wall structure by stepwise core-mediated precipitation, *Macromol. Rapid Commun.* 33 (2012) 326–331.
- [251] J.D. Smart, R.G. Riley, J. Tsibouklis, S.A. Young, F.C. Hampson, J.A. Davis, G. Kelly, P.W. Dettmar, W.R. Wilber, The retention of ¹⁴C-labelled poly(acrylic acids) on gastric and oesophageal mucosa: an in vitro study, *Eur. J. Pharm. Sci.* 20 (2003) 83–90.
- [252] T.T. Kararli, Comparison of the gastrointestinal anatomy, physiology, and biochemistry of humans and commonly used laboratory animals, *Biopharm. Drug Dispos.* 16 (1995) 351–380.
- [253] E. Déat-Lainé, V. Hoffart, G. Garrait, J.-F. Jarrige, J.-M. Cardot, M. Subirade, E. Beyssac, Efficacy of mucoadhesive hydrogel microparticles of whey protein and alginate for oral insulin delivery, *Pharm. Res.* 30 (2013) 721–734.
- [254] S. Kockisch, G.D. Rees, S.A. Young, J. Tsibouklis, J.D. Smart, In situ evaluation of drug-loaded microspheres on a mucosal surface under dynamic test conditions, *Int. J. Pharm.* 276 (2004) 51–58.
- [255] M.J. Toby, J.R. Johnson, P.W. Dettmar, Factors affecting in vitro gastric mucoadhesion. I: Test conditions and instrumental parameters, *Eur. J. Pharm. Biopharm.* 41 (1995) 235–241.

-
- [256] N. Thirawong, J. Nunthanid, S. Puttipipatkachorn, P. Sriamornsak, Mucoadhesive properties of various pectins on gastrointestinal mucosa: An in vitro evaluation using texture analyzer, *Eur. J. Pharm. Biopharm.* 67 (2007) 132–140.
- [257] M. Davidovich-Pinhas, O. Harari, H. Bianco-Peled, Evaluating the mucoadhesive properties of drug delivery systems based on hydrated thiolated alginate, *J. Control. Release Off. J. Control. Release Soc.* 136 (2009) 38–44.
- [258] K. Albrecht, E.J. Zirm, T.F. Palmberger, W. Schlocker, A. Bernkop-Schnürch, Preparation of Thiomers Microparticles and In Vitro Evaluation of Parameters Influencing Their Mucoadhesive Properties, *Drug Dev. Ind. Pharm.* 32 (2006) 1149–1157.
- [259] J.D. Smart, I.W. Kellaway, H.E. Worthington, An in-vitro investigation of mucosa-adhesive materials for use in controlled drug delivery, *J. Pharm. Pharmacol.* 36 (1984) 295–299.
- [260] K. Albrecht, M. Greindl, C. Kremser, C. Wolf, P. Debbage, A. Bernkop-Schnürch, Comparative in vivo mucoadhesion studies of thiomers formulations using magnetic resonance imaging and fluorescence detection, *J. Control. Release Off. J. Control. Release Soc.* 115 (2006) 78–84.
- [261] X. Zheng, K. Tsuchiya, R. Okamoto, M. Iwasaki, Y. Kano, N. Sakamoto, T. Nakamura, M. Watanabe, Suppression of *hath1* gene expression directly regulated by *hes1* via notch signaling is associated with goblet cell depletion in ulcerative colitis, *Inflamm. Bowel Dis.* 17 (2011) 2251–2260.
- [262] D. Preisig, M. Puchkov, J. Huwyler, F.J.O. Varum, R. Bravo, Delayed release pharmaceutical formulation, WO2015040212 A1, 2015. <http://www.google.com/patents/WO2015040212A1> (accessed November 4, 2015).

8 Curriculum vitae

Personal data

First name	Daniel
Last name	Preisig
Date of birth	30.09.1986
Country of birth	Switzerland
Degree	PhD in Pharmaceutical Technology
E-mail	danielpreisig@gmx.ch

Education

1993-1999	Primary school	Speicher, Switzerland
1999-2001	Middle school	Speicher, Switzerland
2001-2005	High school	Trogen, Switzerland
2006-2010	Master degree in Pharmaceutical Sciences University of Basel	Basel, Switzerland
2010	Master thesis in Pharmaceutical Technology Institute of Applied Sciences (Prof. Dr. G. Imanidis) “Absorption mechanisms of poorly water-soluble drugs in the Caco-2 cell model using biorelevant media”	Basel, Switzerland
2012-2015	PhD Thesis in Pharmaceutical Technology University of Basel (Prof. Dr. J. Huwyler), and in collaboration with Tillotts Pharma AG “Development of a mucoadhesive and multiparticulate colon drug delivery system”	Basel, Switzerland

Poster presentations

2010	GPEN, Globalization of Pharmaceutics Education Network	Chapel Hill, NC, USA
2013	3 rd Conference on Innovation in Drug Delivery: Advances in Local Drug Delivery	Pisa, ITA
2015	1st European Conference on Pharmaceutics: Drug Delivery	Reims, FRA
The three posters were also presented at the Swiss Pharma Science Day		Bern, CH

Publication list

- 2014 C. Markopoulos, F. Thoenen, **D. Preisig**, M. Symillides, M. Vertzoni, N. Parrott, C. Reppas, G. Imanidis, *Eur. J. Pharm. Biopharm.* 86; 438-448.
“Biorelevant media for transport experiments in the Caco-2 model to evaluate drug absorption in the fasted and fed state and their usefulness“
- 2014 **D. Preisig**, D. Haid, F.J.O. Varum, R. Bravo, R. Alles, J. Huwyler, M. Puchkov, *Eur. J. Pharm. Biopharm.* 87; 548–558.
“Drug loading into porous calcium carbonate microparticles by solvent evaporation“
- 2015 D. Preisig, M. Weingartner, F.J.O. Varum, R. Bravo, R. Alles, J. Huwyler, M. Puchkov, *Int. J. Pharm.* 487; 157–166.
“Marker-ion analysis for quantification of mucoadhesivity of microparticles in particle-retention assays“
- 2016 **D. Preisig**, R. Roth, S. Tognola, F.J.O. Varum, R. Bravo, Y. Cetinkaya, J. Huwyler, M. Puchkov, *Eur. J. Pharm. Biopharm.* 105; 156–165.
“Mucoadhesive microparticles for local treatment of gastrointestinal diseases“
-